Aus der Medizinischen Klinik und Poliklinik IV

der Ludwig-Maximilians-Universität München

Klinischer Direktor: Prof. Dr. med. Martin Reincke

From Epidemiology to Function:

Identification of a Novel Aldosterone Regulator

Dissertation

zum Erwerb des Doktorgrades der Humanbiologie an der

Medizinischen Fakultät der

Ludwig-Maximilians-Universität zu München

vorgelegt von

Tarik Bozoglu

aus Izmir

GEFÎ

Berichterstatter:	Prof. Dr. med. Felix Beuschlein
Mitberichterstatter:	Prof. Dr. med. Christine Spitzweg
	Prof. Dr. rer. nat. Roland Kappler
	Prof. Dr. med. Ortrud Steinlein
Mitbetreuung durch den promovierten Mitarbeiter:	
Dekan:	Prof. Dr. dent. med. Reinhard Hickel
Tag der mündlichen Prüfung:	16.02.2016

Eidesstattliche Versicherung

Bozoglu, Tarik

Name, Vorname

Ich erkläre hiermit an Eides statt,

dass ich die vorliegende Dissertation mit dem Thema

From Epidemiology to Function:
Identification of a Novel Aldosterone Regulator

selbständig verfasst, mich außer der angegebenen keiner weiteren Hilfsmittel bedient und alle Erkenntnisse, die aus dem Schrifttum ganz oder annähernd übernommen sind, als solche kenntlich gemacht und nach ihrer Herkunft unter Bezeichnung der Fundstelle einzeln nachgewiesen habe.

Ich erkläre des Weiteren, dass die hier vorgelegte Dissertation nicht in gleicher oder in ähnlicher Form bei einer anderen Stelle zur Erlangung eines akademischen Grades eingereicht wurde.

München, 23.04.2015

Ort, Datum   Unterschrift Doktorandin/Doktorand

Avī meī, requiescite in pace.

بِسْمِ اللهِ الرَّحْمٰنِ الرَّحِيْمِ

Contents

1.   Introduction

As sardonically stated by Daniel Defoe, "nothing in life is as certain as death and taxes" [1]. While the Finanzamt ensures the latter, the leading contributor to the prior is cardiovascular disease, causing 1 out of every 2.8 deaths [2]. Within this class, arterial hypertension is the most lethal and prevalent condition, endemic in 30 – 45 per cent of European population [3]. Arterial hypertension is defined as persistent systolic blood pressure above 140 mmHg and diastolic blood pressure above 90 mmHg [4]. While the majority of the cases are due to unknown or insufficiently elucidated causes and designated as "essential hypertension"; several secondary forms of hypertension are identified. Chief among them is primary aldosteronism (PA), which is named after its classical cause of autonomous excess synthesis of the mineralocorticoid aldosterone [5]. The disorder is mainly comprised of Conn's syndrome [6] of aldosterone producing adenomas and idiopathic aldosteronism [7] with uni- or bilateral hyperplasia of the adrenal cortex. Although idiopathy in Koine Greek means "one's own suffering" and defined as "without a known cause" [8]; the fictional but esteemed diagnostician Dr. Gregory House gives an alternative definition: ""Idiopathic", from the Latin, meaning we're idiots 'cause we can't figure out what's causing it" [9]. This sarcastic comment however reflects the truth that the biomedical community has only recently began to emerge from the perplexity surrounding pathophysiology of this disorder. In this dissertation, a quest to explore the genetic and molecular pathophysiology of PA by combining epidemiological and functional studies is reported.

1.1.   The Mineralocorticoid Aldosterone

Life was hard for early tetrapods trying to colonize land during the Paleozoic era. On top of necessary adaptations of mobility, respiration and reproduction to land life [10], they faced the threat of desiccation and maintenance of the "milieu intérieur" [8]. Although they were already equipped with a primitive salt retention apparatus with mineralocorticoid receptors, only after divergence of the mineralocorticoid hormone aldosterone [11] were they able to fully overcome the challenges presented by the Late Devonian extinction, where only sufficiently adapted land vertebrates were able to survive [12]. As such, aldosterone has a crucial and irreplaceable role for all vertebrate life on land. The main physiological role of aldosterone in maintaining homeostasis is through its actions on the renal tissues [13]. The conventional way to describe aldosterone physiology seems to be to categorize it by function, systemic endocrine regulation and molecular regulation of synthesis [14].

1.1.1.   Mechanism of Action

Aldosterone, in its capacity as the main mineralocorticoid in humans, exerts its actions through

genomic and non-genomic effects in the aldosterone sensitive cells of the distal nephron of the kidney, comprising the region from the distal convoluted tubule to the collecting duct (Fig 1.1) [13]. There is evidence, however, that the aldosterone sensitivity of the nephron may extend to the proximal tubule [15] on one side and inner medullary collecting duct [16] on the other. Still, the cortical collecting duct is the most thoroughly investigated part of kidney in relation to aldosterone activity.

The principal cells of the cortical collecting duct, which are involved in sodium reabsorption from the glomerular filtrate it receives from the nephron, are especially sensitive to aldosterone stimulation. These cells form a monolayer that separate the internal and external environs, and facilitate reabsorption of sodium through an apical electrochemical potential and a basolateral active transport system [14]. The transcellular reabsorption of sodium to renal interstitium is then followed by paracellular chloride flux [17] and water diffusion through aquaporins [18]. The regulatory effect of aldosterone on the function of these cells is through its binding to cytosolic mineralocorticoid receptor (MR) of the nuclear receptor family. Normally bound to heat shock proteins, MR dissociates and dimerizes after binding to aldosterone and translocates to the nucleus, acting as a transcription factor for aldosterone sensitive genes [19]. Interestingly, aldosterone sensitivity of these cells does not stem either from exclusive expression of MR in these cells or exclusive affinity of MR to aldosterone, as it has a similar affinity to glucocorticoids. Instead, enzymatic activity of 11-β-hydroxysteroid dehydrogenase 2 (11βHSD2) rapidly oxidizes cortisol to cortisone (or corticosterone to 11-dehydrocortisone) [20], for which MR does not have affinity, hence preventing glucocorticoid activation of the MR. Indeed, due to presence of an inhibitor of this enzyme, glycyrrhizin, excess licorice consumption may trigger pseudo-hyperaldosteronism. [21].

Through a plethora of effects including transcriptional or enzymatic activation of membrane transporters and their regulatory signals, the MR-aldosterone complex facilitates sodium reabsorption and potassium excretion [13]. Among these, upregulation and activation of the amiloride-sensitive epithelial sodium channel (ENaC) [22], the renal outer medullary potassium channel (ROMK) [23] and the thiazide-sensitive sodium-chloride cotransporter (NCC) [24] in the apical membrane and induction of sodium-potassium adenosine triphosphatase (Na^+/K^+ ATPase) activity [25] and sodium–hydrogen antiporter (NHE1) activation [26] in the basolateral membrane account for the major mineral balancing effects of aldosterone in the principal cell. The genomic regulation of these complexes by aldosterone is via direct transcriptional upregulation as in the case of ENaC subunit α, or secondary effects mainly due to upregulation of the serum and glucocorticoid-regulated kinase 1 (SGK1) [27], and through the Kirsten Ras GTP-binding protein-2A (Ki-RasA),

Corticosteroid hormone-induced factor (CHIF) or Phosphoinositide 3-kinase (PI3K) [14]. Through further interplay between SGK1 and "with no lysine" kinase (WNK) pathways, the exact nature of aldosterone action in the kidney, favoring either sodium reabsorption or potassium excretion depending on presence of angiotensin II, is determined [28]

A multitude of non-genomic effects of aldosterone have also been observed, with involvement of protein kinase C activation or increases in second-messenger of cyclic adenosine monophosphate (cAMP), intracellular calcium ($[Ca^{2+}]_i$) and inositol 1,4,5-triphosphate (IP_3) [14; 29; 30]. These mechanisms are fast acting, without the lag-time of genomic effects, and unaffected by transcription and translation inhibitors [31]. Furthermore, it is disputed whether these effects are due to MR-aldosterone complex, or facilitated by a putative aldosterone specific membrane receptor long sought by Martin Wehling and his colleagues [30].

Alongside its effects on the principal cell, aldosterone also participates in the regulation of acid-base balance by its actions on type A intercalated cells that are dispersed through epithelial lining of the distal nephron [32]. Through genomic and acute pathways, aldosterone regulates activities of
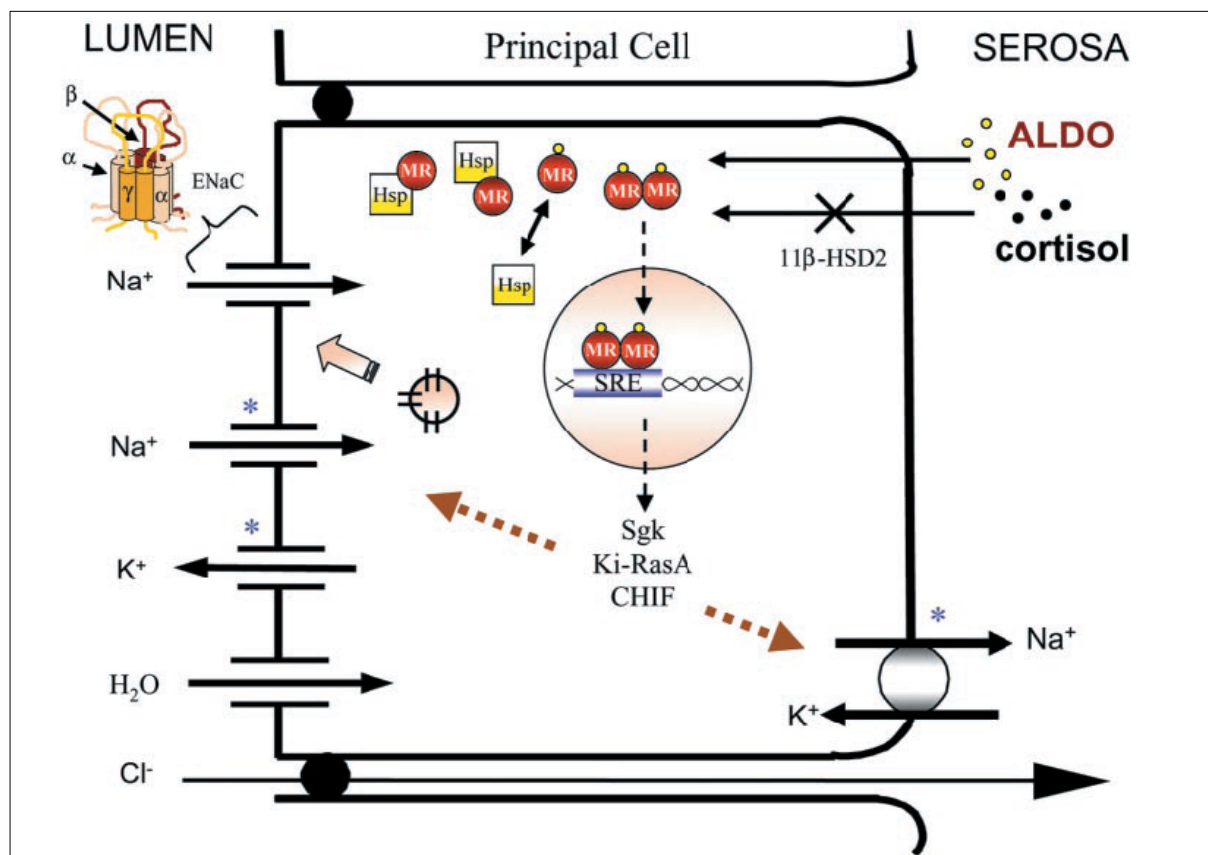
Figure 1.1: Regulation of sodium reabsorption in the kidney principal cell. Aldosterone liberates the mineralocorticoid receptor from bound heat-shock proteins and relocalizes to the nucleus. Glucocorticoids are rapidly degraded by the 11β-hydroxysteroid dehydrogenase. Early actions include increased transporter activity and surface presentation. The late phase of aldosterone induction involves expression of transporter genes. Obtained from Booth, *et al* [31]*.

luminal proton pump and basolateral chloride / bicarbonate exchangers [**33**].

Consistent with the presence of MR in the central nervous system and cardiovascular tissues, these organs are also targets of circulating aldosterone. In the central nervous system, aldosterone has a disadvantage against glucocorticoids for the activation of MR, as MR in this system is not protected by 11βHSD2 [**34**]. Together with the presence of much higher circulating glucocorticoids and the enzymatic activity of 11β-hydroxysteroid dehydrogenase (11βHSD1), which converts inactive cortisone to cortisol, MR in the central nervous system is disproportionately occupied by glucocorticoids [**14**]. As for the cardiovascular tissues, aldosterone has long been regarded to play pathological role due to the induction of hypertension; however, this opinion was much reinforced by the detection of MR and 11βHSD2 in cardiac blood vessels and a possible autocrine effect through cardiac production of aldosterone. By and large, current knowledge on normal physiology of aldosterone in the cardiovascular system is overshadowed by the focus on its pathophysiological effects. [**31**]

1.1.2. Renin-Angiotensin System

The crucial and multifaceted effects of aldosterone require a tight systemic control over its production, without which severe pathological conditions can and do arise. The renin-angiotensin-aldosterone system (RAAS) is the main axis of blood pressure regulation in humans, and therefore responsible for regulation of aldosterone biosynthesis. It provides one of the two most potent physiological signals for aldosterone production, angiotensin II, the other being hyperkalemia. The cascade originates in the kidney, involves components from the liver, vascular epithelia, adrenal and the pituitary gland; ultimately acting on the kidney function (Fig 1.2).

Most kidney anatomical depictions would show that the nephron starts at the glomerulum, where the afferent arteriole branches into many capillaries that effect ultrafiltration, and goes through a length of tubular structures that descend into the medulla and return to the cortex at the thick ascending limb, ultimately merging with other nephrons at the collecting duct. Not readily obvious in such a diagram is the fact that granular smooth muscle cells of afferent and efferent arterioles lay in close proximity to the macula densa cells of cortical thick ascending limb, as can be seen in a cross-section histology staining. Granular smooth cells synthesize and store the hydrolytic enzyme renin in their granules, whereas the macula densa cells have the ability to sense the sodium, potassium and chloride concentrations of the glomerular filtrate through their luminal expression of the Na^+-K^+-$2Cl^-$ cotransporter (NKCC2) [**35**]. The close proximity of these two cell types lead to their designation as the juxtaglomerular apparatus, which functions as the sphygmomanometer of the body. The anatomical proximity of these sensor cells to the glomerulum allows for an intrarenal purinergic

signaling mediated by adenosine and / or adenosine-triphosphate (ATP) [36]. Through evoking this signaling, macula densa cells control the vasoconstriction or vasodilation of afferent arterioles, creating the tubuloglomerular feedback mechanism. Reduction of sodium concentration or glomerular filtration rate results in vasodilation of afferent arterioles, which triggers renin secretion from granular cells. Other factors also lead to vasodilation of afferent arterioles such as detection of arterial blood pressure / volume loss by baroreceptors mediated by β-adrenoreceptor activation and sympathetic nervous system activity via the same route [37]. Along with the systemic effect of renin secretion, reduction of arteriole vascular resistance also leads to immediate increase in glomerular filtration rate.

The next stage in this multi-organ system is the hydrolysis of angiotensinogen, an α-2-globulin peptide which is constitutively produced by the liver. The product, 10 amino acid angiotensin I (AngI) is a substrate for further cleavage by the angiotensin-converting enzyme (ACE) [37]. ACE is highly expressed on the vascular endothelium in tissue bound form, with lung endothelium having the capacity to process whole of the plasma AngI in a single passage [38]. Removal of the two C-terminal amino acids of AngI mainly by the C terminal catalytic domain of ACE [39] produces the active octapeptide angiotensin II (AngII), the effector component of the cascade and a potent vasoconstrictor. Further synergistic effect is provided by ACE mediated metabolization of the vasodilators bradykinin and kallidin into inactive forms [40]. In tissues expressing aminopeptidase A and N, AngII is further lysed to angiotensin III and IV, which plays paracrine roles in these tissues [41].

Angiotensin II is one of the two most potent physiological inducers of aldosterone production by the adrenal cortex [42]. Alongside its steroidogenic effect on the adrenal cortex, it activates a wide range of synergistic responses through its receptors (mainly of type 1) found in the vascular, cardiac, renal and nervous systems [43]. Further effects of AngII include stimulation of the pituitary gland and secretion of anti-diuretic hormone (ADH) [44] and, under increased AngII concentrations by severe volume loss, adrenocorticotropic hormone (ACTH) [45]. In turn, ACTH acts as an acute, protein synthesis independent secretagogue of aldosterone [46], and ADH modulates aquaporin 2 of the principal cells in kidney to facilitate water retention [47].

As the circulating angiotensinogen and endothelial ACE activity are constant and due to the short plasma half-lives of its active components, the regulation of the RAA axis is modulated by a negative feedback loop at the stage of renin secretion. Vasoconstriction of glomerular arterioles by AngII [43] or by purinergic signals from macula densa in response to increased filtrate volume or sodium concentration [36] inhibits renin secretion, as well as by intrarenal α-adrenergic receptor stimulation

[**48**] and by atrial natriuretic peptide [**49**].

Partial or complete sets of components of the RAAS have been observed in cardiac, vascular, brain, renal and adrenal tissues. In contrast to the systemic endocrine RAAS, these tissues exhibit a paracrine / autocrine form of the system. This complementary "tissue RAAS", maintaining localized and longer-term homeostasis, potentially adds another level of complexity to intervention to systemic axis in pathological situations [**37**].

1.1.3. Inside the Glomerulosa Cell: Aldosterone Steroidogenesis and Regulation

The adrenal gland is in effect composed of two separated tissues, that of the medulla and the cortex, each developing from different embryonic origins. [**51**] Whereas the medulla function is focused on secretion of the cathecolamines epinephrine and norepinephrine, the adrenal cortex is responsible for corticosteroid production. Between the adrenal medulla and adrenal capsule, three zonal layers of the cortex have been described by morphology of constituent cells: innermost, the zona
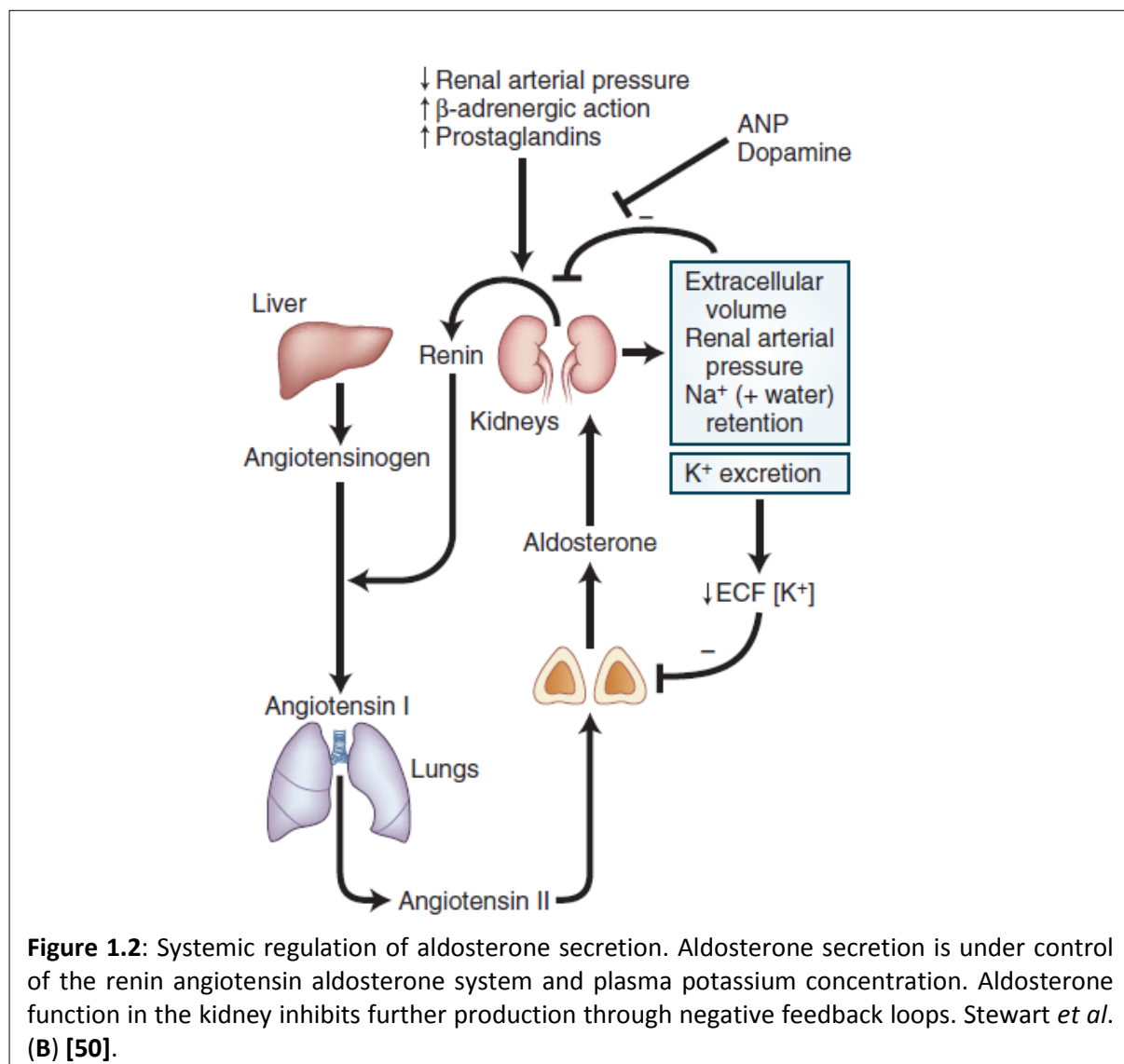
Figure 1.2: Systemic regulation of aldosterone secretion. Aldosterone secretion is under control of the renin angiotensin aldosterone system and plasma potassium concentration. Aldosterone function in the kidney inhibits further production through negative feedback loops. Stewart *et al.* (**B**) [**50**].

reticularis (ZR), zona fasciculata (ZF) and the outermost zona glomerulosa (ZG) [52] along with an undifferentiated stratum of progenitor cells (ZP) between the ZF and ZG (Fig 1.3) [53]. A common steroidogenesis pathway (Fig 1.4) is shared in cells of these zones, with the end product depending on presence or absence of specific enzymes of this pathway [54]. ZR produces adrenal androgens, ZF produces glucocorticoids as part of the energy metabolism in response to ACTH, and ZG focuses on salt and water homeostasis via its production of aldosterone [50]. Although classically defined as a continuous layer, the zona glomerulosa has recently been shown by novel specific antibodies to consist of two units: dispersed cells and clusters. The physiological impact of this divergence is yet to be elucidated [55].

Adrenocortical cells do not have a mechanism for steroid deposition or secretary vesicles, and consequently, upon stimulatory signals, corticosteroids are to be produced *de novo* from cholesterol, primarily from uptake of plasma high-density lipoprotein [56]. Cholesterol stored in cytosolic lipid droplets is then translocated to the mitochondrial inner membrane by the steroidogenesis acute regulatory protein (StAR). This transport process is a common rate limiting step in all adrenocortical cells. In the mitochondria, P450 cholesterol side chain cleaving enzyme (CYP11A1) catalyzes its eponymous reaction, producing pregnenolone. Pregnenolone released to the

Figure 1.3: The adrenal gland: **A**, Rat adrenal gland section immunostained for markers of zona glomerulosa (CYP11B2, blue) and zona fasciculata (CYP11B1, brown). **B**, Schematic diagram of the adrenal cortex. Obtained from Fumiko Mitani (**A**) [51] and Stewart *et al*. (**B**) [50].
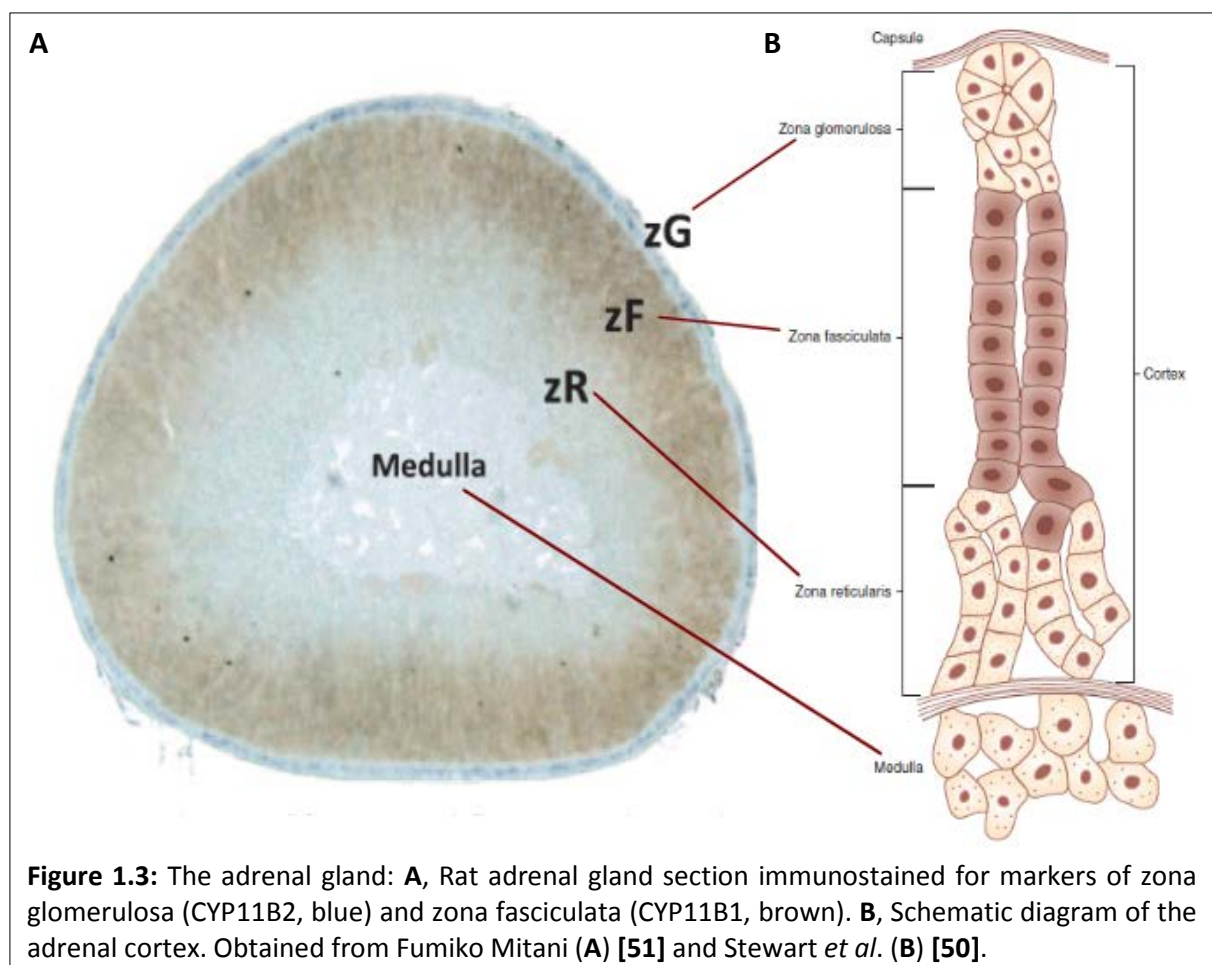
cytosol, and may be converted to other precursors of androgens or glucocorticoids, depending on the zonal type of the cells, by enzymes on the smooth endoplasmic reticulum (ER). Pregnenolone and its derivatives are common in their role as the substrates for the 3β-hydroxyl group dehydrogenation and 5-delta 4-isomerazation, by the isoforms of 3β-hydroxysteroid dehydrogenase (3βHSD) enzyme of smooth ER [14]. Traditionally, isoform 2 of the enzyme was thought to regulate this catalytic activity in the adrenal [57], but emerging evidence challenges this view, as HSD3B1 has been immunolocalized to the ZG, but in pathological aldosterone producing adenomas HSD3B2 has been detected predominantly [58; 59].

Production of progesterone from pregnenolone by 3βHSD activity is followed by steroid 21-hydroxylase activity on the smooth ER of ZG and ZF cells, generating the immediate precursors of mineralocorticoids and glucocorticoids. The final reactions are mediated by the two members of cytochrome P450 11B family of enzymes, located in the inner mitochondrial membrane. Both of the 93 % homologous isozymes have the 11β-hydroxylase activity, which produces cortisol by the ZF localized isoform 1 (CYP11B1). In the ZG, however, 11β-hydroxylation is followed by 18-hydroxylation and 18-methyloxidation, all by P450 11B2, also known as aldosterone synthase (CYP11B2). The final CYP11B2 mediated steps of aldosterone is the last rate limiting step of the pathway [14].

Zona glomerulosa cells under basal conditions are hyperpolarized due to intricate modulation of membrane potential by a number of ion transporters and channels [60]. The ZG cell membrane maintains a selective conductance to potassium ion, with a negative membrane resting potential. This status is maintained by Na^+/K^+ ATPase and leak potassium current through "tandem of P domains in a weak inward rectifying K^+ channel-like, acid-sensitive K^+" channel (TASK). Modulation of this balance of currents is the main mechanism of action for aldosterone secretagogues, as depolarization of the cell is the principal signal that initiates aldosterone synthesis. The two principal depolarizing signals in physiological conditions are AngII and increase in extracellular potassium concentration ($[K^+]_O$). In both types of stimuli, cell depolarization leads to an intracellular calcium flux [61].

AngII effects the calcium rush by binding to its abundant G protein coupled receptors (AT_1) on the membrane. Immediate effect of this is activation of phospholipase C (PLC), which generates the second messenger inositol 1,4,5-trisphosphate and 1,2-diacylglycerol (DAG)by phosphatidylinositol hydrolysis. IP_3 then acts on IP_3 gated Ca^{2+} channels of the ER, resulting Ca^{2+} release from intracellular stores to the cytosol. Simultaneously, AngII binding to its receptor inhibits Na^+/K^+ ATPase and TASK channels, leading to depolarization and increase in membrane potential towards positive. This

voltage reduction triggers an inward Ca^{2+} current through low voltage activated T-type Ca^{2+} channels, as the extracellular calcium concentration ($[Ca^{2+}]_O$) is manyfold higher than intracellular levels ($[Ca^{2+}]_I$). Influx of extracellular calcium is further facilitated by channels that respond to intracellular store depletion. This total increase in the cytosolic Ca^{2+} ($[Ca^{2+}]_I$) also activates PLC, sustaining the initial IP_3 and DAG production [**14; 54; 61**].

Extracellular $[K^+]_O$ increase is also a very potent depolarization signal due to the *glomerulosa* cell's unique potassium sensing ability [**60**]. This increase effectively prevents TASK mediated background current, resulting in a transmembrane T-type calcium influx. By extracellular concentrations of potassium above physiological levels, L-type high voltage channels are also activated. As the $[K^+]_O$ continues to rise, T-type current is inactivated and supplanted by L-type channel activity [**61**].
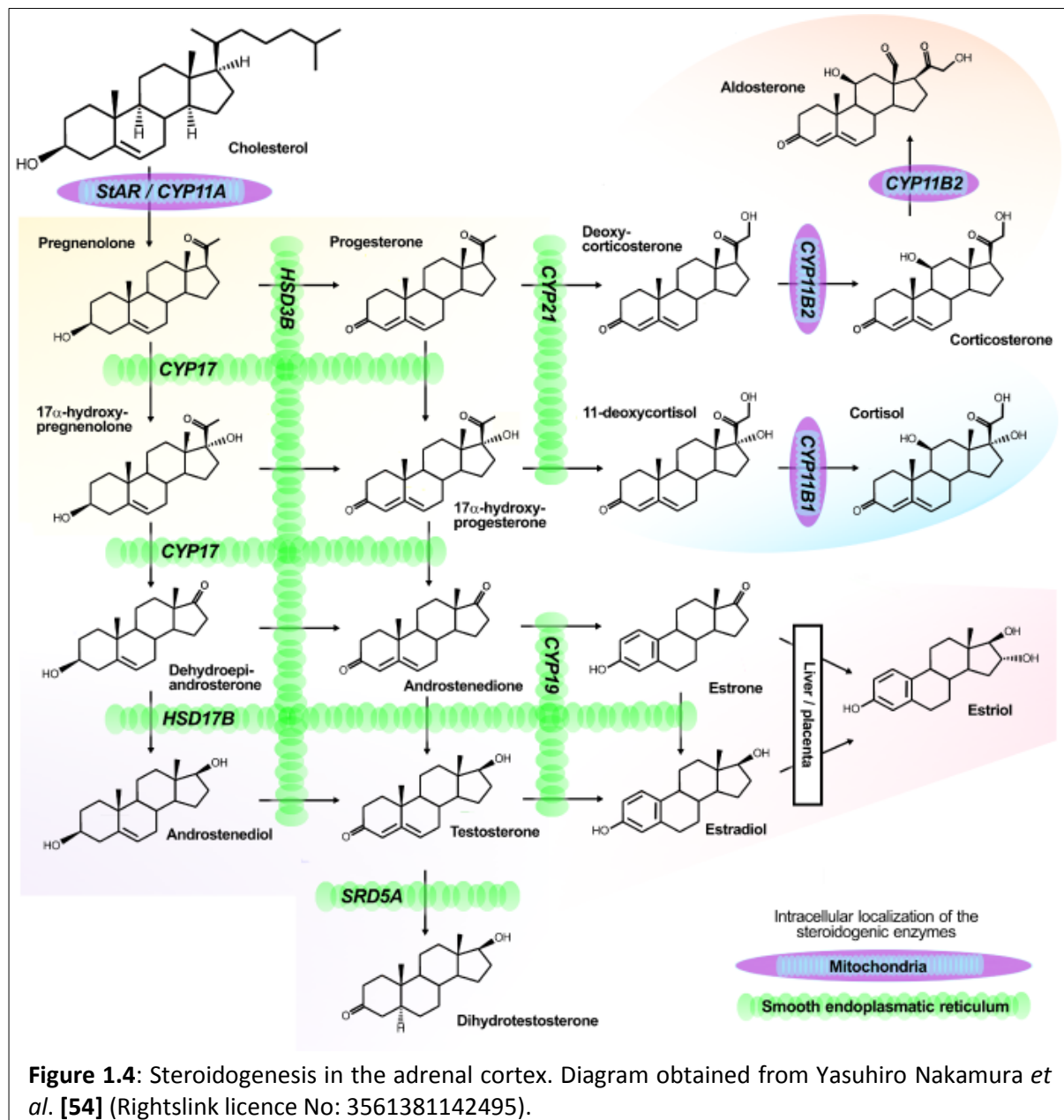
Figure 1.4: Steroidogenesis in the adrenal cortex. Diagram obtained from Yasuhiro Nakamura *et al*. [**54**] (Rightslink licence No: 3561381142495).

The second messengers $[Ca^{2+}]_I$ and DAG activate protein kinase C (PKC). High $[Ca^{2+}]_I$, PKC and DAG-derived 12-Hydroxyeicosatetraenoic acid (12-HETE) in turn activates p38 [62] and p44/42 [63] mitogen-activated protein kinase (MAPK) pathways and calcium binding messenger protein calmodulin (CaM) [64]. CaM mediation is a requirement of calcium induced phosphorylation of calcium / calmodulin dependent kinases (CAMK) I and IV [65]. These pathways ultimately modulate the three rate-limiting steps of aldosterone synthesis, StAR, 3βHSD and CYP11B2. In the acute phase, without de novo enzyme production, the effects depend on StAR activation by PKC. Increased mitochondrial steroidogenic capacity by elevated formation of pyridine dinucleotide NADPH in response to $[Ca^{2+}]_I$ increase may also play a role at this point [61]. Activation of p44/42 MAPK pathway activates steroidogenic factor 1 (SF1) which transcriptionally activates StAR when the inhibitor of this process DAX1 is repressed, also modulated by p44/42 MAPK [66]. CAMK activation leads to transcriptional activation of neuronal growth factor-induced clone B (NGFI-B) family of transcriptional factors (NR4A1 and NR4A2) as well as phosphorylating members of "activator transcription factor (ATF) / cyclic adenosine monophosphate response element (CRE) binding protein (CREB)" family of transcriptional factors [65]. NGFI-B factors can bind to regulatory *cis*-acting NGFIB response elements (NBRE-1 and Ad-5) in the 5' promoter region of CYP11B2, along with CRE sites for ATF / CREB. NGFIB response elements are also identified upstream of HSD3B isoforms 1 [67] and 2 [68]. Through activation of these transcriptional factors, de novo 3βHSD and CYP11B2 production occurs, effecting the long term response to stimulation.

ACTH as a stimulator of aldosterone essentially acts by inducing second messenger cAMP system through binding to its G-protein coupled receptor [69]. Resultant activation of protein kinase A (PKA) is responsible for StAR phosphorylation alongside PKC [70]. However, long term stimulation by ACTH suppresses aldosterone production and reforms the adrenal cortex in favor of glucocorticoid production [71]. There is also a great deal of cross-play between the calcium and cAMP second messenger systems, such as calcium dependency of cAMP formation by ACTH signaling and cAMP dependent activation of L-type calcium current; hinting at the complexity of control behind these cellular events [60].

1.2. Primary Aldosteronism

Just as Charles Darwin was considered the best qualified person for the post of naturalist of the second voyage of *HMS Beagle*, more than a century later, Jerome Conn was perhaps the best man to diagnose the 34-year-old hypertensive patient "MW", due to his studies on body acclimatization to the tropics [72]. Unlike Darwin, who published his theory ahead of "Mendel's peas", Conn fatefully oversaw the removal of his patient's tumor only a year after characterization of what the tumor was

found to overproduce. In his presidential address [6] at the Society of Clinical Research, he presented his case, "primary hyperaldosteronism", with the clinical features of alkalosis, hypokalemia and hypernatremia, all due to the adrenal tumor; having his name given to a syndrome in the fashion of Addison or Crohn. Even as idiopathic cases of PA were reported with no associated tumor, he went on to demonstrate the renin independency of aldosterone production in the disorder [73]. The medical community's approach to diagnosis of PA with considering hypokalemia as a *sine qua non* for the disease gave way to very low prevalence estimates for the next four decades. However, in the last twenty years, a switch to diagnosis based on renin independent aldosterone production as a screening marker sparked what was termed as a "renaissance of the syndrome" [74], as prevalence estimates soared up to 30 % of hypertensives, depending on the study cohort [75]. The current guideline in effect in Germany composed by the Endocrine society during this renaissance defines PA as "a group of disorders in which aldosterone production is inappropriately high, relatively autonomous, and non-suppressible by sodium loading" [76].

1.2.1. Pathogenesis

As important as aldosterone is in an average mammalian diet, in humans, considering the modern salt consumption levels, excess of the hormone is severely damaging to the cardiovascular and renal systems. The most prominent symptom is arterial hypertension, usually resistant to anti-hypertensive therapy and of higher stages. Higher aldosterone levels are found to be predictive of hypertension [77]. Indeed, 5 to 10 percent of total hypertensive population is estimated to be affected by PA, rendering this the prevailing cause of non-idiopathic hypertension [76]. In addition to hypertension, a wide range of cardiovascular (ischemic heart disease, arrhythmia, myocardial fibrosis, inflammatory invasion of vasculature) [14] and renal (nephrosclerosis, proteinuria) [78] complications are characteristic of the disease. Recent evidence also suggests that organ damage is aggravated by oxidative stress induced by excess circulating aldosterone [79].

Although the cutoff between low renin essential hypertension (LREH) and primary aldosteronism is recognized to be arbitrary, the effects of PA are most certainly of adrenal origin. 95 per cent of total PA cases are caused by a benign aldosterone producing adenoma (APA) or bilateral idiopathic adrenal hyperplasia (BAH). This medically correctly [80], but semantically misleadingly termed "benign" neoplasm was the original case described by Conn, hence named after him as Conn's syndrome. They are estimated to represent ~1/3 of the PA cases, contrasted by a more common ~2/3 of diffuse or micronodular bilateral hyperplasia of the adrenal [81]. The proportion of unilateral and bilateral disease is also debated, with different groups coming to varying conclusions [82]. Rarer forms of the disease include unilateral primary adrenal hyperplasia, and the three Mendelian forms

of the disease, familial hyperaldosteronism (FH) types I, II and III. An aldosterone producing adrenal carcinoma is also occasionally encountered, with one such case giving rise to the model cell line NCI-H295R [**83**].

Genetics of PA, aside from the rare FH I, was largely unknown until recently. FH I was found to be due to a chimeric gene arising from the strong homology of aldosterone synthase and 11β-hydroxylase, giving regulatory control of aldosterone production to ACTH [**84**]. The syndrome was therefore named as glucocorticoid-remediable hyperaldosteronism. In the last three years, however, several landmark studies established the causative somatic mutations of more than half of the APAs [**85**], as well as FH III [**86**]. The mutated genes in these adenomas encode membrane channels and transporters of potassium and calcium, and the mutations disrupt ion homeostasis of the cell [**86-89**]. These findings arguably place the syndrome in a post-renaissance baroque era, drawing enhanced interest of the scientific community.

1.2.2. Diagnosis and Treatment

According to the current guidelines, PA is diagnosed with a three tiered procedure [**76; 90**]; that is screening, confirmation and subtype evaluation. Hypokalemia has long been abandoned as a case-finding tool in the face of standardized aldosterone to renin ratio (ARR) measurements, and actual rate of hypokalemic individuals with PA represent now a minority. Plasma aldosterone concentration (PAC) under normal physiological conditions strongly correlate with plasma renin activity (PRA), and an increase of the ratio of the two is suggestive of the disease. As PRA measurements comes with interassay replicability challenges, higher throughput plasma renin concentration (PRC) assays, which basically quantify the same factor [**91**], has been adopted instead. However, as the renin denominator of the ratio is the main covariant, specificity of the test at low renin levels are challenged. In current practice, an ARR screening is recommended to drug-resistant, advanced stage or all hypertensives, depending on the advisory committee. Cessation of antihypertensive medication that affects the RAAS up to several weeks before testing is highly recommended, with an option to switch to blood pressure control via medications that doesn't have a known impact on the system in life-threatening conditions.

A positive ARR, while indicative, is not considered as diagnostic. PA is confirmed by one of the four suppression tests, depending on patient's status and feasibility of a stationary versus ambulatory setting. Saline infusion & plasma aldosterone concentration, oral saline uptake and renal aldosterone excretion, and the more sensitive fludrocortisone suppression tests are recommended in most cases. These tests establish the relative autonomy of aldosterone production in the patients and considered to be diagnostic. In cases where salt loading compromises the patient, captopril

challenge is applied, suppressing renin but not aldosterone [76].

A confirmed case of PA requires subtype evaluation to aid the physician in deciding the therapy strategy. The first step in this direction is adrenal computed tomography. It is known that this method has very low sensitivity for smaller APAs and a lack of specificity for unilateral disease, but it can eliminate the possibility of larger masses such as carcinomas. In addition, adrenal CT provides valuable preparation for the next stage, adrenal vein sampling (AVS). This procedure is definitive, but both invasive and requires a specialist radiologist. Adrenal CT is very useful for providing a better success rate in the especially difficult catheterization of the right adrenal vein [76].

Treatment of PA depends on the lateralization of disease. For unilateral subtypes, a surgical approach with laparoscopic adrenalectomy always improves and often cures the condition. For bilateral hyperplasia, this prognosis is not achievable surgically, so a management with MR antagonists spironolactone or eplerenone is preferred [76]. The latter, being the newer and more specific aldosterone antagonist with fewer side effects, may be cost-inhibitory due to its manyfold price compared to the former [92]. Furthermore, eplerenone is not approved for the treatment of hypertension of PA in many countries.

The main problems with current practices in diagnosis and management of PA are low specificity of ARR screening, inefficiency of adrenal CT both in specificity and sensitivity, invasiveness and inherent difficulty of AVS [93], and a therapeutic strategy in bilateral disease built on lifelong management of MR mediated aldosterone damage with only limited remission [94]. However, recent developments start to offer alternatives at every turn. ARR still is the established norm for screening, but regression based statistical approaches and independent determination of renin decrease and aldosterone increase has been proposed [95]. Subtype classification with a CT-AVS method is now challenged by an ^{11}C-metomidate PET-CT [96]. Development of novel specific antibodies against CYP11B homologs, as well as against other markers of healthy and pathological aldosterone producing cells, as in the case of 3βHSD isozymes, may avail immunochemistry based diagnostic approaches [97]. The recent surge in elucidating the underlying genetics of PA identifies targets of novel drugs like digoxin (ATP1A1) or amlodipine (CACNA1D) [72], as well as enabling prospective less invasive genetic diagnosis methods [98].

1.3. Strategies for Elucidation of Genetic Mechanisms

Primary aldosteronism is a very heterogeneous disease. In addition to its previously described subtypes, heterogeneity is becoming increasingly evident within subtypes based on molecular, morphological and genetic signatures. Obscured by this heterogeneity, however, lies a significant

heritable portion of the disease [**77**]. Although aiming in-depth elucidation of pathophysiological mechanisms of PA is a daunting task in the face of complexity to be overcome, researchers have several potent methods in their armamentarium to rise to the challenge ahead.

1.3.1. Mouse Models

Pharmacological approaches such as 11-desoxycorticosterone acetate (DOCA)-salt sensitive rats has long been used to generate animal models for endocrine hypertension [**99**]. In addition, development of embryonic stem cell based techniques to produce gene knockout mice has been a Nobel prize-worthy success [**100**]. This methodology enabled generation of genotype-driven mouse models, in which a particular genotypic change is characterized phenotypically. In the context of PA research, several such models have been generated. An angiotensin II receptor 1A mutant mice with constitutively active AT_2 receptor developed hypertension. Targeting ion homeostasis by knockouts of leakage potassium channels TASK1, TASK3 or voltage- and Ca^{2+}-activated K^+ channel (BK) yielded varying levels of phenotypic similarity to PA in humans [**101-105**]. Although this kind of approaches greatly enhances the understandings of underlying basic physiology of aldosterone synthesis, without an epidemiological basis, they prove insufficient to explain human pathophysiological mechanisms of PA. In addition, some gene knockouts maybe particularly damaging, as the effects are present during developmental stages. A strategy to overcome this is inducible or tissue specific knockouts, which gives researchers spatial and temporal control over the effects of the genetic manipulation [**106**].

A reversal of direction in the generation of mouse models is possible through utilization of DNA damaging reagent of *N*-ethyl-*N*-nitrosourea (ENU). Treatment of male mice with ENU produces point mutations in the spermatozoa, and subsequent mating and cross-breeding gives rise to offspring that can be screened for a particular phenotype. One such mutagenesis screen has already produced eight separate mouse lines with heritable primary aldosteronism [**107**], and subsequent elucidation of causative mutations will presumably yield new interesting targets for further study.

1.3.2. Exome Sequencing

Towards the end of the last decade, two proof of concept studies established the feasibility of obtaining sequence data from whole exomes, as a compromise in the face of unattainability of whole genome sequencing [**108; 109**]. This methodology has been particularly impactful in PA research, as the already present large collections of APAs were sequenced to reveal novel causative mutations with wide-spread prevalence [**110**]. The seminal paper revealing KCNJ5 mutations as a common culprit in APAs [**86**] was followed by the identification of mutations in ATP1A1, ATP2B3

[**87**], CACNA1D and β-catenin [**88**]. Investigations into the prevalence of these mutations revealed the genetic basis of more than half of all APAs [**111**].

Notwithstanding its success in charactering genetics of surgically obtainable tumors, the methodology of exome sequencing is not well suited in the case of idiopathic bilateral hyperplasia, since the preferred method of MR antagonist treatment deprives researchers of large collections of adrenalectomy specimens to work on. Other shortcomings of the methodology is based on the fact that 99 % of the DNA, including regulatory sequences and miRNA sites, is left uncharacterized, as well as epigenetic modifications, which are known to be heritable across generations [**112**]. The exome datasets used to prepare the sequencing platforms do not always have to correlate with the actual transcriptome, which can be more faithfully analyzed by RNA sequencing techniques. As high throughput methods continue to develop, exome sequencing may presumably be supplanted by more advanced whole genome, epigenome and transcriptome probing technologies.

1.3.3. Genome-Wide Association Studies

Heritability of traits as a ratio of genetic variance to phenotypic variance has been put forth in the early twentieth century as the field of quantitative genetics was emerging [**113**]. Even though the value of twins in discerning effects of "nature versus nurture" was known for a long time [**114**], it took an additional fifty years, rediscovery of Mendelian genetics and an alumnus of LMU to successfully establish classical twin study [**115**]. In these studies phenotypic similarities are compared in both monozygotic and dizygotic twins; with any excess similarity in identical twins are attributed to greater genetic similarity and form the basis of an estimation of heritability [**116**]. Estimations of "narrow sense heritability" excluding non-additive genetic effects of epistasis, dominance and genotype-environment interactions, has been used as an indicator of the genetic contribution to phenotypic variation ever since [**117**].

Association of genetic variations with disease susceptibility is a long standing hypothesis dating back to initial observations of enzyme polymorphisms [**118**]. Although initially testing this hypothesis was limited by the availability of only a meager set of markers in the form of restriction fragment length polymorphisms; the advent of PCR enabled identification and utilization of short tandem repeats and single nucleotide polymorphisms in association studies. However, these early association studies, in general, overestimated the effect size of discovered associations and were largely non-reproducible [**119**]. Simultaneously, development of genetic maps [**120**] allowed linkage analysis studies to identify with great success the genetics of traits with Mendelian inheritance. As the penetrance of the phenotype decreases or when the trait is multifactorial as in most common

diseases or quantitative traits, typical genome-wide linkage analysis with a 10 cM resolution has yielded only limited success [121] (Fig 1.5). Even if linkage to a susceptibility locus was detected, a burdensome task of pinpointing the causal gene remained [122]. On the other hand, purely hypothesis driven method of candidate gene approach [123] has very low odds of hitting the spot among 30000 genes in the human genome, along with millions of gene variants [124]. In the case of PA, insufficiency of both approaches is evident in the Framingham Heart Study as neither genome-wide linkage analysis nor candidate gene association identified components of the estimated heritability [77].

This conundrum was overcome by advances on two fronts in the early 2000s as was foreseen by proponents of association studies [125]: Major innovations in genetics such as the completion of the Human Genome Project [126] and HapMap database of single-nucleotide polymorphisms (SNP) [127] presented scientists with dense genome-wide coverage of markers. Developments in DNA array technology in the last decade made "chips" a term of not only electronics and gastronomy, but biology as well [128]; thus enabling ever increasing number of simultaneous genetic tests with SNP arrays with affordability [129].

The observations of the large effect size of common ApoE-ε4 allele in late onset Alzheimer's [130] substantiated the "common disease-common variant" hypothesis, which states that "common alleles with frequencies over 1 % constitute the majority of the genetic risk for common disorders" [131]. Equipped with this theoretical groundwork and advances in high-throughput genotyping, and encouraged by early success stories from use of SNPs [132], researchers rapidly adopted the genome-wide association study (GWAS) method. In less than a decade, over 1751 GWA studies and 11912 SNP-trait associations were published [133]. Among these, numerous SNP-phenotype associations were reported for hypertension parameters of systolic and diastolic blood pressure [134-136]. Moreover, the power of GWA studies are immensely enhanced by implementation of genotype imputation methods [137] allowing for meta-analyses of multiple studies with various genotyping platforms, which often leads to identification of false negative associations that score below the typical threshold of $p<5x10^{-8}$ for genome-wide association in individual studies [138].

In spite of the relatively short time that has passed, findings from the first GWA study, associating age-related macular degeneration [139] are already giving rise to new therapeutic approaches [140; 141]. Translation of GWAS results to clinical strategies takes more time and effort in the case of metabolic or endocrine diseases. Rather than directly identifying therapeutic targets; the main value derived from these studies is new insights to etiology of the disorder at hand [142]. Considering that the estimated ARR heritability is quite substantial [77; 143], discovering the genetic components of

PA is a logical first step towards clinical advances. In this capacity, hypothesis-free methodology [144] of GWA studies and complementary functional research presents with a promising strategy in the quest for further understanding the pathophysiology of the disease [145].

Figure 1.5: Spectrum of allele frequency and effect size of variations. Top right set of variations gave credence to CDCV hypothesis. Effectiveness of linkage analysis and GWA studies are limited to region the within dotted lines. Bottom left group of variations possibly give rise to "missing heritability" phenomenon [XXX] (see in section 5.1) requires novel methodology to identify. Diagram obtained from Teri A. Manolio [146] (Rightslink license No: 3556991200117).

1.4. Objectives of the Study

The genetics of primary aldosteronism is experiencing a revitalized interest, as more and more pathophysiological causes are identified. Even in this age of discoveries, the majority of PA etiologies remain obscure, although readily available methodology being exhaustively utilized. Genome-wide association studies, despite its under-delivery of clinically meaningful markers, can help biologists by signaling potential loci to investigate. The combination of population genetics with *in vitro* and *in vivo* functional investigations was put to use in this study to elucidate novel genes of particular relevance to PA pathophysiology. The specific objectives of the study was to identify an aldosterone to renin ratio associated locus by genome-wide association study and exhaustively investigate the genes hosted therein as potential components of aldosterone biosynthesis and regulation by functional studies conducted in relevant model cell lines and animals.

2. Materials & Methods

2.1. Materials

2.1.1. Reagents

Material	Product Number	Company
10 % SDS-PAGE gel	456-1033	Bio-Rad
100 bp DNA Ladder	N3231S	New England Biolabs
3,3'-diaminobenzidine (DAB)	D4293	Sigma-Aldrich
ACTH (Synacthen)	480881	Novartis
Advanced DMEM/F12	12634	Gibco
Agarose	35-1020	PeqLAB
Aldosterone	A9477	Fluka
Angiotensin II	A9525	Fluka
Boric acid	100160	Merck-Millipore
Bovine Serum Albumin fraction V (BSA)	5482	Sigma-Aldrich
Bovine γ-Globulin	G5009	Sigma-Aldrich
Bromophenol blue	B0126	Sigma-Aldrich
Buffer RLT Plus lysis buffer	1053393	QiaGen
Calcium chloride (CaCl$_2$)	793639	Sigma-Aldrich
Calmidazolium	C3930	Sigma-Aldrich
Citric acid	251275	Sigma-Aldrich
Collagenase II	17101	Gibco
Complete protease inhibitor cocktail	11836153001	Roche
ddH$_2$O		Central Warehouse
Dexamethasone (Fortecortin)	H02AB02	Merck-Soreno
Dichloromethane	106050	Merck-Millipore
Diethylenetriaminepentaaceticacid (DTPA)	D6518	Sigma-Aldrich
Di-sodium hydrogen phosphate (Na$_2$HPO$_4$ x 2 H$_2$O)	71633	Fluka
DL-Dithiothreitol (DTT)	D0632	Sigma-Aldrich
DMEM/F-12	31330	Gibco
DNA Loading Dye, 6x	R0611	Fermentas
Edathamil (EDTA-Na$_2$)	E5134	Sigma-Aldrich
Eosin Y solution	HT110232	Sigma-Aldrich
Ethanol, absolute (EtOH)	108543	Merck-Millipore
Ethanol, technical (EtOH)		Central Warehouse
Ethidium Bromide (EtBr)	2218	Roth
Ethylene diamine tetraacetic acid (EDTA)	E6758	Sigma-Aldrich
Europium labeled streptavidin	1244-360	Perkin-Elmer
Fetal bovine serum (FBS)	10500064	Invitrogen
Forskolin	F3917	Sigma-Aldrich
Fura-2-AM ratiometric Ca^{2+} dye	F-1201	Invitrogen
Glacial acetic acid	137000	Merck-Millipore
Glucose	G0350500	Fluka
Glycerol	104092	Merck-Millipore

Glycine	104169	Merck-Millipore
GoTaq Green Master Mix	M7122	Promega
H_2O, sterile (Braun Aqua ad iniectabilia)		Central Warehouse
Hematoxylin	HHS32	Sigma-Aldrich
HEPES buffer	15630-049	Gibco
Hexadimethrine bromide	H9268	Sigma-Aldrich
HRP substrate Western Lightning Plus-ECL	NEL103E001EA	Perkin Elmer
Human M-CSF	216-MC-005	R&D Systems
Hydrocortisone	N/A	Pfizer
Hydrogen peroxide (H_2O_2)	107298	Merck-Millipore
Insulin–transferrin–selenium supplement (ITS)	41400	Gibco
Isoflurane	05260-05	Abbott
Isopropanol	100995	Merck-Millipore
KCl	104936	Merck-Millipore
KN-93	K1385	Sigma-Aldrich
Magnesium chloride ($MgCl_2$)	M8266	Sigma-Aldrich
Metafectene Pro transfection reagent	T040	Biontex
Methanol	106009	Merck-Millipore
Neomycin sulfate	A2198	AppliChem
Normal goat serum	005-000-001	Jackson Immuno Research
Normal human serum	31876	Thermo Scientific
PageRuler prestained protein ladder	26616	Thermo Scientific
Paraffin	107337	Merck-Millipore
Paraformaldehyde (PFA)	P6148	Sigma-Aldrich
Penicillin / streptomycin (Pen-Strep)	15140	Invitrogen
Permount	SP15-500	Fisher Scientific
Phenylmethanesulfonylfluoride (PMSF)	P2721	DiaSorin
Phosphate Buffered Saline (PBS) Dulbecco's	14190-094	Gibco
Phosphate Buffered Saline PBS	P4417	Sigma-Aldrich
PhosSTOP phosphatase inhibitor cocktail	4906845001	Roche
Poly-d-lysine	P7886	Sigma-Aldrich
Polyethylenglycol 10000 (PEG-10000)	821881	Merck-Millipore
Potassium carbonate (K_2CO_3)	104928	Merck-Millipore
Potassium-hydrogen-phthalate (KHP)	104874	Merck-Millipore
Puromycin	P9620	Sigma-Aldrich
Renin substrate, plasma from 5/6 nephrectomized rats	N/A	CharlesRiver
RIPA buffer	R0278	Sigma-Aldrich
RNase-free water	129112	Qiagen
RPMI 1640	61870	Gibco
shRNA control transduction particles	SHC202V	Sigma-Aldrich
shRNA SLC26A2 transduction particles	SHCLNV-NM_000112	Sigma-Aldrich
siRNA CSF1R specific	sc-29220	Santa Cruz
siRNA negative control	1022076	Qiagen
Skim milk powder	70166	Sigma-Aldrich

Sodium azide (NaN_3)	822335	Merck-Millipore
Sodium chloride (NaCl)	1064040500	Merck-Millipore
Sodium chloride, Braun NaCl 0.9 %		Central Warehouse
Sodium hydrogen carbonate ($NaHCO_3$)	137013	Merck-Millipore
Sodium lauryl sulfate (SDS)	L3771	Sigma-Aldrich
Sodium maleate	63260	Sigma-Aldrich
SsoFast EvaGreen RT-PCR master mix	172-5200	Bio-Rad
Thenoyltrifluoroacetone (TTFA)	T27006	Sigma-Aldrich
Tri-N-octylphosphinoxide (TOPO)	814868	Merck-Millipore
Tris-hydroxymethylaminomethane (TRIS base)	252859	Merck-Millipore
Trisodium citrate	S1804	Sigma-Aldrich
Triton X-100	X100	Sigma-Aldrich
TURBO DNase	AM2238	Ambion
Tween 20	P1379	Sigma-Aldrich
Tween 40	P1504	Sigma-Aldrich
Xylene	108661	Merck-Millipore

2.1.2. Commercial Kits

Material	Product Number	Company
BCA protein assay	23227	Thermo Scientific
Corticosterone EIA	AC-14F1	Immunodiagnostic Systems
ImmPRESS Anti-Mouse	MP-7402	Vector Laboratories
LIAISON Cortisol	13261	DiaSorin
LIAISON Direct Renin	310470	DiaSorin
RENCTK, angiotensin I RIA	P2721	DiaSorin
RevertAid First Strand cDNA Synthesis	K1621	Fermentas
RNeasy Plus Mini	74134	QiaGen
Vectastain Elite ABC	PK-6100	Vector Laboratories

2.1.3. Labwares

Material	Product Number	Company
Centrifuge tubes	Central Warehouse	Sarstedt
Hybond-P PVDF membranes	YA3236	Amersham
hydrophilic PTFE membranes	PICM01250	Merck-Millipore
Hyperfilm ECL photographic films	28-9068-36	GE Healthcare
Lignocel wood fibre bottom covering	C120	J.Rettenmaier & Söhne
Maxisorp microtiter plates	439454	Nunc
Micropipette tips	Central Warehouse	Sarstedt
QIAshredder spin-columns	79654	QiaGen
RNaseZap wipes	AM9786	Ambion
Scalpel	200170011	PFM
Standard pelleted chow	1314	Altromin
Standard pelleted food	2018	Harlan Laboratories

Super PapPen liquid blocker pen	MKP-1	G.Kisker
Superfrost Plus microscope slides	J1800AMNZ	Menzel
Tissuelyser 5 mm steel beads	69989	QiaGen
Vacutainer Li-heparin coated tubes	366664	BD Bioscience
Whatman filter paper	Central Warehouse	Schleicher & Schuell

2.1.4. Instruments

Material	Product Number	Company
Analog microscope camera	MPS52	Leica
Analytical balance	CPA225D	Sartorius
Automatic microtiter plate washer	M8/2R	TECAN
Centrifuge, benchtop	75005521	Heraeus
Centrifuge, benchtop	5415D	Eppendorf
Centrifuge, cell culture	Ultra 2S	Hettich
Centrifuge, swing-bucket rotor	5804R	Eppendorf
CO_2 incubator	HeraCell	Thermo Scientific
HeraSafe laminar flow hood	KS 15	Thermo Scientific
Inverted microscope	DM IL	Leica
LIAISON Analyser	9122290001	DiaSorin
Microplate absorbance reader	Sunrise	Tecan
Mini-PROTEAN II electrophoresis system	165-2940	Bio-Rad
Mx3000P qPCR system	401512	Stratagene
Nanodrop 1000 spectrophotometer	ND1000	Thermo Scientific
Phase-contrast microscope	DM2500	Leica
Photographic film developer	Curix 60	Agfa
Pipetboy acu 2 pipettor	155 000	Integra Biosciences
Pipetman micropipettes	F167500	Gilson
Powerpac 300 electrophoresis power supply	165-5050	Bio-Rad
Primus 25 Advanced thermocycler	95-4002	PeqLab
Rotary microtome	HM335E	Microm
Spin tissue processor	STP 120	Thermo Scientific
Stereo microscope	ES2	Leica
SubCell GT agarose electrophoresis system	170-4481	Bio-Rad
TissueLyser LT	85600	QiaGen
Trans-Blot SD semi-dry transfer cell	170-3940	Bio-Rad
UV gel imaging system	iX20	Intas
VICTOR fluorometer	1420	Perkin-Elmer
Vortex Genie	SI-0256	Scientific Industries
WALLAC DELFIA Plateshake horizontal shaker	1296-003	Perkin-Elmer
Wallac Wizard gamma-counter	1470	Perkin-Elmer

2.1.5. Antibodies

Material	Product Number	Company
Biotinylated goat anti rabbit IgG	BA-1000	Vector Laboratories
HRP conjugated goat anti-mouse IgG	31432	Pierce
HRP conjugated goat anti-rabbit IgG	31460	Pierce
Mouse anti human CYP11B2 antibody (CYP11B2-41-17B)	obtained from Celso Gomez-Sanchez [147]	
Mouse anti-aldosterone antibody	obtained from Celso Gomez-Sanchez [55]	
Mouse anti-β-Actin antibody	A5441	Sigma-Aldrich
Rabbit anti human SLC26A2 antibody	HPA041957	Sigma-Aldrich
Rabbit anti-phospho-CREB1 (pSer133) antibody	SAB4300040	Sigma-Aldrich
Rabbit-anti-mouse immunoglobulin	D0314	DAKO

2.1.6. Electronic Resources

DAVID database for annotation, visualization and integrated discovery [148]

Encode project DNA methylation [149]

Gene Ontology Project [150]

GNF Gene Expression Atlas 2 [151]

HapMap phase II [152]

ImageJ image processing program [153]

KEGG database [154]

PathVar microarray analysis of pathway expression variance [155]

PathVisio pathway drawing and pathway analysis tool [156]

Primer3 primer design program [157]

Prism 3.02 statistics (GraphPad Software)

PubMed [158]

Reactome pathway database [159]

RefSeq database [160]

TargetScan miRNA target prediction [161]

UCSC Genome Browser [162]

WikiPathways pathway database [163]

2.1.7. Cell Lines

Human principal collecting duct cells immortalized by SV4O virus [164]

Adrenocortical carcinoma cell line NCI-H295R [83] (ATCC CRL-2128)

2.1.8. Buffer Formulations

1 % agarose gel	1 % w/v agarose, 0.005 v/v EtBr in TBE
Citrate buffer	1.8 mM citric acid, 8.2 mM trisodium citrate, pH 6.0
Coating buffer	50 mM Na_2HPO_4 x 2 H_2O pH=7.4
DIN salt buffer	50 mM $NaHCO_3$, 9.56 mM NaCl, 1.35 mM K_2CO_3
Enhancement buffer	1 % v/v enhancement solution A, 10 % v/v enhancement solution B
Enhancement solution A	100 mM TTFA, 10 mM TOPO, 20 % v/v Triton X-100
Enhancement solution B	68 mM KHP, 6 % v/v Glacial acetic acid, pH 3.15
Erythrocyte lysis buffer	0.15 M NH_4Cl, 1 mM $KHCO_3$, 0.1 mM Na_2EDTA, pH 7.2
High calcium extracellular solution	5 mM glucose, 1 mM $MgCl_2$, 6.3 mM $CaCl_2$, 5 mM HEPES, and 5 mM KCl; pH 7.4
High potassium extracellular solution	5 mM glucose, 1 mM $MgCl_2$, 1.3 mM $CaCl_2$, 5 mM HEPES, and 20 mM KCl; pH 7.4
IHC CYP11B2 blocking solution	0.1 M Tris base, 0.5 % w/v SDS, pH 7.4
IHC CYP11B2 primary antibody buffer	0.1 M Tris base, 0.1 % v/v Tween 20, 20 % v/v human serum, pH 7.4
IHC SLC26A2 blocking buffer	5 % goat serum in blocking solution
IHC SLC26A2 blocking solution	3 % w/v BSA, 0.5 % v/v Tween 20
In house wash buffer	0.05 % v/v Tween 20 in PBS
LKC buffer	154 mM NaCl, 49.53 mM Tris base, 7.7 mM N_3Na, 0.01 % w/v Tween 40, 0.5 % w/v BSA, 0.05 % w/v Bovine γ-Globulin, 20 µM DTPA, pH 7.75
Maleate buffer	200 mM sodium maleate, 5 mM PMSF, 10 mM EDTA, 0.1 % w/v neomycin sulfate, pH=6.0
PFA solution	4 % PFA w/v in PBS
Ringer-type extracellular solution	137 mM NaCl, 5 mM glucose, 1 mM $MgCl_2$, 1.3 mM $CaCl_2$, 5 mM HEPES, and 5 mM KCl; pH 7.4
TBE	89.15 mM Tris base, 88.95 mM Boric acid, 2 mM EDTA-Na_2, pH=8.2
TBST buffer	20 mM Tris base, 125 mM NaCl, 0.1 % v/v Tween 20, pH 7.6
Tris-EDTA buffer	10 mM Tris base, 1 mM EDTA, 0.05 % v/v Tween 20, pH 9.0
WB 6X loading dye	350 mM Tris base, 10 % w/v SDS, 0.6 % w/v bromophenol blue, 30 % v/v glycerol, 600 mM DTT, pH 6.8
WB blocking buffer	5 % w/v skim milk powder in TBST
WB running buffer	25 mM Tris base, 200 mM glycine, 0.1 % w/v SDS
WB transfer buffer	25 mM Tris base, 200 mM glycine, 20 % v/v methanol

2.2. Genome-Wide Association Study

A genome-wide association study was performed on the participants of the population-based Cooperative Health Research in the Region of Augsburg (KORA) study of the Helmholtz Zentrum München [165]. 4261 subjects participated in the baseline S4 study, with 3080 of these further participating in the 7-year follow-up F4 survey. The study was conducted with written informed consents of all participants and approval of the ethics committee of the Bavarian Medical

Association. 10 hours fasting venous blood samples were obtained between 07:30 and 10:30 in a seated position from the F4 cohort subjects [166]. Blood samples were stored at -80°C after centrifugation. Plasma aldosterone concentration was assayed as described in section 3.3.1 by Jenny Manolopoulou and Ariadni Spyroglou (Medizinische Klinik und Poliklinik IV, University of Munich). Plasma renin concentration was measured using an automated chemiluminescence immunoassay (LIAISON Direct Renin, Germany) by the group of Martin Bidlingmaier (Medizinische Klinik und Poliklinik IV, University of Munich). Participants with a renin or aldosterone concentration of more than 1000 ng/L were excluded from the study. Single-nucleotide polymorphism genotyping of 1814 individuals from the cohort was accomplished with Affymetrix Genome-Wide Human SNP 6.0 arrays in accordance with the manufacturer's instructions by Rajesh Rawal and Christian Gieger (Institute of Genetic Epidemiology, Helmholtz Zentrum München). Birdseed2 clustering algorithm [167] was used in genotype determination. Positive and negative control DNA was applied every 96 samples for quality control purposes. Average genotyping efficiency was 98 % per chip after excluding subjects with less than 93 % overall genotyping efficiency. Genotype imputation with IMPUTE v0.4.2 [168] based on HapMap phase II [152] resulted in a total of ~2.7 million directly genotyped or imputed single-nucleotide polymorphisms. 28 individuals under hypertensive treatment were excluded as interference of anti-hypertensive agents with ARR screening is well documented [169; 170]. Analysis of genome-wide association between genotyped and imputed markers and aldosterone to renin ratios was performed on the remaining 1786 subjects, using a linear regression model adjusting for age and sex.

2.3. Animal Experiments

Mouse necropsy was performed for harvesting murine tissues to profile gene expression levels. All animal studies were performed according to protocols examined and approved by the Regierung von Oberbayern (Az. 55.2-1-54-2531-36-07, 55.2-1-54-2531-134-07) and according to the German Animal Protection Law. Three female C3HeB/FeJ mice from the same litter were raised in the animal house of the Medizinische Klinik und Poliklinik IV. Mice were kept on a 12 hours light / dark circle in an ambient temperature of 25±2°C with relative humidity of 60±5 %, in standard mouse cages (15 cm x 27 cm x 42 cm) with wood fibre bottom covering (Lignocel Fa. J.Rettenmaier & Söhne). They were fed with standard pelleted chow #1314 (Altromin, Lage, Germany), *ad libitum* with free access to tap water. The chow diet was composed of 22.5 % crude protein, 5 % crude fat, 4.5 % crude fibre, 6.5 % crude ash. At 12 weeks of age, animals were euthanized by isoflurane inhalation (Forene, Abbot). Adrenal glands, kidneys, lungs, heart, lean muscles, spleen, brain, fat and ovaries were collected. Adrenal glands were cleaned of adjacent fat with a stereo microscope. All collected tissues were immediately snap frozen in liquid nitrogen and stored at -80°C until further processing.

Stimulation and suppression of aldosterone production in mice were previously performed by Ariadni Spyroglou, Medizinische Klinik und Poliklinik IV, University of Munich [**42**]. 12-week-old female C3HeB/FeJ mice were given either intraperitoneal injections of 0.2 nmol angiotensin II (Fluka, Taufkirchen, Germany), 50 µl/g NaCl 0.9 % (B Braun, Melsungen, Germany) or 2 % KCl in water ad libitum. For each treatment, mice were euthanized by isoflurane inhalation at various time points (for angiotensin II and NaCl injections, 10, 20, 30, 40, 60 and 120 minutes; for KCl, 1, 4 and 7 days) with five mice per time point in addition to baseline group receiving no treatment. Adrenal glands were cleaned of adjacent tissue, snap frozen and stored at -80°C.

Adrenal glands and plasma samples of SLC26A2 knock-in mutant mice were obtained from Antonio Rossi, Department of Molecular Medicine, University of Pavia. Animal studies were performed according to protocols examined and approved by the Animal Care and Use Committee of the University of Pavia. Generation of this mouse model was previously described [**171**]. Briefly, the A386V substitution found in a non-lethal form of DTD was introduced via a targeting vector into AB1 ES cells. Male chimeras were generated by injecting recombinant ES cells in BDF1x C57Bl/6J mouse blastocysts, which were in turn mated with C57Bl/6J females to yield heterozygous animals. Through subsequent breeding, homozygous mutants were generated.

Wild type and homozygous *Slc26a2* mutant mice were grown in a pathogen-free animal facility with ambient temperature of 25±2°C, relative humidity 60±5 %, and a 12h-12h light-dark circle, fed with standard pelleted food #2018 (Harlan Laboratories, Udine, Italy) *ad libitum* with free access to tap water. Mice were sacrificed at 8 weeks of age. Adrenal glands of wild type (7 males and 9 females) and mutant (11 males and 4 females) were cleaned of adjacent tissue and snap frozen for RNA extraction. Trunk blood for hormone assays and adrenals glands for histology experiments were collected from another set of animals (5 male and 5 female wild types, 4 male and 5 female mutants). 0.25 ml of blood from each animal was collected to Li-heparin coated tubes and centrifuged (10000 x *g*, 10 min) to obtain plasma, stored at -20°C. Adrenal samples were fixed in 4 % formaldehyde solution overnight at 4°C and subsequently embedded in paraffin.

2.4. Hormone Assays

2.4.1. Aldosterone Measurement

Aldosterone concentrations in plasma samples and cell culture supernatant were measured by an in-house developed fluorescence immunoassay [**172**]. In principle, sample aldosterone and a biotinylated aldosterone tracer binds competitively to anti-aldosterone antibody on coated microtiter plates. Bound tracer is detected by addition of Europium labeled streptavidin.

Microtiter plates are coated in two steps for the assay. Polyclonal rabbit-anti-mouse immunoglobulin is diluted in coating buffer to yield 300 ng per well and incubated overnight at 4°C. Incubation is followed by 3X wash with an in house wash buffer. Anti-aldosterone antibody produced in mouse as previously described [147] is diluted 1:200000 in LKC buffer and added to the wells, incubating overnight at 4°C, after which the plates were ready for the assay. A standard curve is prepared by diluting 10 mg/ml aldosterone in ethanol down to several concentrations between 10 pg/ml and 2000 pg/ml in DIN salt buffer. Control samples were obtained by pooling mouse samples with low (50 pg/ml) or high (200 pg/ml) plasma aldosterone concentration. Biotinylated aldosterone tracer was prepared previously as per described methods [173].

Cell culture supernatant was directly used in the assay, whereas aldosterone from plasma samples were extracted by adding 1 ml of 50 mg/L polyethylene glycol 10000 in dichloromethane solution to 50 µl of sample and 30 minutes of low speed vortexing. The organic phase was separated and evaporated, reconstituted with 175 µl 5.9 % methanol in DIN salt buffer, yielding four-fold dilution of the original sample. 50 µl of the sample was added to assay plate wells, along with 5 pg / 100 µl tracer in LKC buffer, incubating overnight at 4°C. After incubation, wells were washed 3X, 200 µl europium labeled streptavidin diluted 1:1000 in LKC buffer was added for 30 minutes at room temperature. Following a 6X wash, wells were incubated with 200 µl of enhancement buffer for 15 minutes at room temperature and fluorescence of biotinylated aldosterone was measured by a fluorometer (VICTOR, Perkin-Elmer), calculating concentration through use of standard curve generated from the on-plate standard concentration points.

2.4.2. Plasma Renin Activity Assay

Plasma renin activity of mouse plasma samples were measured by a commercial angiotensin I radioimmunoassay kit (RENCTK, Diasorin) using nephrectomized rat plasma as substrate, with a modified protocol [101]. Reaction mixes were set up containing 50 µl probe diluted with maleate buffer, 22.2 µl rat renin substrate from bilaterally nephrectomized male rats diluted 1:3 with maleate buffer, 27.7 µl of the generation buffer and 2 µl PMSF. Mixture was divided into two 51 µl volumes, incubated 90 minutes on ice or in a 37°C water bath. 45 µl of each was incubated for 23 hours at room temperature in RIA coated tubes along with the calibrators. Tubes were then aspirated and radioactivity was measured with a gamma counter. Renin activity in ng/(ml*hour) units were calculated as per the formula provided by the kit's instructions.

2.4.3. Cortisol Measurement

Cortisol concentrations of cell culture supernatants were measured using a commercial kit (LIAISON

Cortisol, Diasorin) as per kit instructions by Philipp Grimminger, Medizinische Klinik und Poliklinik IV, University of Munich. Unused cell culture media was initially tested for cross-reactivity, and measurements were performed with a LIAISON Analyzer (Diasorin).

2.4.4. Corticosterone Measurement

Corticosterone concentrations of mouse plasma samples were assayed with a commercial enzyme immunoassay kit (Corticosterone EIA, Immunodiagnostic Systems) as per manufacturer's instructions. 30 µl of plasma per animal was used. Absorbance of each well at 450 nm was measured with a microplate reader (Sunrise, Tecan). Concentrations were calculated from absorbance values using formula provided with the kit's instructions.

2.5. Cell Culture

All culture cells were grown in sterile conditions in a humidified atmosphere (95 % CO_2). Media compositions for individual cell types were as follows:

Human principal collecting duct cells immortalized by SV4O virus: (cell line generated by Domiqiue Prie and colleagues at INSERM, Paris [164], obtained from Wolfgang Neuhofer, Department of Physiology, University Clinic Munich): DMEM/F-12 (Gibco #31330) supplemented with 2 % fetal bovine serum (Invitrogen #10500064), 1 % insulin–transferrin–selenium supplement (Gibco #41400), 1 % penicillin / streptomycin (Invitrogen #15140), and 50 nM dexamethasone (Merck-Soreno). Cells were passaged weekly with a seeding ratio of 1:10. Cells with passage numbers between 5 and 15 were used for experiments.

Adrenocortical carcinoma cell line NCI-H295R [83] (American Type Culture Collection, #CRL-2128): RPMI 1640 medium (Gibco #61870) supplemented with 10 % fetal bovine serum (Invitrogen #10500064), 1 % insulin–transferrin–selenium supplement (Gibco #41400), 1 % penicillin / streptomycin (Invitrogen #15140), and 100 nM hydrocortisone (Pfizer). Cells were passaged weekly with a seeding ratio of 1:7. Cells with passage numbers between 15 and 25 were used for experiments.

Primary culture of human adrenal gland cells: Use of human tissue samples for this study was approved by the Ethics Commission of Klinikum der Universität München (Project No: 379-10; 17.01.2011). Surgically obtained human adrenal gland tissue was treated with collagenase II (1 mg/ml, Gibco #17101) and erythrocyte lysis buffer (150 mM NH_4Cl, 1 mM $KHCO_3$, 0.1 mM Na_2EDTA, pH 7.2). Cells were cultured in Advanced DMEM/F12 media (Gibco #12634) supplemented with 10 % fetal bovine serum (Invitrogen #10500064) and 1 % penicillin / streptomycin (Invitrogen #15140).

Cells were kept in culture for 7 days before experiments.

2.5.1. siRNA Mediated CSF1R Expression Knockdown

NCI-H295R cells were seeded with 200000 cells per well in 24-well plates, and incubated 24 hours after seeding. Metafectene Pro transfection reagent (Biontex # T040) was used as per manufacturer's instructions to transfect scrambled negative control siRNA (Qiagen #1022076) or CSF1R specific siRNA (Santa Cruz #sc-29220), with 200 pmol siRNA and 6.25 µl transfection reagent per well. Cells were incubated with the transfection complex for six hours. Cell media were renewed, and cells and culture supernatant was harvested for expression and hormone analysis 2 days after transfection.

2.5.2. CSF1 Stimulation

200000 NCI-H295R cells per well were seeded in 24-well plates and incubated for 24 hours. Media was replaced, with the fresh media containing 0, 16, 80, 400, 2000, 10000 or 50000 pg/ml recombinant human M-CSF (R&D Systems #216-MC-005). After 24 hours of incubation with M-CSF, media supernatant was harvested for aldosterone measurement.

Human primary adrenal gland cells, seeded at 10000 cells per well in 48-well plates 7 days prior to experimentation, were given fresh media containing 0, 10 or 100 ng/ml M-CSF. After 24 hours of incubation, the supernatant was collected for aldosterone measurement.

2.5.3. shRNA Mediated Knockdown of SLC26A2

Knockdown of SLC26A2 expression in NCI-H295R and cortical collecting duct cells are achieved with lentiviral transduction of non-targeting control (Sigma Mission SHC202) and SLC26A2 specific shRNA expression vectors (Sigma Mission #SHCLNV-NM_000112). A set of five shRNA sequences expressed by the TRC2-pLKO-puro Vector were used, with the clone of highest silencing efficacy being selected for further experiments (Table 2.1).

Protocol for transduction of the viral particles was obtained from The RNAi Consortium. For both NCI-H295R and cortical collecting duct cells, the same procedure was used, aside from the initial number of cells seeded. 10000 NCI-H295R cells or 5000 collecting duct cells per well were seeded in 96-well plates in their respective normal growth media. After being let grow for 24 hours, cell media was refreshed, with the addition of 2 µg/ml hexadimethrine bromide (Sigma #H9268). Lentiviral particles were added to cells with a multiplicity of infection of 10, and plates were centrifuged at 700x g for 30 minutes at 37°C. Media was changed after overnight incubation, and 48 hours after transduction, selection of recombinant cells with 7 µg/ml puromycin (Sigma #P9620) was initiated.

Cells were grown under selective pressure for three passages, after which antibiotic was applied at every third passage. After the third passage, samples from each clone were assayed for SLC26A2 expression.

TRC Number	Targeted Region	Clone ID	Sequence
TRCN0000285035	CDS	NM_000112.3-2344s21c1	CCGGTTCCCTAACCAACGGAGAATACTCGAGTATTCTCCGTTGGTTAGGGAATTTTTG
TRCN0000273694	CDS	NM_000112.3-1262s21c1	CCGGCCGATTCCTATTGAACTTGTTCTCGAGAACAAGTTCAATAGGAATCGGTTTTTG
TRCN0000273695	CDS	NM_000112.3-1091s21c1	CCGGCTCAACCTTCCTCGGACTAATCTCGAGATTAGTCCGAGGAAGGTTGAGTTTTTG
TRCN0000273644	3' UTR	NM_000112.3-4199s21c1	CCGGGCCCTTTCTATCCAGCCTTATCTCGAGATAAGGCTGGATAGAAAGGGCTTTTTG
TRCN0000273646	CDS	NM_000112.3-1417s21c1	CCGGTGTAGATGCAATAGCTATTTCCTCGAGGAAATAGCTATTGCATCTACATTTTTG

Table 2.1: shRNA clones and coding sequences targeting SLC26A2.

2.5.4. Aldosterone Stimulation of Collecting Duct Cells

Wild type or lentivirally transduced (targeting and non-targeting) collecting duct cells were seeded in 24-well plates with a density of 50000 cells per well in normal growth media. After 48 hours of growth, cells were switched to DMEM/F-12 without supplements or serum. Following 18 hours of serum starvation, 1 µM of aldosterone (Fluka) was given in fresh DMEM/F-12, and incubated for 24 hours. Cells were then harvested for RNA extraction.

2.5.5. Steroidogenic Stimulation or Suppression of NCI-H295R Cells

Wild type or lentivirally transduced (targeting and non-targeting) NCI-H295R cells were seeded in 24 well plates at 200000 cells per well and grown for 48 hours. For stimulation or suppression of aldosterone production, cells were given fresh media containing 10 mM KCl (Merck #104936), 100 nM angiotensin II (Sigma #A9525), 2 µM ACTH (Novartis #480881), 10 µM Forskolin (Sigma #F3917), 3 µM calmidazolium (Sigma #C3930) or 3 µM KN-93 (Sigma #K1385). Cells were incubated for 24 hours, after which cell culture supernatant and cells were harvested for hormone, gene expression and protein assays.

Stimulation experiments were repeated under serum-starved conditions for simultaneous assaying of cortisol and aldosterone production of NCI-H295R cells. After seeding and initial growth of 48 hours, cells were incubated with serum and additive-free media for 24 hours, followed by

application of 10 mM KCl, 100 nM angiotensin II, 10 µM Forskolin for 48 hours before harvesting cells and supernatant.

2.5.6. Steroidogenic Stimulation of Primary Adrenal Cells

Human primary adrenal gland cells, seeded at 10000 cells per well in 48-well plates 7 days prior to experimentation, were given fresh media containing 10 mM KCl, 100 nM angiotensin II or vehicle. After 24 hours of incubation, cells were lysed for RNA purification.

2.5.7. Quantification of Intracellular K^+, Na^+ and Cl^- Concentrations

Wild type or lentivirally transduced (targeting and non-targeting) cells were seeded on poly-D-lysine (Sigma # P7886) coated hydrophilic PTFE membranes (Millipore #PICM01250) in 24-well plates with a seeding ratio of 100000 collecting duct cells per well or 250000 NCI-H295R cells per well and grown for 48-hours in their respective normal growth media. Cells were then transferred to the facilities of Dr. Wolfgang Neuhofer (Department of Physiology, University Clinic Munich), who proceeded with shock freezing, cryosection preparation and electron microprobe analysis, as described before [**174**]. Briefly, after cells were grown into a confluent monolayer, filters were covered with a thin layer of 20 % w/v BSA containing growth media and frozen with -196°C 3:1 v/v propane-isopentane mixture. 1 µm cryosections were prepared and freeze-dried. Electron microprobe analysis with an energy dispersive X-ray detector equipped scanning electron microscope and subsequent quantification was performed by previously established procedure [**175**].

2.5.8. Quantification of Intracellular Ca^{2+} Concentration in NCI-H295R Cells

Intracellular Ca^{2+} concentrations of lentivirally transduced control and SLC26A2-knockdown NCI-H295R cells were measured in the laboratory of Richard Warth (Medical Cell Biology, University of Regensburg) [**176**]. Briefly, cells grown on cover slips were loaded with 50 µM fura-2-AM ratiometric Ca^{2+} dye for 30 minutes at 37°C. Either Ringer-type (137 mM NaCl, 5 mM glucose, 1 mM $MgCl_2$, 1.3 mM $CaCl_2$, 5 mM HEPES, and 5 mM KCl; pH 7.4) or high calcium or potassium (same as Ringer-type except for NaCl replaced with 5 mM $CaCl_2$ or 15 mM KCl) extracellular solutions were used. Mean fluorescence values for single cells were calculated after measurements with a filter wheel–based imaging system (Universal Imaging Corporation) mounted on an inverted microscope (Zeiss, Axiovert 200) at 37°C.

2.6. Histological Procedures

Use of human tissue samples for this study was approved by the Ethics Commission of Klinikum der

Universität München (Project No: 379-10, 17.01.2011).

2.6.1. Paraffin Embedding of Tissue Samples

Human and murine tissue samples for histology experiments were fixed immediately after collection in 4 % PFA solution overnight at 4°C. Tissues were then washed with PBS and dehydrated, cleared and infiltrated with paraffin by a spin tissue processor (Thermo Scientific #STP 120) (1X 30 % EtOH, 1X 70 % EtOH, 1X 80 % EtOH, 1X 96 % EtOH, 3X 100 % EtOH, 2X Xylene, 2X liquid paraffin at 60°C). Samples were then embedded in paraffin blocks. 4 μm sections were cut by a microtome and slides were left to dry overnight at room temperature.

2.6.2. Hematoxylin and Eosin Staining

Slides were dewaxed and rehydrated with 2x3 min Xylene, 2x3 min 100 % EtOH, 2x3 min 95 % EtOH, 3 min ddH$_2$O. 3 seconds of hematoxylin (Sigma #HHS32) staining was immediately followed by rinsing briefly with ddH$_2$O, then under running tap water for one minute. After rinsing with ddH$_2$O, slides are counterstained for 10 seconds with 0.5 % glacial acetic acid containing eosin Y solution (Sigma #HT110232). Slides were dehydrated (2x30 sec 95 % EtOH, 2x30 sec 100 % EtOH, 2x30 sec Xylene) and mounted with Permount (Fisher #SP15-500)

2.6.3. Immunohistochemistry

Paraffin embedded human adrenal and aldosterone producing adenoma sections were stained with polyclonal rabbit anti human SLC26A2 antibody (Sigma-Aldrich #HPA041957) or monoclonal mouse anti human CYP11B2 antibody (CYP11B2-41-17B) obtained from Celso Gomez-Sanchez (Endocrinology, University of Mississippi Medical Center) [55]. Paraffin embedded murine adrenal sections were stained with a polyclonal rabbit anti mouse SLC26A2 antibody (Sigma #SAB2106645). Two different protocols were used for immunohistochemistry of SLC26A2 and CYP11B2:

SLC26A2 Staining: Slides were rehydrated (2X 5 min xylene, 2X 5 min 100 % EtOH, 2X 5 min 95 % EtOH, 2X 5 min ddH$_2$O) and heat induced epitope retrieval with citrate buffer (1.8 mM citric acid, 8.2 mM trisodium citrate, pH 6.0) was applied. Endogenous peroxidases were blocked with 0.3 % H$_2$O$_2$ in PBS for 10 minutes. Samples were incubated with a blocking buffer composed of 5 % goat serum in blocking solution (3 % BSA w/v, 0.5 % Tween 20 v/v) for 30 minutes at room temperature, followed by overnight incubation at 4°C with primary antibody diluted in blocking buffer (1:40 for Sigma #HPA041957; 1:200 for Sigma #SAB2106645). After a 15 minute wash with PBS, biotinylated goat anti rabbit IgG (Vector Laboratories #BA-1000) diluted 1:200 in blocking buffer was applied for 30 minutes at room temperature. For visualization of bound antibody complex, Vectastain Elite ABC kit (Vector Laboratories #PK-6100) was used as per manufacturer's instructions, staining sections with

3,3'-diaminobenzidine (Sigma #D4293) for 1 to 5 minutes. Slides were washed with PBS, counterstained with hematoxylin, dehydrated (2X 1 min 95 % EtOH, 2X 1 min 100 % EtOH, 2X 5 min Xylene) and mounted with Permount.

CYP11B2 Staining: Rehydration (2X 10 min Xylene, 2X 2 min 2-propanol, 2 min 95 % EtOH, 2 min 70 % EtOH, 2 min 30 % EtOH, 5 min ddH$_2$O) and heat induced epitope retrieval with Tris-EDTA buffer (10 mM Tris, 1 mM EDTA, 0.05 % Tween 20, pH 9.0) was applied to the sections. Endogenous peroxidases were blocked with 0.3 % H$_2$O$_2$ in methanol for 10 minutes. Samples were incubated with a blocking buffer composed of 20 % normal human serum (Thermo Scientific # 31876) in blocking solution (0.1 M Tris, 0.5 % SDS, pH 7.4) for 1 hour at room temperature, followed by overnight incubation at 4°C with primary antibody (CYP11B2-41-17B) diluted 1:200 in primary antibody buffer (0.1 M Tris, 0.1 % Tween 20, 20 % human serum, pH 7.4). After a 25 minute wash with PBS, ImmPRESS Anti-Mouse Kit (Vector Laboratories #MP-7402) was applied according to manufacturer's protocol. Sections were stained with 3,3'-diaminobenzidine for 2 to 20 minutes and counterstained with hematoxylin, followed by dehydration (2 min 30 % EtOH, 2 min 70 % EtOH, 2 min 95 % EtOH, 2X 2 min 2-propanol, 2X 10 min Xylene) and mounting with Permount.

2.7. Western Blot

Protein extraction and quantification: Cells in 24-well plates were harvested for protein by washing 2X with ice-cold PBS and directly adding RIPA buffer (Sigma #R0278) supplemented with protease (Roche #11836153001) and phosphatase inhibitor cocktails (Roche #04906845001). Cells were lysed on ice for 15 minutes while shaking at 300 rpm, scraped from wells, collected to tubes and centrifuged at 13000 rpm for 10 minutes at 4°C. Supernatant was stored at -80°C after aliquoting to minimize freeze-thaw cycles. Protein concentration was quantified with BCA protein assay (Thermo Scientific #23227) according to supplied protocol. BSA standards (Sigma #05482) between 0.0625 and 2 mg/ml were prepared in the same matrix as protein samples. Concentrations were calculated based on absorbance measurements at 562 nm with a microplate reader (Sunrise, Tecan).

Protein samples were diluted to a uniform 1 µg/µl concentration. Samples were denatured by adding an 6X SDS containing loading dye (350 mM Tris, 10 % SDS, 0.6 % bromophenol blue, 30 % glycerol, 600 mM DTT, pH 6.8) and incubating @95°C for 5 min. 20 µg of each sample was symmetrically loaded to two 10 % SDS-PAGE gels (Bio-Rad #456-1033) along with PageRuler prestained protein ladder (Thermo Scientific #26616). The gels were run for 25 minutes under 250 V in the Mini-PROTEAN II electrophoresis system (Bio-Rad) with 1X running buffer (25 mM Tris, 200 mM glycine, 0.1 % SDS). Size-separated protein on gels were transferred to methanol activated Hybond-P PVDF membranes (Amersham # YA3236) in the Trans-Blot SD semi-dry transfer cell (Bio-

Rad) in a "wet sandwich" of filter papers soaked in transfer buffer (25 mM Tris, 200 mM glycine, 20 % methanol) under 15 V for 45 minutes. The membranes were blocked with 5 % skim milk powder (Sigma #70166) in TBST buffer (20 mM Tris, 125 mM NaCl, 0.1 % Tween 20, pH 7.6) for 1 hour. Rabbit anti-phospho-CREB1 (pSer133) antibody (Sigma #SAB4300040) was diluted 1:1000; mouse anti-β-Actin antibody (Sigma #A5441) was diluted 1:5000 in blocking buffer. Each membrane was incubated with a primary antibody overnight at 4°C. After 1 hour TBST wash and 15 minute blocking, membranes were incubated with HRP conjugated secondary antibodies diluted 1:5000 in blocking buffer (goat anti-mouse IgG, Pierce #31432; goat anti-rabbit IgG, Pierce #31462). Detection was achieved by soaking the membranes with HRP substrate Western Lightning Plus-ECL (Perkin Elmer, #NEL103E001EA) and capturing the resulting chemiluminescence on Hyperfilm ECL photographic films (GE Healthcare #28-9068-36) and subsequent development of the film with Curix 60 developer (Agfa). Developed films were scanned with 2400 dpi resolution, and band intensities were quantified by ImageJ image processing program [**153**] as described previously [**177**].

2.8. Gene Expression Analyses

2.8.1. RNA Purification and Reverse Transcription

Purification of total RNA from tissue and cell culture samples were accomplished using silica column binding based methodology of RNeasy Plus Mini Kit (Qiagen #74134). Prior to extraction of RNA, working space was cleared of RNase contamination using RNaseZap wipes (Ambion #AM9786). Surgically obtained human tissue samples and murine tissues from sacrificed animals were weighed in centrifuge tubes before freezing in liquid nitrogen. Frozen tissues were cut down to below 30 mg pieces with a surgical knife on dry ice without letting thaw. In case of small tissue samples of murine adrenal glands and murine ovaries, both tissues from the same animal were processed together. Tissues were homogenized in lysis buffer using TissueLyser LT (Qiagen #85600) bead mill system with 5 mm steel beads. Cells from cell culture experiments were twice washed with ice cold PBS, and lysed directly by adding lysis buffer, and homogenized using QIAshredder spin-columns (Qiagen #79654). Subsequent treatments of homogenized lysates until elution in RNase-free water were according to instructions of RNeasy Plus Mini Kit.

Concentration and purity (260 / 280 and 260 / 230 nm absorbance ratios) of eluted samples were determined with Nanodrop 1000 spectrophotometer (Thermo Scientific). Integrity of the RNA was ensured by observation of sharp 18S and 28S RNA bands after 1.5 % agarose gel electrophoresis. DNA contamination in purified RNA was controlled by a PCR reaction using the primers for genomic human beta-actin (5'-TCATGAAGTGTGACGTGGACATCC-3' & 5'-CCTAGAAGCATTTGCGGTGGACGATG-3') or murine CYP11B2 (5'-TGCATGGCATGGTATCAATC-3' & 5'-CATCCGTCTTCCTTTTTCCA-3') with

GoTaq Green Master Mix (Promega #M7122) with recommended reaction (0.4 µM primers, 1 µl template in 25 µl total volume) and thermocycler conditions (2 min 95°C initial denaturation; 35 cycles of 30 sec 95°C, 45 sec 60°C, 45 sec 72°C; 5 min 72°C final extension) in a Primus 25 Advanced thermocycler (Peqlab #95-4002). In the case of observable DNA contamination, RNA samples were treated with TURBO DNase (Ambion #AM2238) as instructed by manufacturer.

2.8.2. Quantitative Real-Time Polymerase Chain Reaction

Purified total RNA was reverse transcribed with RevertAid First Strand cDNA Synthesis Kit (Fermentas #K1621) using oligo(dT)$_{18}$ primers according to kit instructions (1 µg RNA per 20 µl reaction). Gene expression levels were quantified by Mx3000P quantitative polymerase chain reaction system (Stratagene #401512). Amplification reactions were set up in duplicates using SsoFast EvaGreen RT-PCR master mix (Bio-Rad #172-5200) with 400 nM of each primer in 12 µl total volume and ran with a 2-step amplification program consisting of 3 minute initial denaturation at 95°C, 40 cycles of 10 seconds denaturation at 95°C followed by annealing / extension at primer melting temperature. At the end of amplification, a melting curve was generated by incremental fluorescence readings with 0.5°C steps from 55°C to 95°C. Primers were designed using reference sequences from RefSeq database [160] with the aid of Primer3 oligonucleotide design tool [157]. Primer sequences and melting temperatures are listed in table 2.2. For each primer pair, amplification efficiency was determined using serial dilutions of target tissue or cell cDNA. Only primers with amplification efficiencies between 1.90 and 2.05 were used. Primer specificity was confirmed by the amplification product size via 1 % agarose gel electrophoresis. A calibrator was prepared by pooling all samples of each assay, and expression level of target gene in each sample was calculated relative to this calibrator. Target gene expression levels were normalized by HPRT1 in human adrenal tissues and NCI-H295R cells, 18S RNA in human collecting duct cells and *Actb* in murine tissues. Normalized gene expression levels are presented as percentages of control samples.

Quantification of SLC14A2 expression in collecting duct cells was carried out by Wolfgang Neuhofer (Department of Physiology, University Clinic Munich) by RT-PCR.

2.8.3. Microarray Analyses

Transcriptome analysis and KCNJ5, ATP1A1 and ATP2B3 mutations genotyping of 91 aldosterone producing adenoma and 11 control adrenal samples along with were conducted by the research group of Maria-Christina Zennaro (Institut National de la Santé et de la Recherche Médicale, Paris). Samples were collected from patients of the Hypertension Unit at Hôpital Européen Georges Pompidou in Paris between 1994 and 2008, with approval from local ethics committee.

Methodology of sample phenotyping, microarray hybridization and data analysis were described previously [110].

Gene (Accession)	Species	Strand	Sequence (5' > 3')	Annealing Temperature
CAMK1 (NM_003656.4)	human	fwd	CATCGCCTACATCTTGCTCTG	60°C
		rev	TTCTTCTTGATCTGCTCACTCAC	
CYP11B1 (NM_000497.3)	human	fwd	GGGTGGCCTACAGACAACATC	60°C
		rev	GGCGACAGCACTTCTGGATT	
CYP11B2 (NM_000498.3)	human	fwd	ACTCGCTGGGTCGCAATG	60°C
		rev	AGTGTCTCCACCAGGAAGTGC	
HPRT1 (NM_000194.2)	human	fwd	TGCTGACCTGCTGGATTACA	60°C
		rev	CCTGACCAAGGAAAGCAAAG	
HSD3B1 (NM_000862.2)	human	fwd	AGAAGAGCCTCTGGAAAACACATG	60°C
		rev	TAAGGCACAAGTGTACAGGGTGC	
HSD3B2 (NM_000198.3)	human	fwd	AGAAGAGCCTCTGGAAAACACATG	60°C
		rev	CGCACAAGTGTACAAGGTATCACCA	
NFAT5 (NM_138714.3)	human	fwd	TCAGCTTACCACGGACAACA	60°C
		rev	ATGGCCTTCCAGCTTTACTGT	
NR4A1 (NM_002135.4)	human	fwd	TCGGGGATACTGGATACACC	60°C
		rev	TGTTCGGACAACTTCCTTCA	
NR4A2 (NM_006186.3)	human	fwd	AGTCTGATCAGTGCCCTCGT	60°C
		rev	CTGGGTTGGACCTGTATGCT	
SCNN1A (NM_001038.5)	human	fwd	CAACCAGGTCTCCTGCAAC	60°C
		rev	GGGTTTCCTTCCTCATGCT	
SLC26A2 (NM_000112.3)	human	fwd	CAATGCCCATAGTGCTCCTT	60°C
		rev	ATCCACTCAGCAAGGCATCT	
Actb (NM_007393.3)	mouse	fwd	ACCCGCGAGCACAGCTTCTT	60°C
		rev	TCTGGGCCTCGTCACCCACATA	
Cyp11a1 (NM_019779.3)	mouse	fwd	GCTGGAAGGTGTAGCTCAGG	60°C
		rev	CACTGGTGTGGAACATCTGG	
Cyp11b2 (NM_009991.3)	mouse	fwd	CAGGGCCAAGAAAACCTACA	60°C
		rev	ACGAGCATTTTGAAGCACCT	
Hsd3b1 (NM_008293.3)	mouse	fwd	AAGGAGGAATTCTCCAAGCTG	60°C
		rev	GAGCTGCAGAAGATGAAGGC	
Hsd3b6 (NM_013821.3)	mouse	fwd	ATCAGAACCAGCCATTCCAA	60°C
		rev	AAAACCCTCCTGCTCCAGTT	
Slc26a2 (NM_007885.2)	mouse	fwd	CTGCCCTGACACTGATGCTA	60°C
		rev	ACGTGAGGATGGTGAAGGAG	
Star (NM_011485.4)	mouse	fwd	GACCTTGAAAGGCTCAGGAAGAAC	63°C
		rev	TAGCTGAAGATGGACAGACTTGC	

Table 2.2: Real-time PCR primer sequences and melting temperatures.

Whole-transcript gene expression microarray analysis covering 36,079 RefSeq transcripts was conducted to investigate differential expression of genes between control and SLC26A2 knockdown NCI-H295R cells. Mock and SLC26A2 knockdown cells were seeded in 6-well plates in triplicates, 1000000 cells per well, and incubated with normal growth media for 48 hours. Subconfluent cell monolayer was lysed and RNA was purified as described in section 2.8.1. Subsequent cRNA synthesis, microarray hybridization and data analysis were carried out by Kompetenzzentrum für Fluoreszente Bioanalytik (KFB, Regensburg) using GeneChip Human Gene 1.0 ST Arrays (Affymetrix #901086). Functional annotation of differentially expressed genes was carried out using DAVID [148], and pathway mapping was accomplished by PathVisio [156] using pathway maps from WikiPathways [163].

2.9. Statistical Analyses

Values are presented as mean ± standard error of the mean. Statistical significance of RT-PCR and hormone assay results was determined by unpaired, 2-tailed Student's t test or one-way analysis of variance (ANOVA) with the Prism3.02 package (GraphPad Software). Statistical significance in graphs was denoted by asterisks as *: $P<0.05$, **: $P<0.01$, and ***: $P<0.001$. Statistical significance in microarray gene expression analyses were determined by the Mann-Whitney test. Pathway association of genes differentially expressed in SLC26A2 knockdown cells was determined by Fisher Exact test.

3. Results

3.1. Genome-Wide Association Study

A genome-wide association study was conducted with participation of 1786 subjects of the Cooperative Health Research in the region of Augsburg F4 cohort [165]. The individuals were genotyped with Affymetrix Genome-Wide Human SNP 6.0 arrays, and their plasma aldosterone and renin concentrations were determined to calculate their aldosterone to renin ratio phenotypes [166]. Subsequent association analyses demonstrated a strong linkage of aldosterone to renin ratio to a locus at 5q32 with genome-wide significance (P=6.78×10^{-11}) (Fig. 3.1A). The associated locus contained four genes: solute carrier family 26 (anion exchanger), member 2 (SLC26A2), tigger transposable element derived 6 (TIGD6), HMG box domain containing 3 (HMGXB3) and colony stimulating factor 1 receptor (CSF1R) (Fig. 3.1B). CSF1R and SLC26A2 were chosen for functional characterization based on an evaluation of the literature on PubMed [158] and publicly available expression data [151], as discussed in section 4.2.

3.2. Colony Stimulating Factor 1 Receptor (CSF1R)

3.2.1. Adrenal Expression Levels

The locus that was found to be associated with high aldosterone to renin ratio by genome-wide association study contained colony stimulating factor 1 receptor (CSF1R). Among the four genes in the locus, this was the most thoroughly studied one in the literature. Although screening for reports on this gene's possible function in aldosterone biosynthesis yielded no particular leads, it was considered prudent to be investigated further. Therefore, the expression level of the gene was measured with RT-PCR, comparing normal (100±18 %) and diseased human adrenal tissues (adenoma: 130.4±39.8; carcinoma: 69.8±31.3 %), along with the cell line NCI-H295R (0.021±0.006 %) (Fig. 3.2). The results indicated no significant difference in tissue samples (normal vs. adenoma P=0.53; normal vs. carcinoma P=0.44). It was also shown that the expression in the adrenal cancer cell line was detectable, yet at very low levels (5000-fold less than in adrenal tissue).

3.2.2. Expression Knockdown

In an attempt to eliminate the residual expression of CSF1R, NCI-H295R cells were transfected with siRNA specific to CSF1R. The gene silencing had an efficacy of 65 % of the controls (100±26.1 vs 65.4±21.6 %) (Fig. 3.3A), but did not to give rise to any difference in aldosterone production of the cells (100±6.7 vs 108±2.4 pg/ml; P=0.32) (Fig. 3.3B).
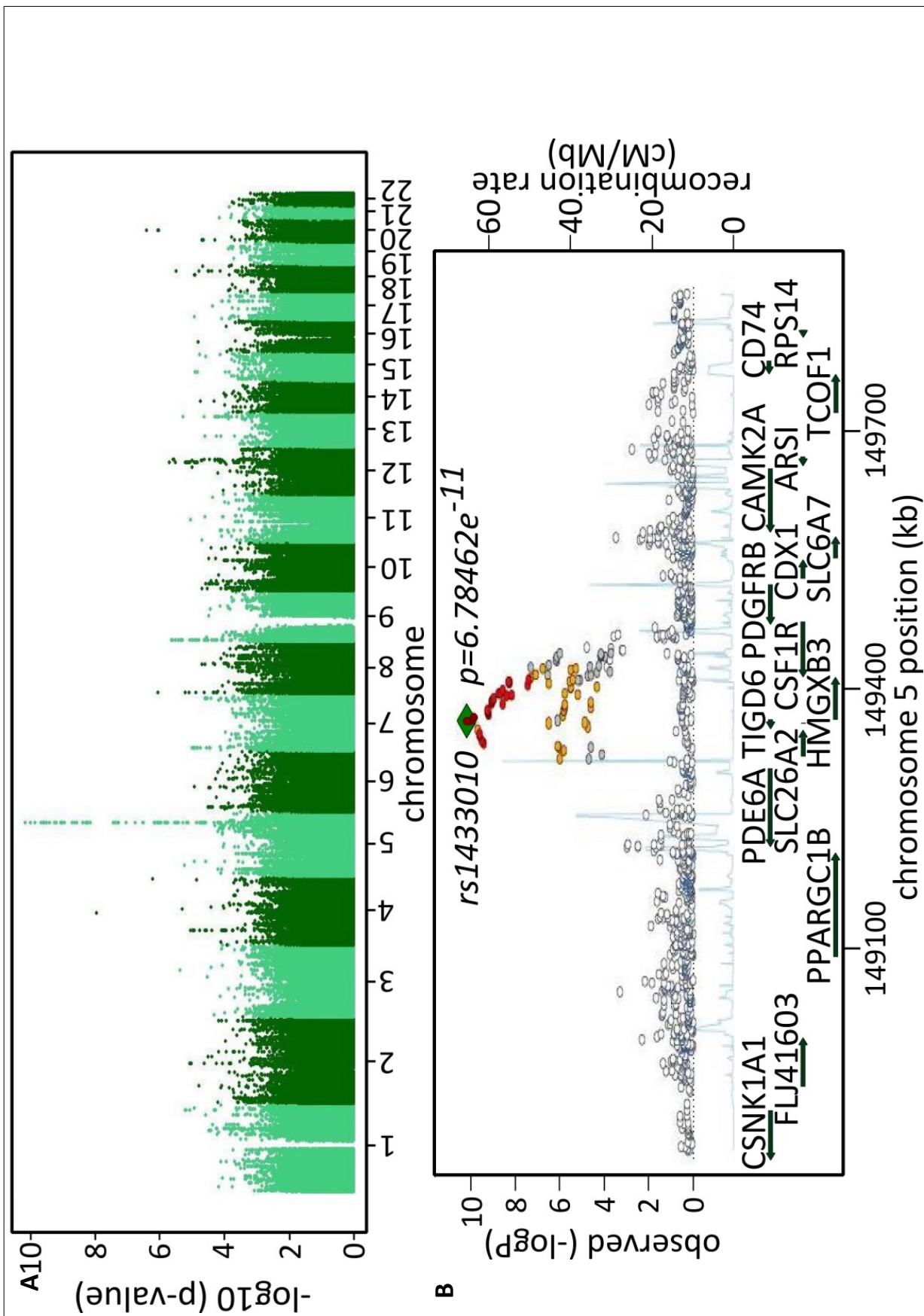
Figure 3.1: Genome-wide association study for aldosterone to renin ratio. **A**, genome-wide Manhattan plot, demonstrating genome-wide significant locus at chromosome 5. **B**, in detail plot of the associated locus depicting significance as a function of genomic position. Lead SNP is indicated with an enclosing diamond. SNPs in linkage disequilibrium with the lead SNP are colored red ($r^2 > 0.8$) or yellow ($0.2 < r^2 < 0.5$). White and gray colors indicate no LD with the lead SNP ($r^2 < 0.2$) and unavailable LD information, respectively. Recombination rate estimates from HapMap Phase II **[152]** are given in light blue, and RefSeq genes **[160]** in green arrows of scale with orientation indicated by direction.
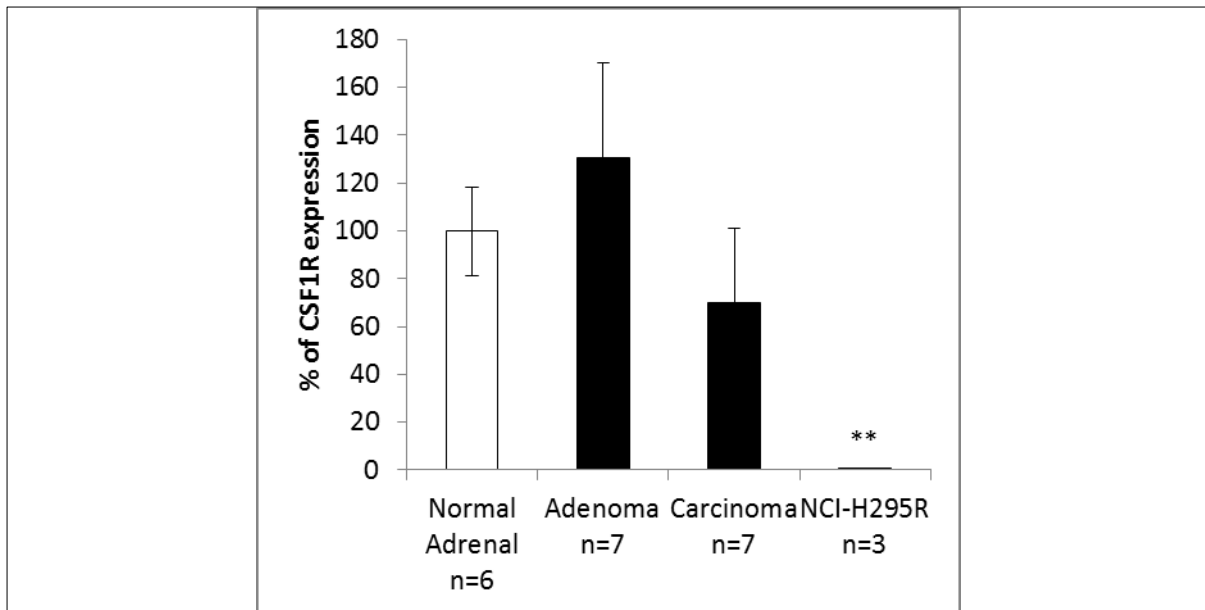
Figure 3.2: CSF1R expression in human adrenal tissue and cell line samples as percentage of normal adrenals. CSF1R expression in adrenocortical cell line NCI-H295R was three orders of magnitude less than normal adrenals. * depicts significant differences compared to control group (Normal Adrenal).
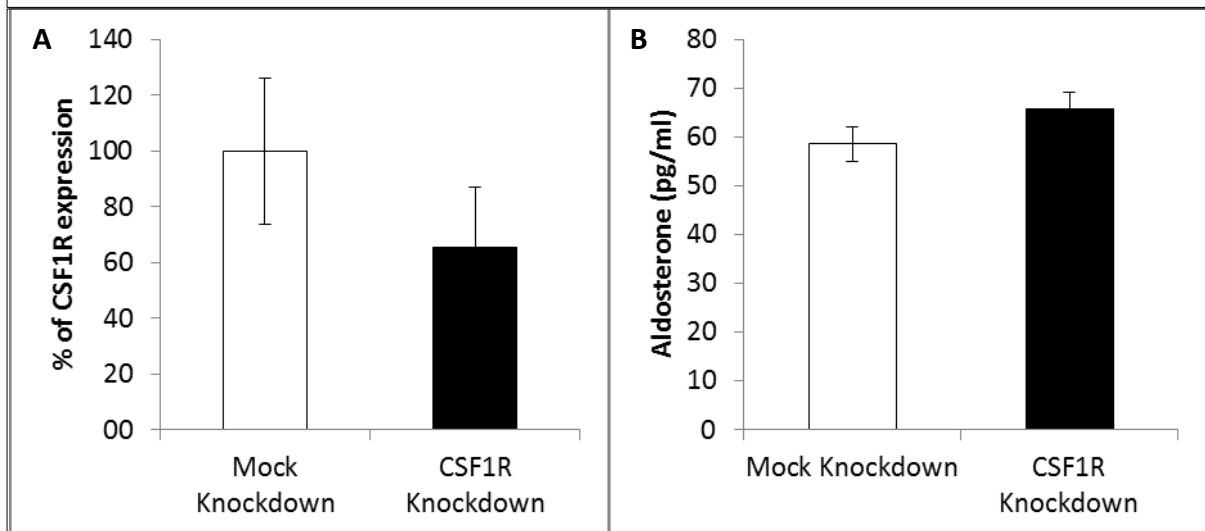
Figure 3.3: Aldosterone output of NCI-H259R cells after CSF1R knockdown. **A**, CSF1R expression of NCI-H295R cells transfected with scrambled or specific siRNA yielded a low knockdown efficacy. **B**, Aldosterone output difference of cells after knockdown was statistically not significant. For all groups, n=3.

3.2.3. Ligand Induction

The CSF1 receptor is normally found in an auto-inhibited state before binding to the ligand and subsequent auto-phosphorylation [**178**]. As a possible strategy to elevate the CSF1R activity in NCI-H295R and to better elucidate whether it has any functional impact in aldosterone production, the receptor was stimulated by incubating the cells with its ligand, CSF1. However, measuring aldosterone output of the cells treated with various concentrations of CSF1 revealed that stimulation
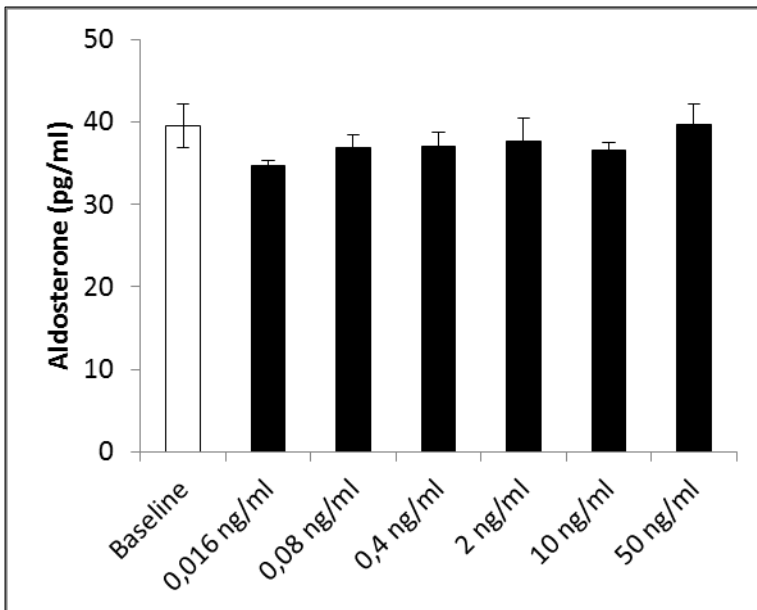
Figure 3.4: Aldosterone output of NCI-H295R cells after 24 hours of incubation with various concentrations of CSF1. Aldosterone production in H295R cells are not affected by M-CSF dosage. For all groups, n=2.
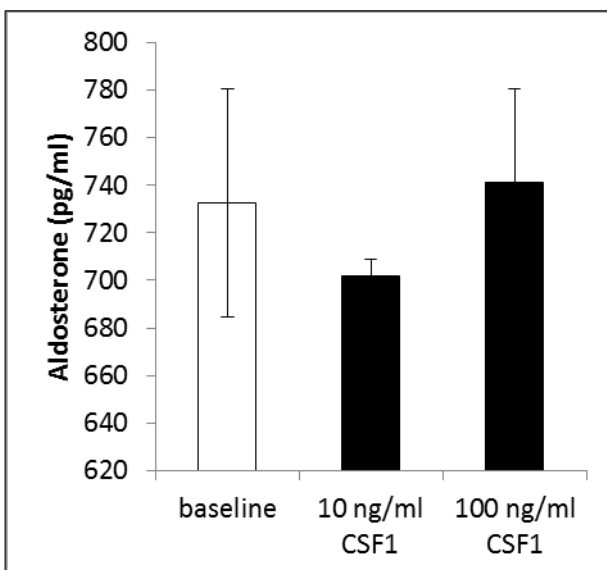
Figure 3.5: Aldosterone output of human adrenal gland primary culture cells after incubation with vehicle, 10 or 100 ng/ml CSF1 for 24 hours. Aldosterone production of primary adrenal cells from cortex adjacent to an adenoma is not regulated significantly by CSF1. For all groups, n=3.

of CSF1R does not affect aldosterone production in NCI-H295R (baseline: 39.6±2.7; 0.016 ng/ml: 34.8±0.1; 0.08 ng/ml: 36.8±1.7; 0.4 ng/ml: 37±1.8; 2 ng/ml: 37.6±2.9; 10 ng/ml: 36.6±1; 50 ng/ml: 39.7±2.5 pg/ml) (Fig. 3.4).

Lack of any relation between CSF1R induction and adrenal aldosterone production was also confirmed by replicating the treatment in primary adrenal cell cultures, as adrenal tissue had manyfold higher expression of the gene. After establishing primary cell cultures from human adrenal gland samples obtained from adrenalectomy, low (10 ng/ml) and high (100 ng/ml) doses of CSF1 was used to stimulate its receptor, and the aldosterone accumulation in the culture media was assayed (baseline: 732.7±47.8; low: 701.6±7.5; high: 741.2±39.2 %). Again, comparison of the treatment conditions revealed no significant difference of aldosterone concentration (baseline vs low P=0.56; baseline vs high P=0.9) (Fig. 3.5).

3.3. Solute Carrier Family 26 (Anion Exchanger), Member 2 (SLC26A2)

SLC26A2, also known as diastrophic dysplasia sulfate transporter (DTDST) after its role in the pathophysiology of the synonymous disorder (DTD), is an anion transporter with affinity to sulfate, oxalate and chloride [**179**]. These properties suggested a possible role for the transporter in the nephron ion recycling.

3.3.1. SLC26A2 in Aldosterone Function on Kidney

The mineralocorticoid aldosterone, the dysregulation of which gives way to PA, acts on distal tubule of the kidney to facilitate Na^+
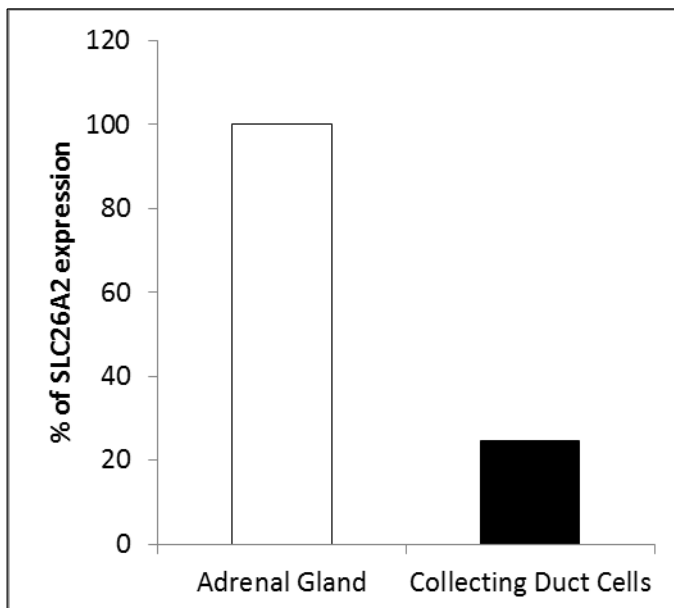
Figure 3.6: Baseline expression of SLC26A2 in collecting duct cells. SLC26A2 is expressed in collecting duct cells, albeit less than human adrenal tissue levels. For all groups, n=1.

reabsorption. As there was the possibility of high ARR associated locus having an impact on aldosterone function as aldosterone production, the cortical collecting duct was also investigated with regard to the genes present in the locus. After obtaining and growing a culture line of human principal kidney cortical collecting duct cells [**164**], baseline expression level of SLC26A2 gene was determined. SLC26A2 was found to be expressed in these cells in the same order of magnitude as adrenal tissue (adrenal: 100 vs collecting duct cells: 24.7 %) (Fig. 3.6).

3.3.2. Collecting Duct Cells Response to Aldosterone

Aldosterone's mechanism of action includes transcriptional upregulation of the epithelial sodium channel alpha subunit (SCNN1) to increase Na^+ permeability of the apical membrane. SLC26A2 expression changes due to and during this process was investigated by inducing the mineralocorticoid receptors of the kidney cells by aldosterone incubation. Transcript levels of CSF1R, SLC26A2 and SCNN1A were determined under serum starved conditions. Along with the expected upregulation of SCNN1A in response to aldosterone (baseline 100±14.2 vs aldosterone 338 ±20 %; $P<0.001$) (Fig. 3.7A), a significant, 1.5-fold increase of SLC26A2 was also detected (baseline: 100.0±10.8 vs aldosterone: 158.1±14.6 %; $P=0.03$) (Fig. 3.7B).

3.4. SLC26A2 Gene Silencing in Collecting Duct Cells

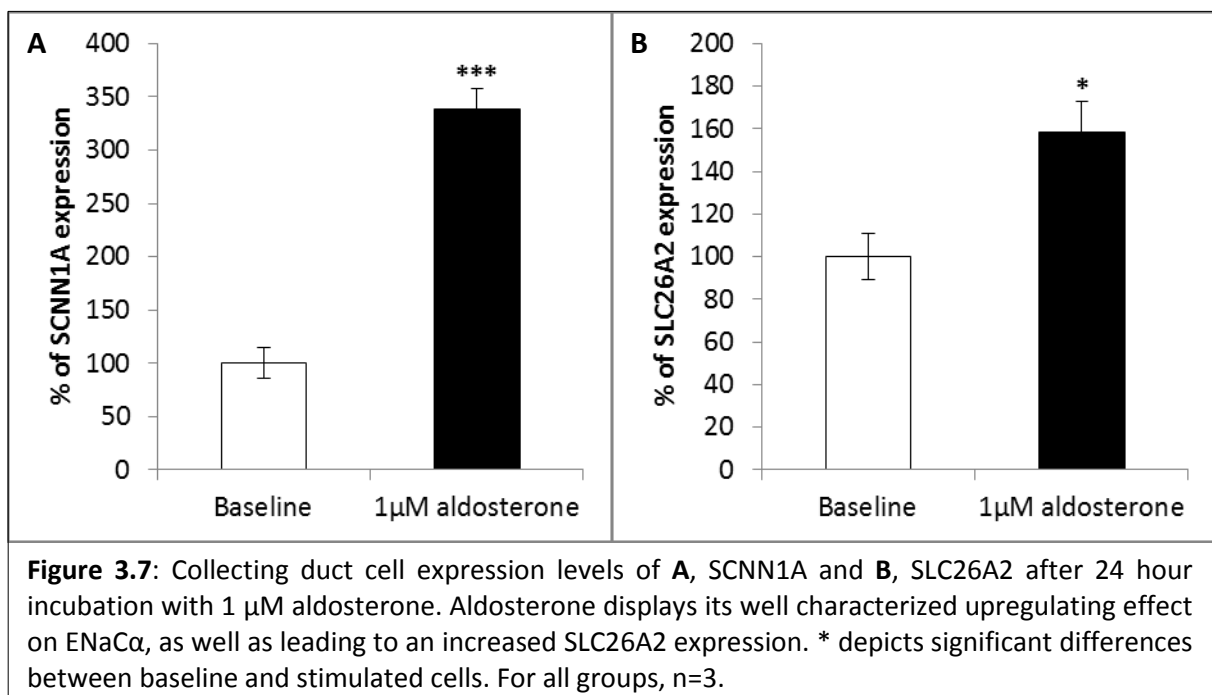### 3.4.1. Effect of Gene Silencing on Aldosterone Response

The observation of increased SLC26A2 expression during the regulation of epithelial sodium channel by aldosterone led us to investigate of whether SLC26A2 has a function in the pathway from aldosterone receptors to SCNN1A upregulation. To this end, the SLC26A2 expression was knocked

down in collecting duct cells. Lentiviral delivery of shRNA was chosen as the method of gene silencing for the benefit of a constitutive expression of shRNA, which yields a long term suppression of gene expression.

Using lentiviral particles encapsulating viral vectors with shRNA specific to SLC26A2, a collecting duct cell line with suppressed SLC26A2 expression was established, along with a control cell line with nontargeting shRNA expression. Employment of shRNA expression suppressed approximately two-thirds of gene expression, with a higher efficacy in aldosterone stimulated cells (baseline: 100±5.6 vs 35.4±0.7; aldosterone: 120.5±15.5 vs 30.6±2.5 %) (Fig. 3.8A). No upregulation of SLC26A2 was observed upon aldosterone stimulation neither in control cells (P=0.28) nor upon silencing of SLC26A2 (P=0.14). Quantification of SCNN1A levels revealed that the knockdown did not cause a significant alteration in sodium channel expression in cells with or without aldosterone stimulation (baseline: 18.6±3 vs 25.5±0.3; aldosterone: 100±25 vs 80.4±4.6 %) (Fig. 3.8B). However, the aldosterone induced increase of SCNN1A expression was less profound in the knockdown cells, although this difference did not achieve statistical significance (mock: 5.4±1.3-fold vs KD: 3.2±0.2-fold; P=0.18).

3.4.2. Osmotic Stress Genes

The need to maintain a high osmotic gradient in principal collecting duct cells to reabsorb sodium in hypertonic conditions puts the cells in osmotic stress. NFAT5 is a transcription factor that directs multiple responses of these cells: it regulates uptake and synthesis of organic osmolytes that

Figure 3.7: Collecting duct cell expression levels of **A**, SCNN1A and **B**, SLC26A2 after 24 hour incubation with 1 µM aldosterone. Aldosterone displays its well characterized upregulating effect on ENaCα, as well as leading to an increased SLC26A2 expression. * depicts significant differences between baseline and stimulated cells. For all groups, n=3.
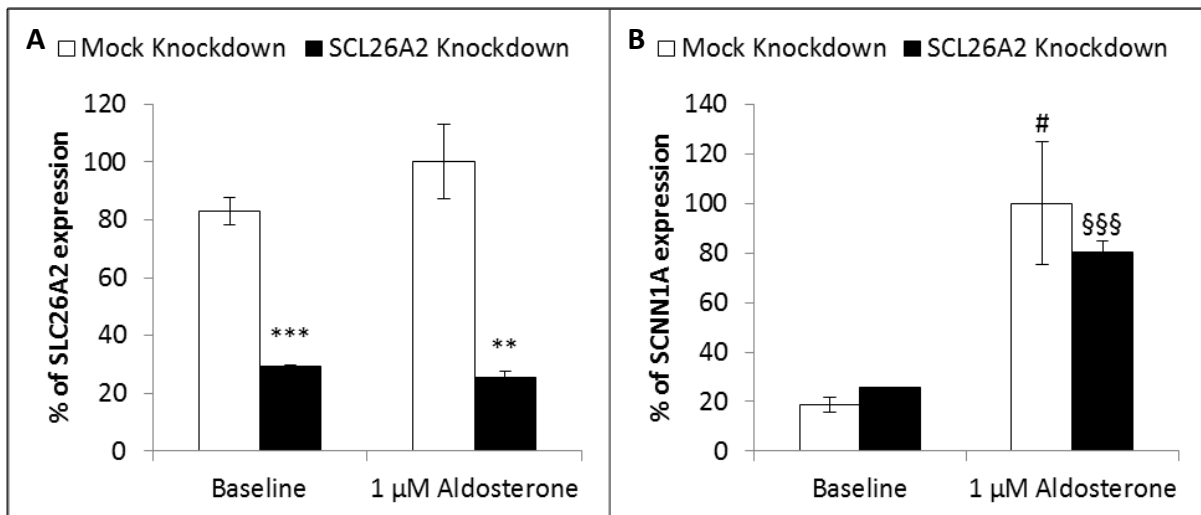
Figure 3.8: shRNA mediated SLC26A2 knockdown in aldosterone stimulated collecting duct cells. **A**, The efficacy of the knockdown was similar in baseline and stimulated conditions. **B**, SCNN1A expression upregulation by aldosterone was not prevented by knockdown, but was reduced in intensity. * depicts significant differences between Mock and SLC26A2 Knockdown ce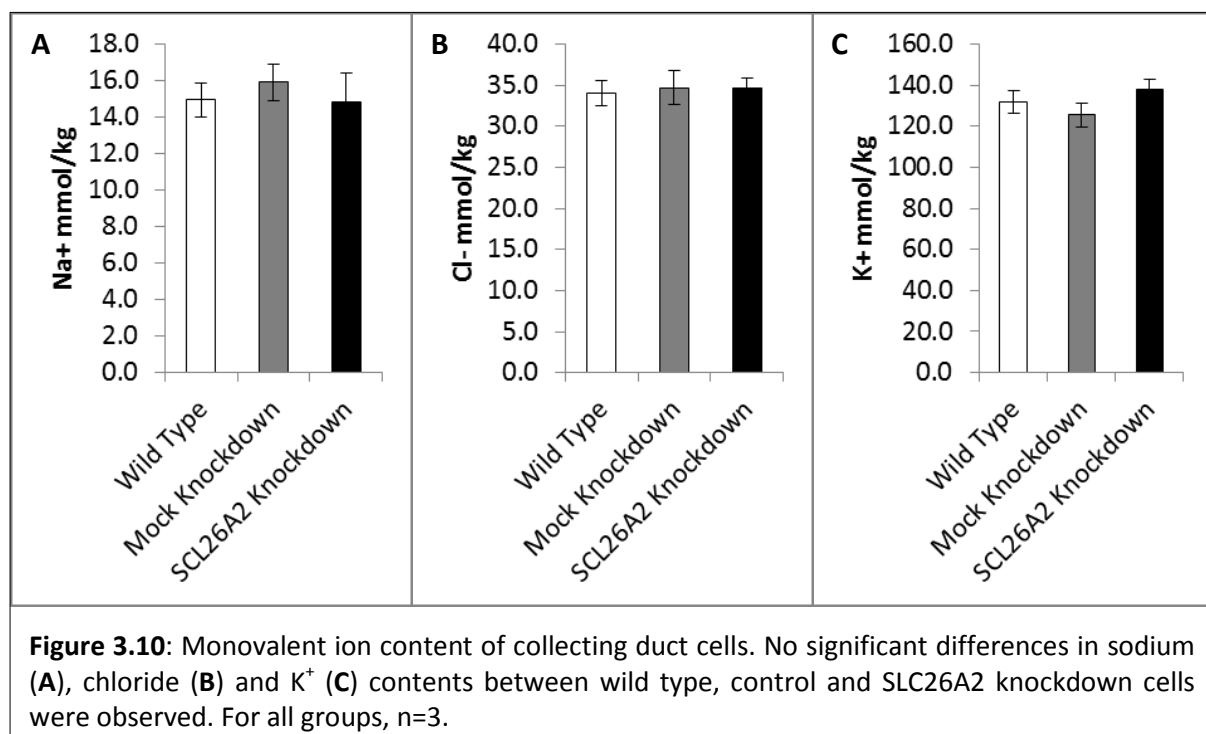lls of the same treatment; # depicts significant differences between baseline and stimulated Mock Knockdown cells; § depicts significant differences between baseline and stimulated SLC26A2 Knockdown cells. For all groups, n=3.

increase intracellular tonicity while lowering the ionic strength, therefore preventing disruption of protein structure and function. NFAT5 also protects the cells against urea by promoting expression of HSP-70 and urine transporter SLC14A2 (UT-A) and water channel AQP2, which contributes as well to urea concentrating process [**180**]. After failing to observe any significant direct alterations in principal cell response to aldosterone by SLC26A2 knockdown, it was suspected that the knockdown may upset the interplay between sodium and water reabsorption processes and cellular defenses against osmotic stress. In fact, SLC26A2 knockdown was observed to reduce the expression of NFAT5 under baseline or aldosterone stimulated culture, and the reduction in baseline condition satisfied statistical significance criteria (baseline: 100±4.2 vs 58.6±3.3 %; P=0.001; aldosterone: 59.5±19 vs 38.9±4 %; P=0.35) (Fig. 3.9A). As expected, a subsequent decrease in SLC14A2 levels in SLC26A2 knockdown cells was also observed (baseline: 100±14.1 vs 69.6±28.9 %; P=0.4; aldosterone: 109.3±22.1 vs 68.5±11.8 %; P=0.18) (Fig. 3.9B).

3.4.3. Intracellular Ion Content

SLC26A2 knockdown collecting duct cells were further studied to determine their intracellular electrolyte levels by electron microprobe analysis, in order to observe whether the osmotic stress response differences in knockdown cells affect Ion concentrations. In comparison to wild type or nontargeting shRNA controls, knockdown cells presented no significant changes in levels of sodium (WT: 14.9±0.9; mock: 15.9±1; KD: 14.8±1.6 mmol/kg; mock vs KD P=0.6) (Fig. 3.10A), chloride (WT:

34±1.5; mock: 34.7±2.1; KD: 34.7±1.2 mmol/kg; mock vs KD P=1) (Fig. 3.10B) or potassium (K^+) (WT: 131.7±5.5; mock: 125.4±5.6; KD: 137.9±4.6 mmol/kg; mock vs KD P=0.1) (Fig. 3.10C).

Figure 3.9: Expression of osmotic stress genes in SLC26A2 knockdown collecting duct cells. **A**, osmotic stress regulator NFAT5 was expression decreased in response to both aldosterone and SLC26A2 suppression. **B**, Mean SLC14A2 expression expression was lower in knockdown cells, but did not respond to stimulation of cells by aldosterone. * depicts significant differences between Mock and SLC26A2 Knockdown cells of the same treatment; § depicts significant differences between baseline and stimulated SLC26A2 Knockdown cells. For all groups, n=3.

Figure 3.10: Monovalent ion content of collecting duct cells. No significant differences in sodium (**A**), chloride (**B**) and K^+ (**C**) contents between wild type, control and SLC26A2 knockdown cells were observed. For all groups, n=3.

3.5. Adrenal SLC26A2 Expression

A literature scan for this gene failed to identify any reports on its potential role in adrenal function. However, evaluation of publicly available microarray based expression data from GNF Gene Expression Atlas 2 [151] indicated a high adrenal and adrenocortical expression of the gene (Fig. 3.11).

3.5.1. Tissue Specific Expression

Confirmation of the microarray data from the literature, indicating above-median expression of SLC26A2 in adrenal tissue, was the initial step of confirming the hypothesis that this locus could be involved in the pathogenesis of primary aldosteronism. Using primers targeting the SLC26A2 gene, relative expression levels in human reference RNA mix (100±16.7 %), liver (73±14.5 %) and pancreas (744±115.6 %) were quantified and compared with normal adrenal (3365±367 %) and Conn's adenoma tissues (2831±1013 %), depicting a profile of differential expression levels throughout the organism (one-way ANOVA P=0.035) (Fig. 3.12).

As a genetically modifiable model organism, mice play an important role in studies of aldosterone physiology and hyperaldosteronism [102; 105]. Therefore, *Slc26a2* expression in murine tissues was profiled. Expression was quantified in adrenal, kidney, lung, heart, liver, muscle, spleen, brain, ovary and fat tissues (Fig. 3.13). *Slc26a2* levels in adrenal glands were found to be significantly higher compared to the other tissues (adrenal : 100±4.3 %; kidney: 40.1±3 %, P<0.001; lung: 35.5±2.4 %, P<0.001; heart: 51.7±0.9 %, P<0.001; liver: 19.4±1 %, P<0.001; muscle: 62.6±11.7 %, P=0.04; spleen: 5.6±0.1 %, P<0.001; vs brain: 12.9±1.5 %, P<0.001; vs ovary: 34.1±4.6 %, P<0.001; vs fat: 68.3±6.7 %, P=0.016).

3.5.2. Adrenal Expression by Disease State

The high adrenal SLC26A2 expression opened up the possibility of altered expression profile of this gene in adrenal disease. To address this question, expression levels in 11 control adrenals and a large set of 91 APAs were quantified and compared. Interestingly, a significant decrease in SLC26A2 levels in APAs was observed (31.2±4.2 vs 12.4±1.1; P<0.001) (Fig. 3.14A). However, within the adenomas, there were no significant differences between the mutation status of recently identified [86; 87] causative genes KCNJ5, ATP1A1 or ATP2B3 ($^-$/$^-$: 10±1.2; KCNJ$^+$: 15.2±2.1; ATPase$^+$: 10.2±2.4; P=0.22) (Fig. 3.14B) or between sexes (females: 12.8±1.6 vs males: 11.8±1.6; P=0.77) (Fig. 3.14C).

Lowered mean transcript levels of SLC26A2 in aldosterone producing adenomas were validated on the protein level by immunohistochemistry. Normal human adrenal samples and adrenal adenomas

Figure 3.11: Microarray based expression levels of SLC26A2 among human tissues in the Gene Atlas platform data.
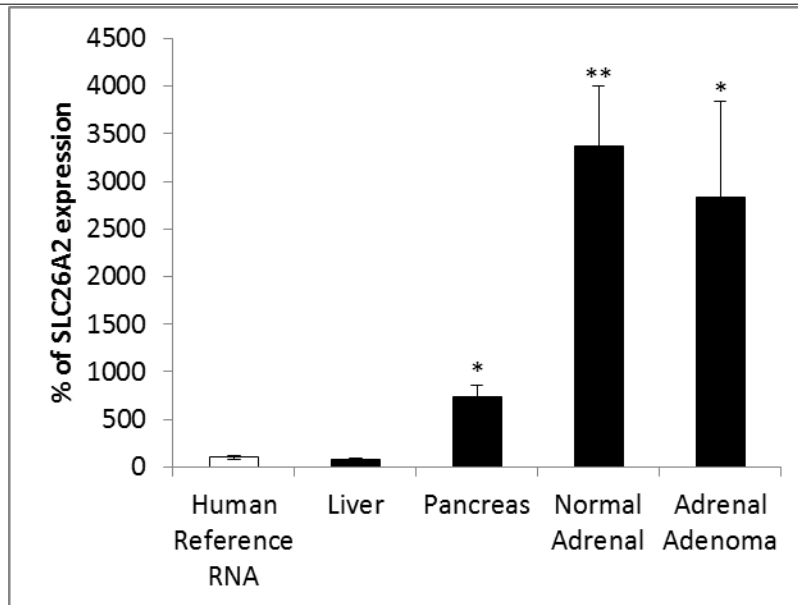
Figure 3.12: SLC26A2 expression in human tissue samples. Expression in adrenal tissues was significantly higher compared with other reference, liver or pancreas samples ($P<0.05$). * depicts significant differences compared to control group (Human Reference RNA). For all groups, n=2.
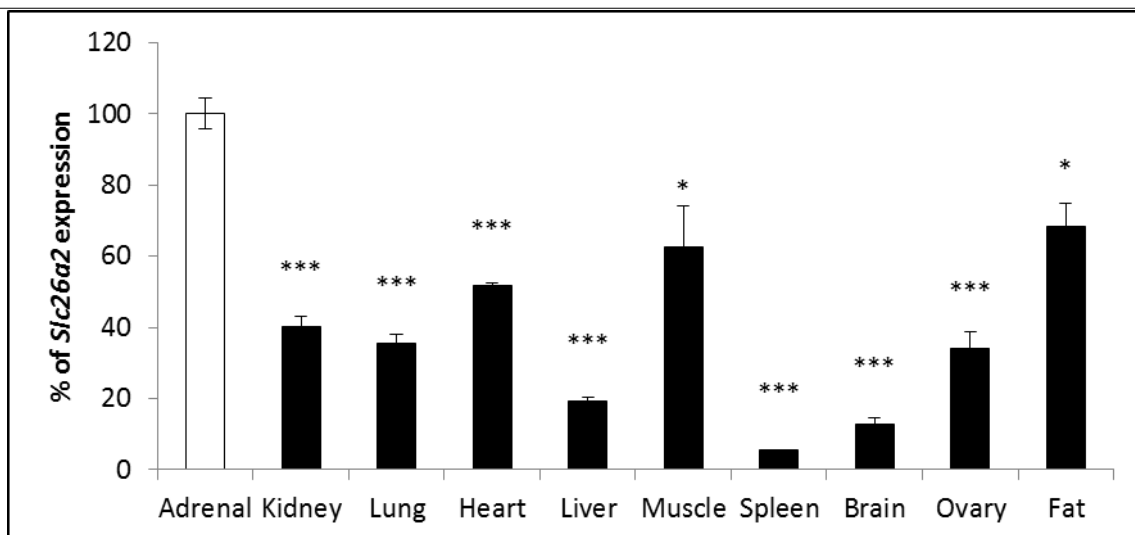
Figure 3.13: *Slc26a2* expression in murine tissues. Expression in adrenal glands was significantly higher than each of the screened tissues. * depicts significant differences compared to control group (Adrenal). For all groups, n=3.

were screened with anti-CYP11B2 antibodies and visualized by peroxidase reaction. No staining was observed in negative controls lacking the primary antibodies (Fig. 3.15A,B). Intensive CYP11B2 expression was evident in adenomas (Fig. 3.15D) whereas in normal adrenals, CYP11B2 was localized to a thin sub-capsular region and islets as expected [**55**] (Fig. 3.15C). Immunohistochemical detection of SLC26A2 expression in these samples was carried out using a polyclonal rabbit anti-human SLC26A2 antibody. Subsequent visualization revealed SLC26A2 expression throughout the cortex of normal adrenals (Fig. 3.15E). In comparison, staining was diminished in APAs (Fig. 3.15F).
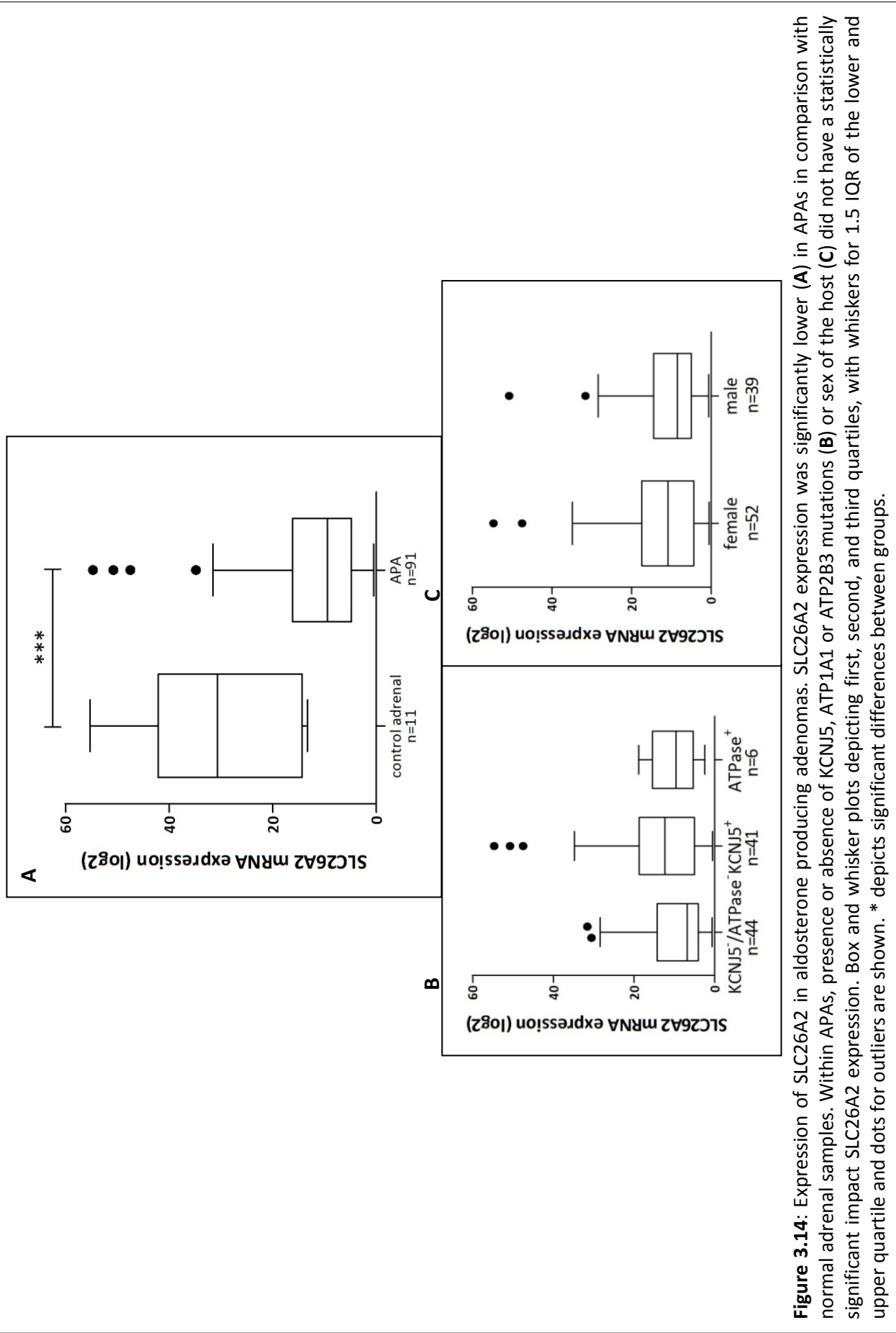
Figure 3.14: Expression of SLC26A2 in aldosterone producing adenomas. SLC26A2 expression was significantly lower (**A**) in APAs in comparison with normal adrenal samples. Within APAs, presence or absence of KCNJ5, ATP1A1 or ATP2B3 mutations (**B**) or sex of the host (**C**) did not have a statistically significant impact SLC26A2 expression. Box and whisker plots depicting first, second, and third quartiles, with whiskers for 1.5 IQR of the lower and upper quartile and dots for outliers are shown. * depicts significant differences between groups.
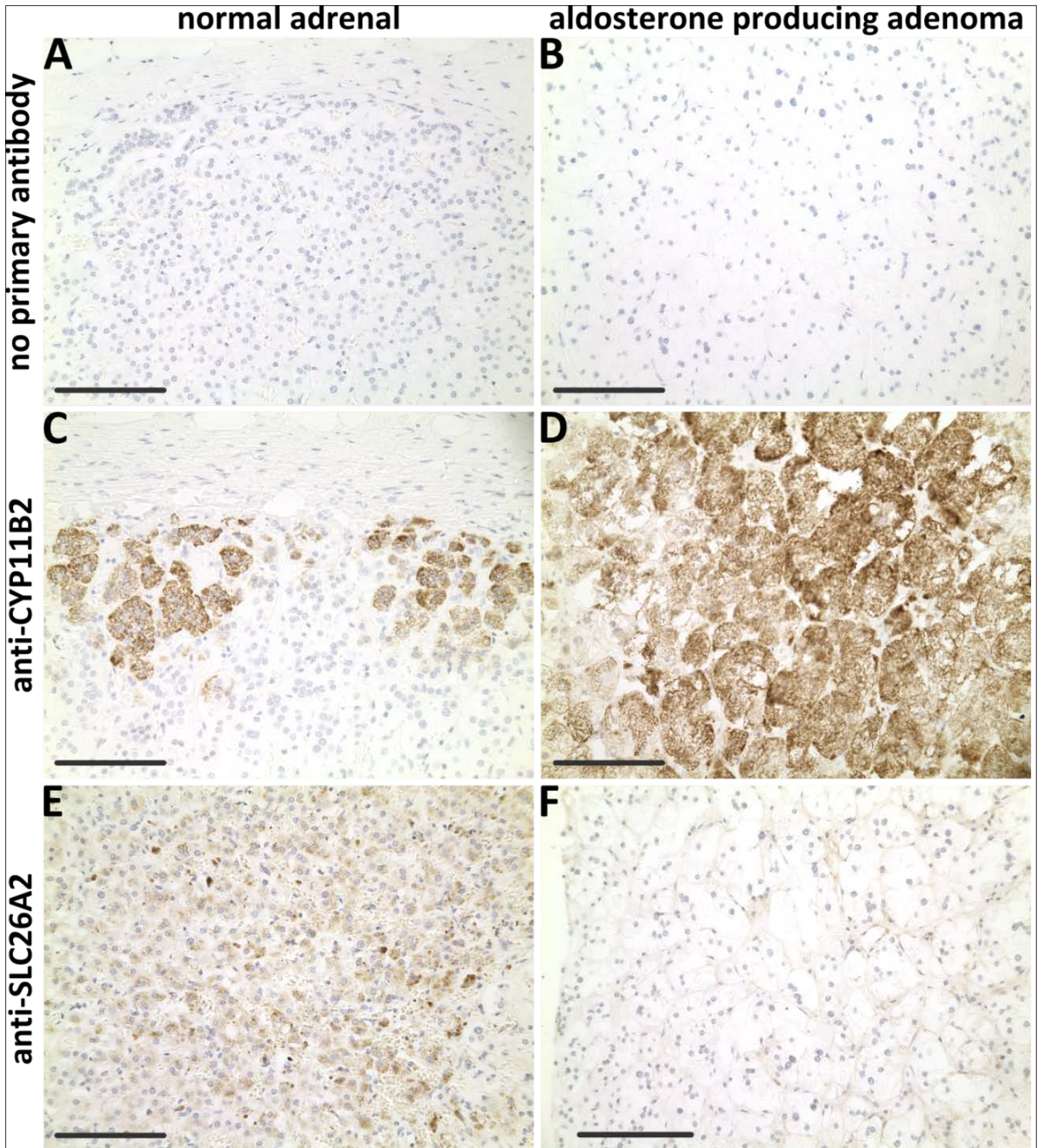
Figure 3.15: Immunohistochemical detection of CYP11B2 (**C,D**) and SLC26A2 (**E,F**) expression in adrenal tissue. No unspecific staining in the lack of primary antibody was detected (**A**,**B**). CYP11B2 staining was localized to ZG in normal adrenals (**C**) compared to more intense and broad immunopositivity in APA (**D**). In contrast, SLC26A2 was detected throughout the adrenal cortex with a higher intensity in normal adrenal (**E**) in comparison with APA (**F**). Bars represent 125 μm.

3.6. Effects of Aldosterone Regulators on Adrenal SLC26A2 Expression

3.6.1. *in vivo*
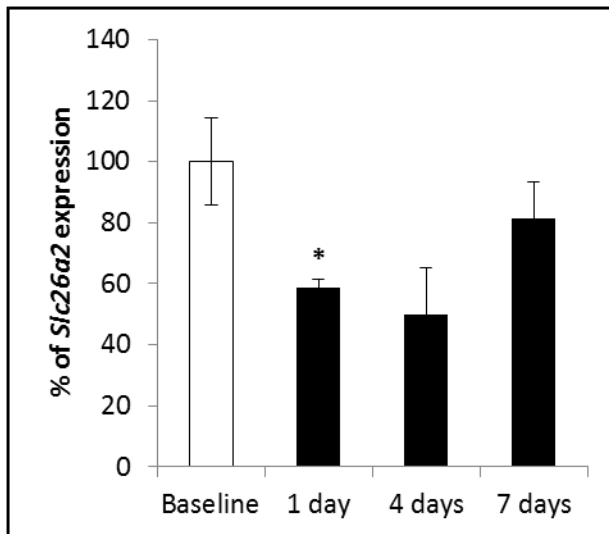
Figure 3.16: Regulation of *Slc26a2* expression *in vivo* by K⁺. Expression in adrenal glands of mice fed with a high K⁺ diet was initially significantly lowered, with recovering after seven days. * depicts significant differences compared to control group (Baseline). Baseline, n=4; treatment groups, n=5.

Observations of high adrenal and decreased APA expression of SLC26A2 led us to suspect a potential effect of the solute carrier on aldosterone production. Initially, coregulation of *Slc26a2* expression with aldosterone was investigated. Therefore, mice were treated with secretagogues of aldosterone, and the adrenal *Slc26a2* expression was measured. As high blood K⁺ levels are the most potent factor in aldosterone, effects of K⁺ were investigated. Mice on a high K⁺ diet through their water supply were tested at four time points showed a significant decrease in gene expression (baseline:

100 ± 14.4; day 1: 58.6 ± 2.7 %; $P=0.015$; day 4: 49.8 ± 15.6 %; $P=0.054$; day 7: 81.6 ± 11.7 %; $P=0.34$), within days, tending to recover as the decrease being reduced to non-significant levels within a week (Fig. 3.16).
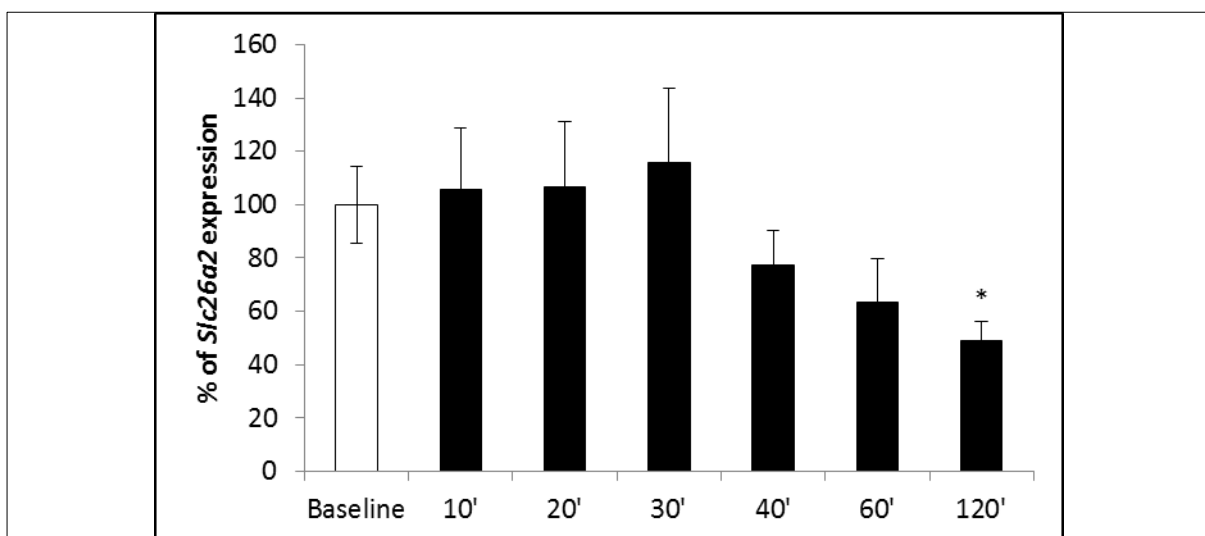
Figure 3.17: Regulation of *Slc26a2* expression *in vivo* by AngII. Expression in adrenal glands of mice injected with AngII decreased within 40 minutes. After two hours, the downregulation was statistically significant. * depicts significant differences compared to control group (Baseline). Baseline, n=4; treatment groups, n=5.

As described previously, angiotensin II exerts control of the RAA system on aldosterone production by initiation of the signaling cascade in zona glomerulosa cells to express *Cyp11b2* and therefore to secrete aldosterone. In this context, acute effects of AngII treatment in murine adrenal glands in relation to *Slc26a2* expression were observed. Expression changes were determined within a 2-hour time period. *Slc26a2* expression began to decrease after 40 minutes (baseline: 100±14.4 vs 40': 77.3±13 %, *P*=0.28), with a significant reduction being observed after 2 hours (48.8±7.3 %, *P*=0.012) (Fig. 3.17).

Intravenous sodium loading is a regularly employed clinical test in the diagnosis of PA. By elevating the plasma sodium levels, renin production in the kidney is inhibited, which in turn leads to inhibition of aldosterone production in the adrenals via the RAAS. *Slc26a2* expression in adrenal glands was observed after suppression of RAAS by this method in mice. Even though a decrease in expression was observed within twenty minutes (100±14.4 vs 59.6±11 %, *P*=0.057), overall, the treatment yielded no statistically significant changes in the expression profile (*P*=0.48) (Fig. 3.18).

Figure 3.18: Suppression of renin by injecting mice by sodium loading did not affect adrenal *Slc26a2* expression. Baseline, n=4; treatment groups, n=5.
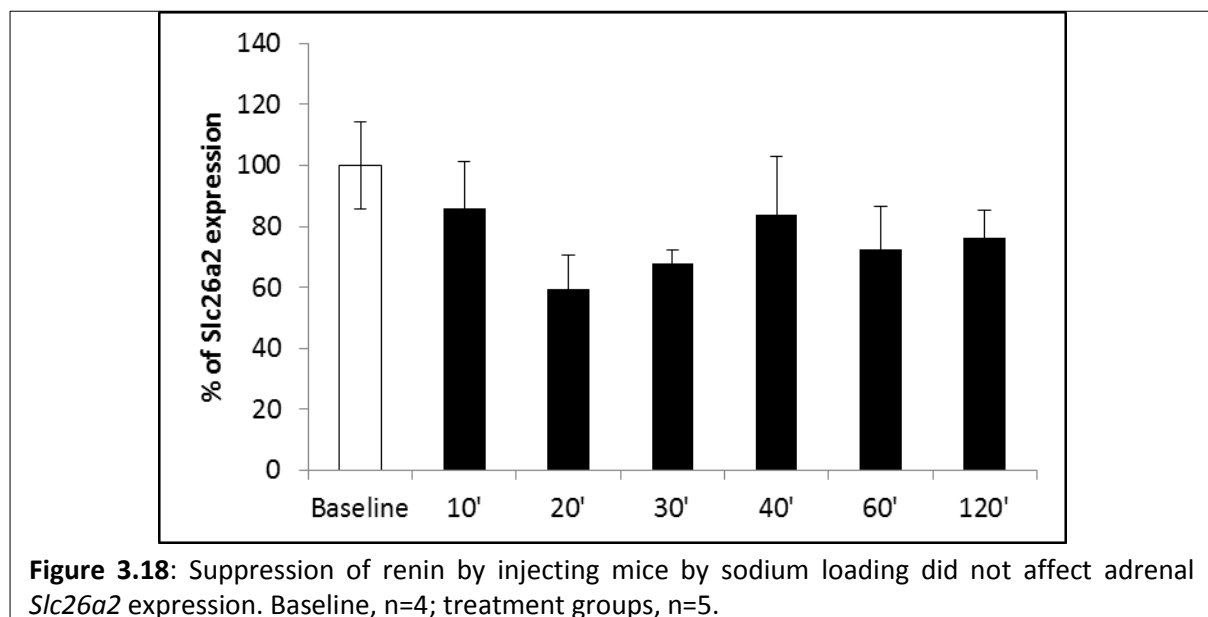
3.6.2. *in vitro*

The model cell line for studies on aldosterone biosynthesis and metabolism is the human adrenocortical cancer cell line NCI-H295R [**181**]. Interestingly, incubation of these aldosterone producing cells with elevated K^+ concentration in their growth medium led to an increase in their expression of SLC26A2 (100±6.7 vs 163.8±16.8 %, *P*=0.027) (Fig. 3.19). Incremental increase of K^+, however, had no effect on the magnitude of this increase.
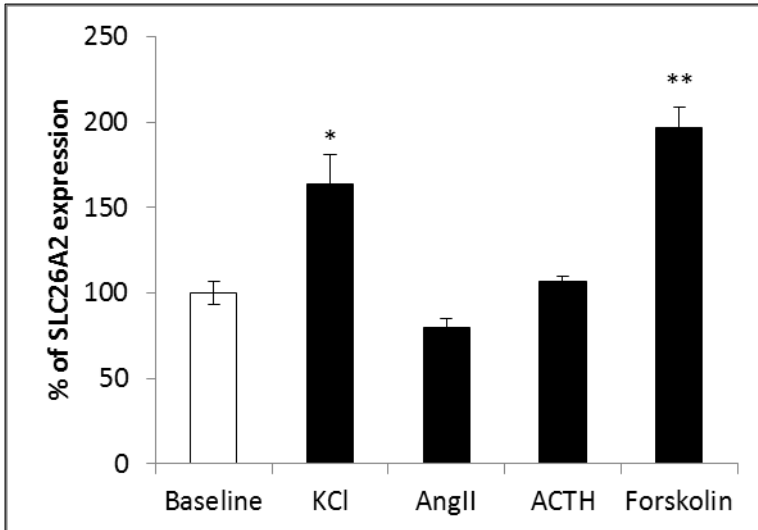
Figure 3.19: *In vitro* transcriptional regulation of SLC26A2. NCI-H295R cells were stimulated with aldosterone secretagogues K⁺, AngII, synthetic ACTH and forskolin. SLC26A2 expression was upregulated significantly by K⁺ and forskolin, unaffected by ACTH and mildly decreased by AngII. * depicts significant differences compared to control group (Baseline). For all groups, n=3.

The NCI-H295R cells are sensitive to signals stimulating the aldosterone production, mainly AngII, K^+ and forskolin. These stimulators of aldosterone production were utilized for better elucidation of aldosterone - SLC26A2 coregulation. As compared to cells grown with regular media, those with angiotensin added to the media displayed a less-than-significant reduction in the SLC26A2 transcript levels (79.6±5.4 %, *P*=0.076). Low ACTH responsiveness [182] of H295R cells were demonstrated as synachten had no observable effects to SLC26A2 expression (106.4±3.6 %, *P*=0.45), whereas elevation of cyclic AMP levels independently using forskolin yielded a significant upregulation (196.8±11.6 %, *P*=0.002) (Fig. 3.19).
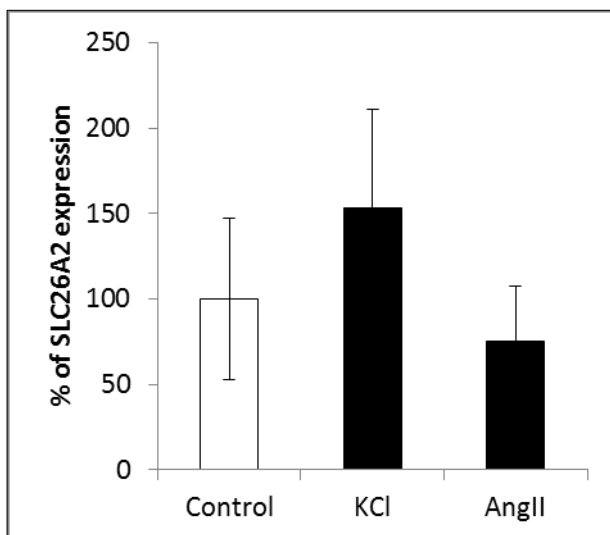
Figure 3.20: Transcriptional regulation of SLC26A2 in adrenal cells. SLC26A2 levels of the primary adrenal cell culture was elevated by K⁺ and slightly lowered by AngII, mimicking H295R cell response. For all groups, n=2.

A cancer-derived cell line may provide an easily handled and versatile tool to perform experiments, but the origins of the line may cause problems and artifacts in comparison to physiological conditions. It may, therefore, be deemed prudent to use primary cell lines when possible. Using the small amount of tumor adjacent normal adrenal tissue attached from adrenalectomy samples, primary cultures were prepared and treated with increased K^+ or AngII. The effects of these stimulators on the primary adrenal culture cells replicated that of NCI-H295R cells, the increase by K^+ (100±47.1 vs 153±57.7 %, *P*=0.55) and the decrease by AngII (75.5±31.9 %, *P*=0.71) (Fig. 3.20). Statistical tests, however, yielded no

significance due to intragroup variation, possibly due to heterogeneous cell composition in the source tissue sample.

3.7. Adrenal SLC26A2 Gene Silencing

The evidence derived from observing the effects of aldosterone stimulators on SLC26A2 expression indicated a potential regulatory role of the SLC26A2 itself on the production of mineralocorticoids. To test this hypothesis, a suppression of SLC26A2 expression using RNA interference was aimed. Using lentiviral delivery of expression vectors encoding non-targeting or SLC26A2-specific shRNA, cell lines with decreased expression and control lines were established. Non-targeting shRNA did not significantly alter SLC26A2 expression compared to wild type cells (107.1 ± 4.2 vs 100 ± 4.3 %, P=0.3). Expression levels of SLC26A2 were reduced four-fold compared to control cells (100 ± 4.3 vs 23.5 ± 2.3
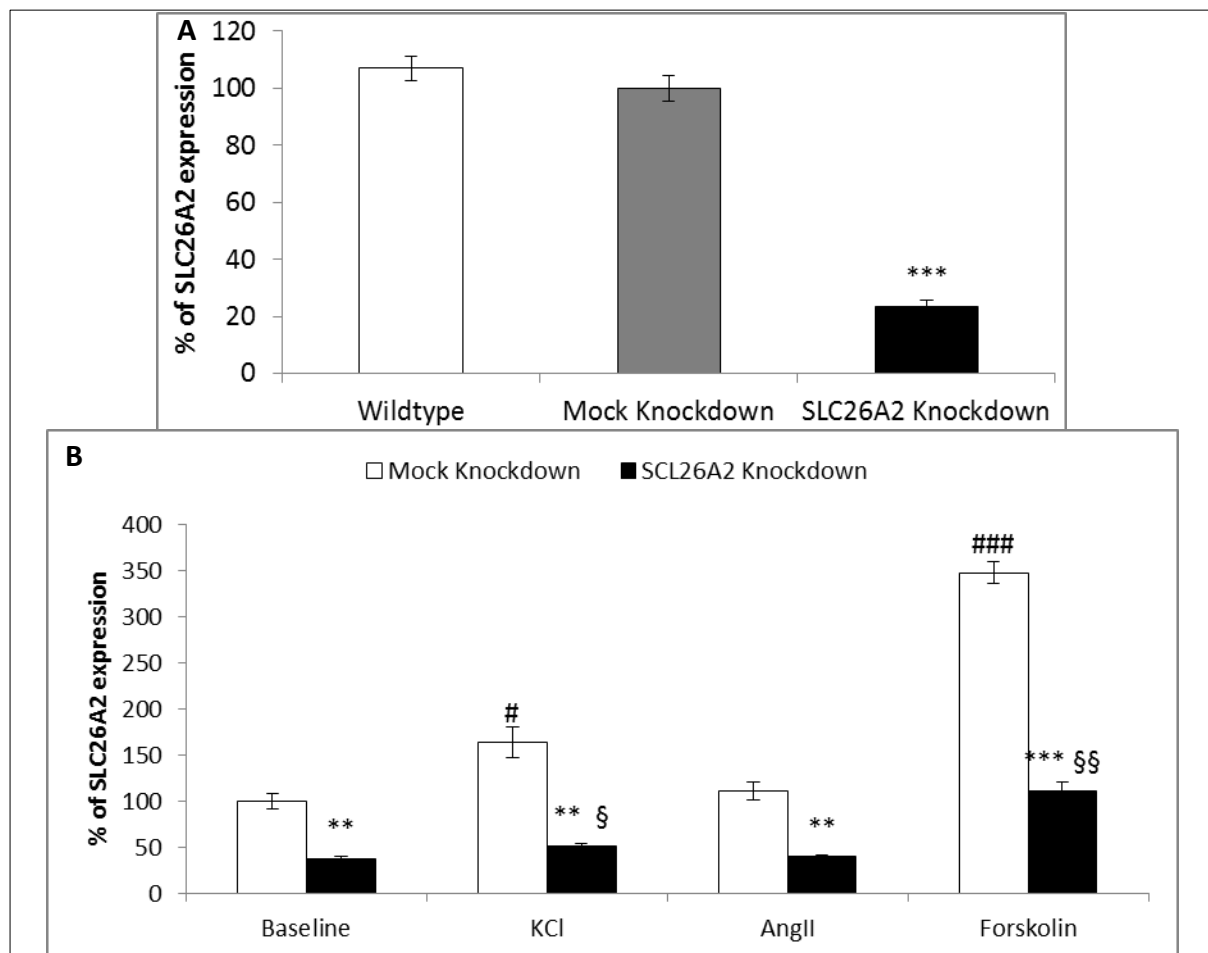
Figure 3.21: shRNA mediated SLC26A2 knockdown in NCI-H295R cells. **A**, SLC26A2 expression was silenced with lentivirally delivered constitutively expressed shRNA. SLC26A2 expression was suppressed to 23 % of controls, whereas unspecific shRNA did not alter SLC26A2 levels. **B**, Supression of SLC26A2 expression remained at similar potency after treatment of cells with aldosterone agonists. * depicts significant differences between Mock and SLC26A2 Knockdown cells of the same treatment; # depicts significant differences between baseline and stimulated Mock Knockdown cells; § depicts significant differences between baseline and stimulated SLC26A2 Knockdown cells. For all groups, n=3.

%, *P*<0.001) (Fig. 3.21A), with this ratio remaining in the range of 3 to 4-fold across passages (100±7.9 vs 37.7±1.9 %) (Fig. 3.21B). Knockdown efficacy was similar in culture conditions stimulating aldosterone production, i.e. with increased K$^+$ (3.2±0.2-fold), with AngII (2.8±0.2-fold) and with elevated cAMP levels by forskolin (3.2±-0.3-fold).

3.7.1. Steroidogenesis

Initially, any possible effects of SLC26A2 knockdown on aldosterone production of the cells were investigated. In comparison to unspecific control shRNA expressing cells, which did not affect aldosterone production (WT: 129.8±24.8 vs mock: 100±18.9 %, *P*=0.12) (Fig. 3.25B), the knockdown line demonstrated a profound increase in aldosterone output (64.6±1.1 vs 432.7±23 pg/ml, *P*<0.001) (Fig. 3.22). The increase in aldosterone production upon knockdown was also observed in stimulating conditions provided by presence of increased KCl (1419.8±15.4 vs 1950.5±20.1 pg/ml, *P*<0.001), AngII (98.9±2.8 vs 778.8±43.3 pg/ml, *P*<0.001) or forskolin (800.6±35.6 vs 1630.6±14.6 pg/ml, *P*<0.001).
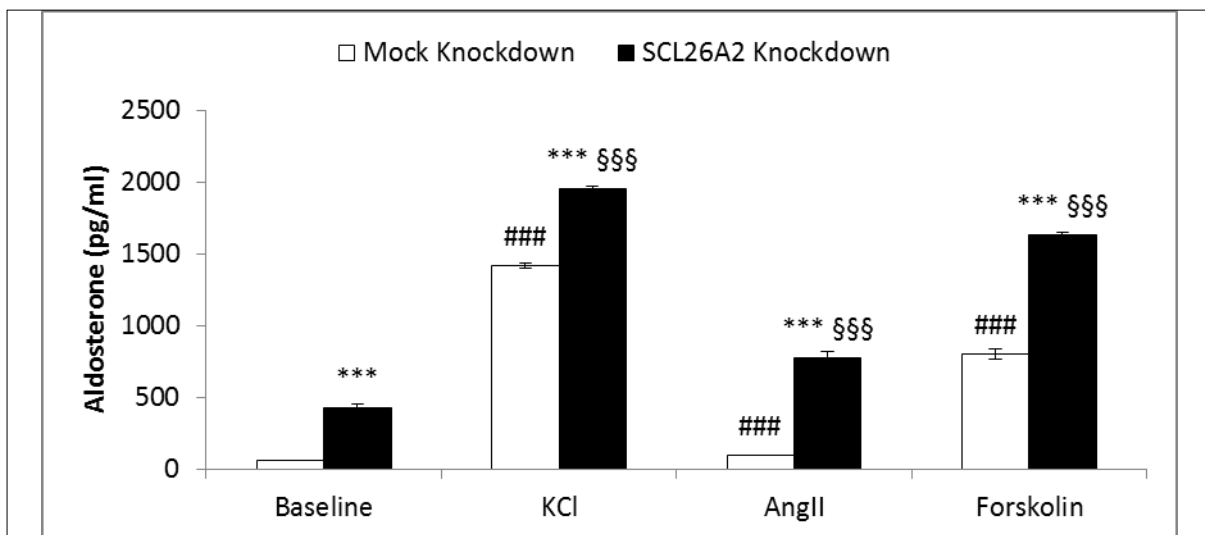
Figure 3.22: Aldosterone production of SLC26A2 knockdown NCI-H295R cells. Aldosterone output of knockdown cells were significantly higher in cells with suppressed SLC26A2 expression in both baseline and aldosterone stimulating culture conditions. * depicts significant differences between Mock and SLC26A2 Knockdown cells of the same treatment; # depicts significant differences between baseline and stimulated Mock Knockdown cells; § depicts significant differences between baseline and stimulated SLC26A2 Knockdown cells. For all groups, n=3.

Although SLC26A2 expression was not affected by induction of NCI-H295R cells by synachten, possibly due to low ACTH responsiveness of this cell line (Fig. 3.19), aldosterone production was increased by ACTH, and the reaction of SLC26A2 knockdown cells to ACTH stimulation was significantly more pronounced (mock: 31.2±1.8 vs 80±6.1 pg/ml, 2.6±0.2-fold; KD:224.8±27.6 vs 802±65.9 pg/ml, 3.6±0.3-fold, *P*=0.04;) (Fig. 3.23).
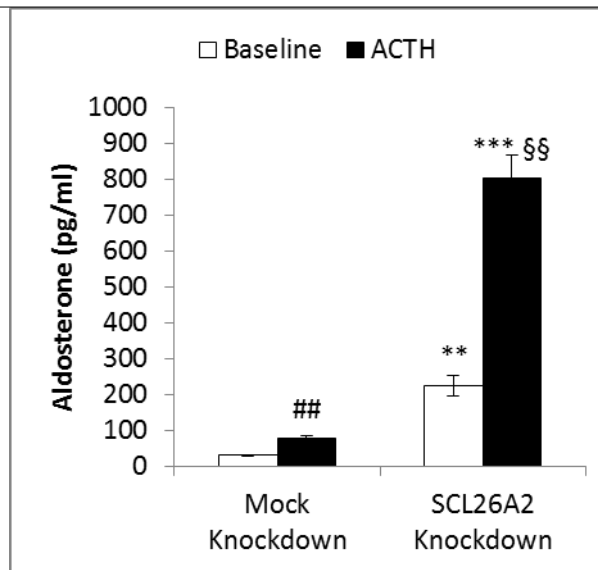
Figure 3.23: Aldosterone production of SLC26A2 knockdown NCI-H295R cells treated with ACTH. Increase in aldosterone production by ACTH stimulation was more pronounced (3.5-fold) in comparison to control cells (2.5-fold). * depicts significant differences between Mock and SLC26A2 Knockdown cells of the same treatment; # depicts significant differences between baseline and stimulated Mock Knockdown cells; § depicts significant differences between baseline and stimulated SLC26A2 Knockdown cells. For all groups, n=3.

The NCI-H295R cell line has the capability of producing cortisol in addition to aldosterone. In order to clarify whether the elevated steroidogenetic effect of SLC26A2 knockdown is specific to aldosterone, cortisol and aldosterone outputs of the cells in serum starved conditions were determined. Synthesis of both steroids increased in knockdown cells under baseline conditions (aldosterone: 8.1±0.6 vs 96.9±12.2 pg/ml, *P*=0.002; cortisol: 76.2±0.3 vs 233.6±22.4 ng/ml, *P*=0.002) (Fig. 3.24A&B); ratio of aldosterone increase over shadowing that of cortisol (aldosterone: 12±1.5-fold vs cortisol: 3.1±0.3-fold, *P*=0.004). Moreover, cortisol output change remained less prominent in presence of stimulators K^+ (aldosterone: 30.9±3.1-fold vs cortisol:3.7±0.5-fold, *P*<0.001), AngII (aldosterone: 13.8±0.6-fold vs cortisol:2.7±0.2-fold, *P*<0.001) and forskolin (aldosterone: 16±0.5-fold vs cortisol:2.1±0.1-fold, *P*<0.001).

3.7.2. Steroidogenic Enzymes

CYP11B2, the rate limiting enzyme of aldosterone biosynthesis, catalyses the last step of the mineralocorticoid production pathway by oxidation of corticosterone to aldosterone in the ZG. CYP11B2 expression and aldosterone output of knockdown cells were simultaneously quantified. Lentiviral transduction alone, in accordance with its effects on aldosterone production (WT: 129.8±24.8 vs mock: 100±18.9 %, *P*=0.12) (Fig. 3.25B), did not affect CYP11B2 expression (WT: 119.2±4.9 vs mock: 100±27.7 %, *P*=0.56) (Fig. 3.25A). Comparison of transcript levels between control and knockdown cells revealed that the increases in aldosterone production after SLC26A2

Figure 3.24: Comparison of aldosterone and cortisol production of serum-starved SLC26A2 knockdown NCI-H295R cells. Aldosterone production increased 12-fold in knockdown cells in baseline conditions (**A**) in comparison to the threefold increase in cortisol output (**B**). Incubation of cells with KCl, AngII and forskolin further increased thealdosterone production change, whereas ratio of cortisol output increase was not affected by the presence of these aldosterone agonists. Values are plotted in base 10 logarithmic scale. * depicts significant differences between Mock and SLC26A2 Knockdown cells of the same treatment; # depicts significant differences between baseline and stimulated Mock Knockdown cells; § depicts significant differences between baseline and stimulated SLC26A2 Knockdown cells. For all groups, n=3.

knockdown (100±18.9 vs 767.9±70.4 %, $P<0.001$) were effected by upregulation of this enzyme (100±27.7 vs 553.1±30.1 %, $P<0.001$).

As the CYP11B2 found in ZG cells catalyzes late pathway of mineralocorticoid synthesis, CYP11B1 similarly facilitates glucocorticoid production in the zona fasciculata. Expression levels of these two enzymes in SLC26A2 knockdown NCI-H295R cells were quantified at baseline and aldosterone stimulating conditions. Expression of both steroidogenic enzymes were elevated in baseline conditions, with CYP11B2 increase being more prominent (CYP11B2: 2.2±0.1 vs CYP11B1: 1.5±0.1-

fold, P=0.004) (Fig. 3.26A&B). It was also observed that the SLC26A2 suppression had a more pronounced effect on CYP11B2 expression compared to CYP11B1 after stimulation with K^+ (1.4±0.1 vs 1.1±0.1-fold, P=0.03) or AngII (2±0.1 vs 1.5±0.1-fold, P=0.03). Forskolin induced elevation of cAMP levels increased transcription of both enzymes in a statistially indistiguishable manner (1.3±0.1 vs 1.4±0.05-fold, P=0.47).

Upstream of the latter steps of corticosteroid genesis catalyzed by P450 cytochromes, conversion of pregnenolone to progesterone, a precursor to all adrenal steroid production is catalyzed by the 3β hydroxysteroid dehydrogenase enzymes. After confirmation of detectability of both types in NCI-H295R cells by RT-PCR, their transcript levels were quantified in knockdown cells grown in normal and stimulatory conditions. Aldosterone agonists regulated the expression levels of HSD3B2 (baseline: 100±5.5, KCl: 277.2±25.2, angII: 173.0±19.1, forskolin: 509.4±49.4 %) (Fig. 3.27A), but not of HSD3B1 (baseline: 100±3.6, KCl: 101.9±15.7, angII: 107±12.4, forskolin: 100.5±3 %) (Fig. 3.27B), in control cells. Inreased expression of HSD3B2 in SLC26A2 knockdown cells compared to control cells was observed in all culture conditions (baseline: 100±5.5 vs 181.4±4.2 %, P<0.001; KCl: 277.2±25.2 vs 557.5±7.3 %, P<0.001; angII: 173.0±19.1 vs 266.8±8.9 %, P=0.011; forskolin: 509.4±49.4 vs 924.1±107.9 %, P=0.025). However, suppression of SLC26A2 did not alter HSD3B1 expression (baseline: 100.0±3.6 vs 91.8±4.6 %, P=0.234).

Aldosterone, same as other steroids, ultimately derives from cholesterol, after a chain of enzymatic convertions. The first link of this chain is the cleavage of the side chain of cholesterol at C20, catalyzed by CYP11A1 in the inner mitochondrial membrane. In SLC26A2 knockdown cells, transcript
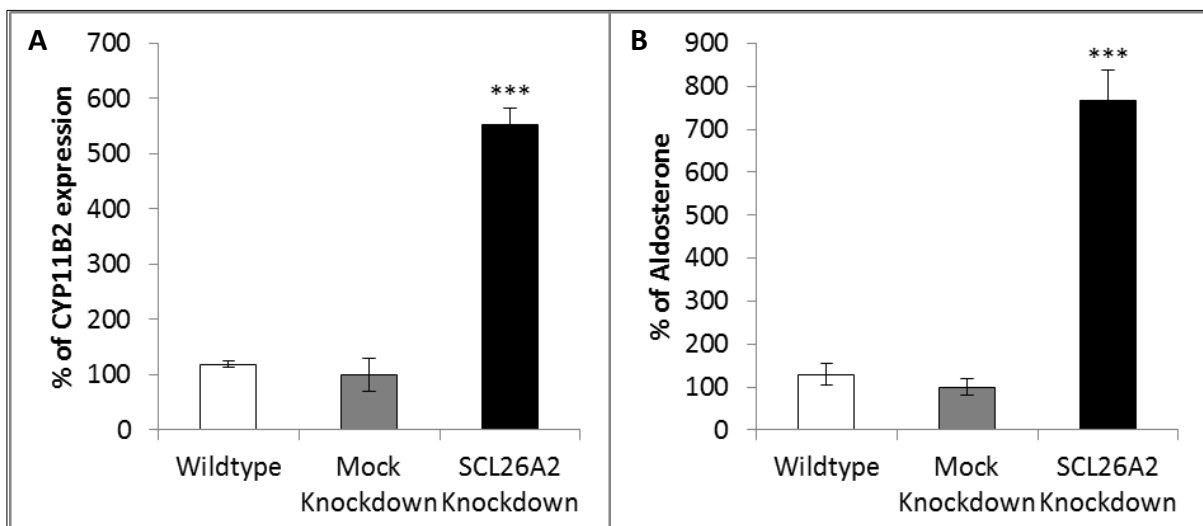
Figure 3.25: CYP11B2 expression of SLC26A2 knockdown NCI-H295R cells. Suppression of SLC26A2 expression increased CYP11B2 expression by 5.5-fold in knockdown cells (**A**) yielding a 7.6-fold aldosterone production increase (**B**). No significant differences between wild type and unspecific shRNA expressing cells were observed. * depicts significant differences between Mock and SLC26A2 Knockdown cells of the same treatment. For all groups, n=3.

Figure 3.26: Comparison of CYP11B2 (**A**) and CYP11B1 (**B**) expression in SLC26A2 knockdown NCI-H295R cells. CYP11B2 expression is 2.2-fold higher in knockdown cells under baseline conditions in contrast of the 1.4-fold increase in CYP11B1. The magnitude of increase was remained higher for CYP11B2 in presence of increased K^+ and AngII. Values are plotted in base 10 logarithmic scale. * depicts significant differences between Mock and SLC26A2 Knockdown cells of the same treatment; # depicts significant differences between baseline and stimulated Mock Knockdown cells; § depicts significant differences between baseline and stimulated SLC26A2 Knockdown cells. For all groups, n=3.

levels of CYP11A1 were found to be increased in comparison to control cells in baseline conditions as well as upon stimulation by aldosterone secretagogs (baseline: 100±12 vs 189.1±48.7 %, *P*=0.15; KCl: 150.8±17.7 vs 332.8±152.8 %, *P*=0.3; angII: 78.4±19 vs 271.4±30.2 %, *P*=0.006; forskolin: 150±15.9 vs 237.9±69.4 %, *P*=0.285) (Fig. 3.28).

On the acute level, the rate of adrenocortical steroid production is limited by the availability of cholesterol as the substrate of the reaction catalyzed by CYP11A1. Steroidogenic acute regulatory protein (STAR) facilitates transport of cholesterol from outer to inner mitochondrial membrane. The increase in aldosterone production upon SLC26A2 knockdown in NCI-H295R cells was found to be
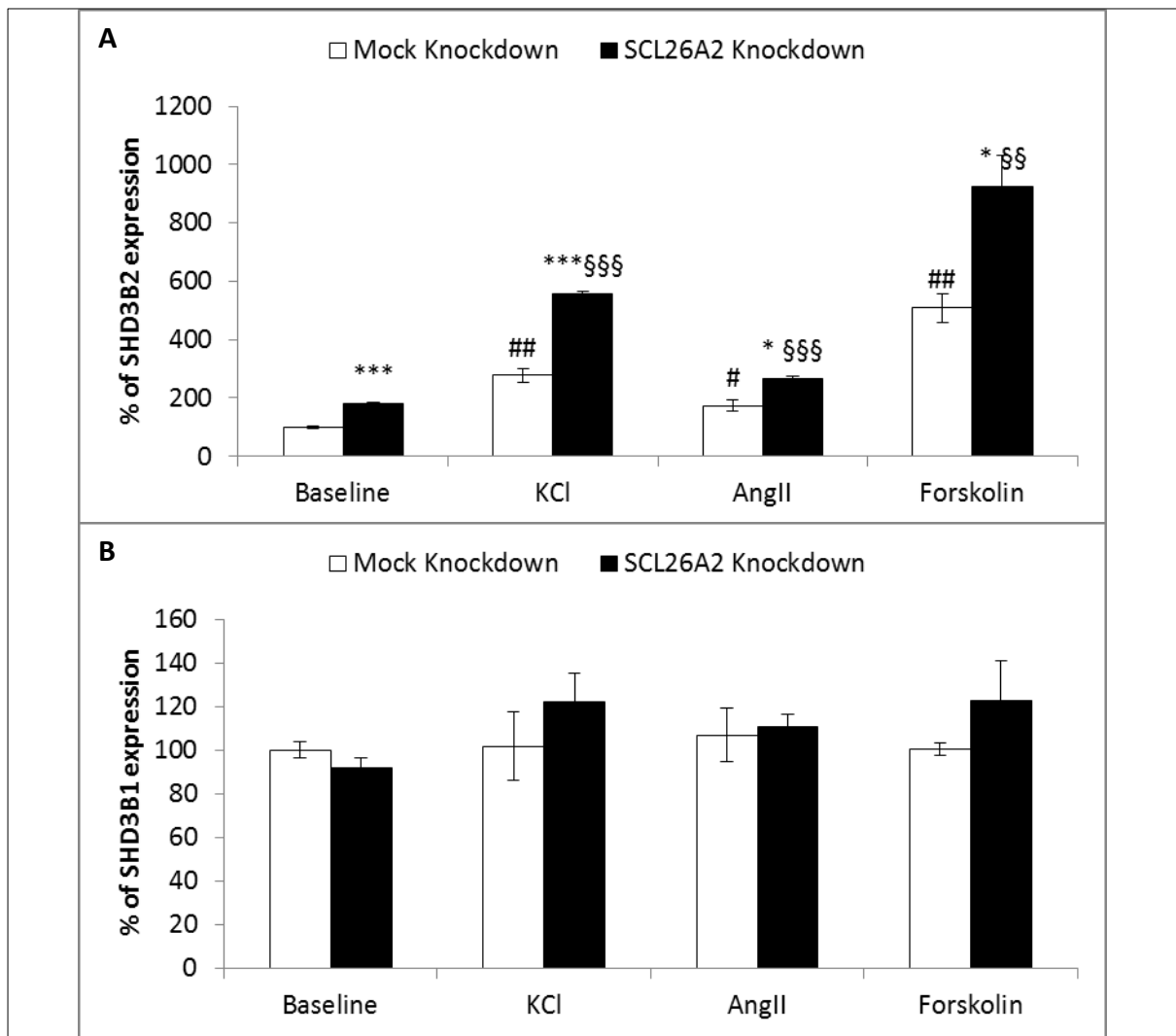
Figure 3.27: 3βHSD expression in SLC26A2 knockdown NCI-H295R cells. **A**, HSD3B2 expression was regulated by K^+, AngII and forskolin, as well as being upregulated in knockdown cells in all culture conditions. **B**, isozyme HSD3B1 expression was not regulated by SLC26A2 knockdown or aldosterone secretagogs. * depicts significant differences between Mock and SLC26A2 Knockdown cells of the same treatment; # depicts significant differences between baseline and stimulated Mock Knockdown cells; § depicts significant differences between baseline and stimulated SLC26A2 Knockdown cells. For all groups, n=3.

not due to the elevated STAR expression, since levels of STAR transcript in knockdown cells were not significantly different than controls in any growth condition aside from AngII induction (60.5±0.6 vs 107.5±2.2 %, *P*<0.001) (Fig. 3.29).

3.7.3. CAM Kinase Cascade

Calcium signalling in ZG cells acts as the main hub for mineralocorticoid production. Calcium / calmodulin dependent kinase 1 (CAMK1) has been shown to drive the upregulation of CYP11B2 in response to increased cytosolic calcium concentrations. Activation of CAMK1 effects increased expression of nuclear factors NR4A1 and NR4A2, which subsequently bind to *cis* elements in
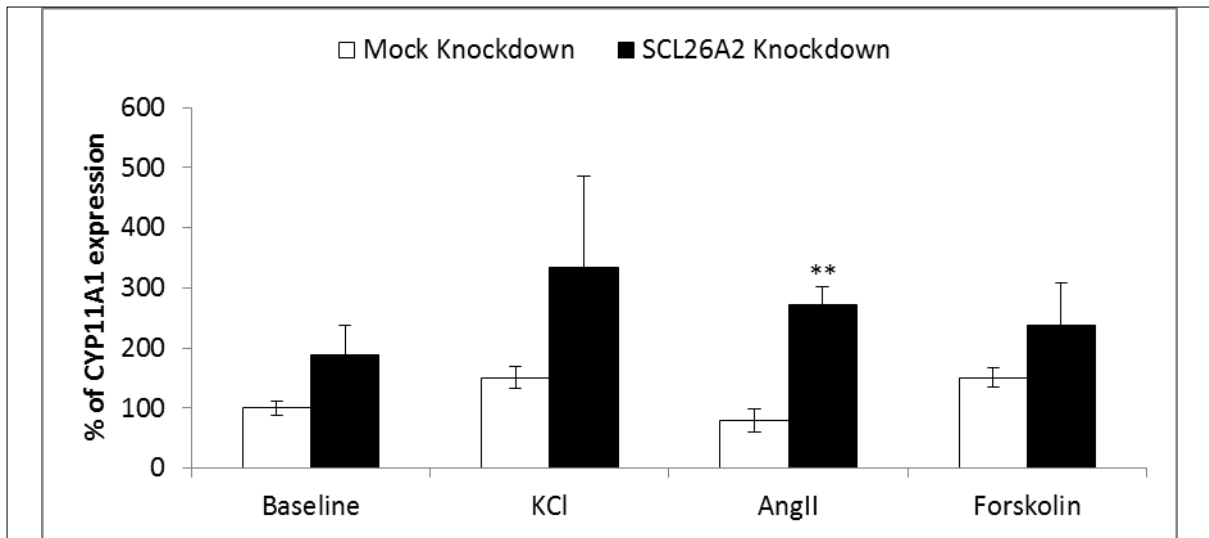
Figure 3.28: Side chain cleavage enzyme P450SCC (CYP11A1) expression in SLC26A2 knockdown NCI-H295R cells was elevated compared to control cells. * depicts significant differences between Mock and SLC26A2 Knockdown cells of the same treatment. For all groups, n=3.
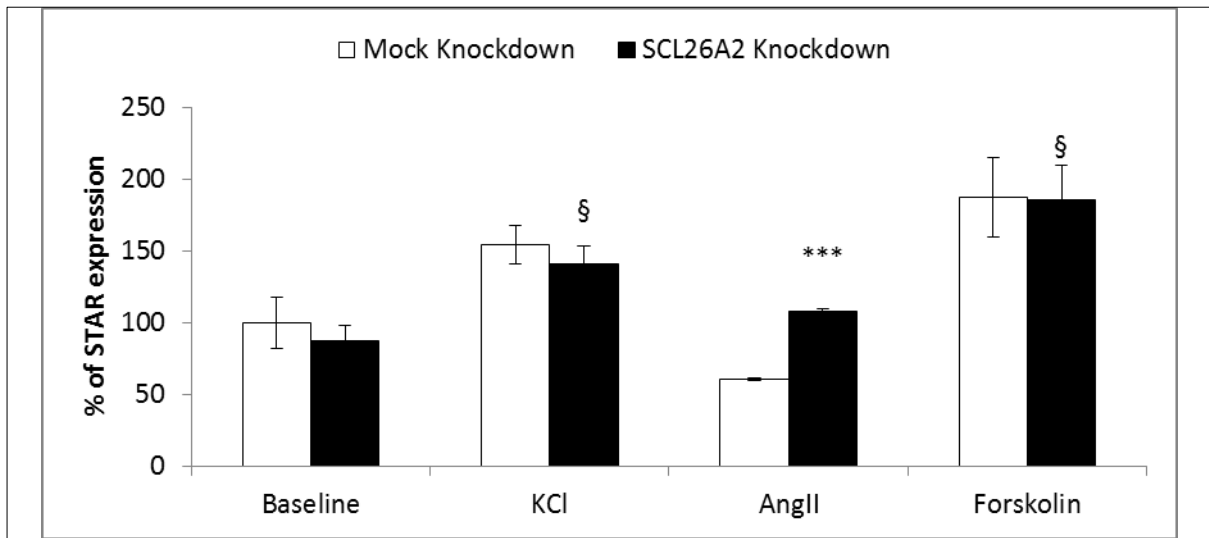
Figure 3.29: Steroidogenic acute regulatory protein (STAR) expression in SLC26A2 knockdown NCI-H295R cells. Expression levels remained in the same levels between knockdown and control cells, except for an upregulation in knockdown cells upon stimulation with AngII. * depicts significant differences between Mock and SLC26A2 Knockdown cells of the same treatment; § depicts significant differences between baseline and stimulated SLC26A2 Knockdown cells. For all groups, n=3.

CYP11B2 promoter, activating its trascription. NCI-H295R cells with the SLC26A2 knockdown was found to have almost two-fold increased CAMK1 mRNA levels under normal growth conditions, and similar increase with agonist induction (baseline: 100 ± 2.5 vs 180.7 ± 4.1 %, $P<0.001$; KCl: 94.4 ± 2.9 vs 154.7 ± 7.5 %, $P=0.002$; angII: 106.2 ± 5.4 vs 239 ± 10.6 %, $P<0.001$; forskolin: 45.2 ± 3.4 vs 77.7 ± 12.5 %, $P=0.067$) (Fig. 3.30A). Correspondingly, the nuclear factors NR4A1 and NR4A2, under transcriptional regulation of CAMK1, also showed increases in expression levels (baseline, NR4A1: 100 ± 1.6 vs 131.4 ± 3.4 %, $P=0.001$; NR4A2: 100 ± 6.1 vs 154.1 ± 6.2 %, $P=0.003$) (Fig. 3.30B&C). Only in the case of
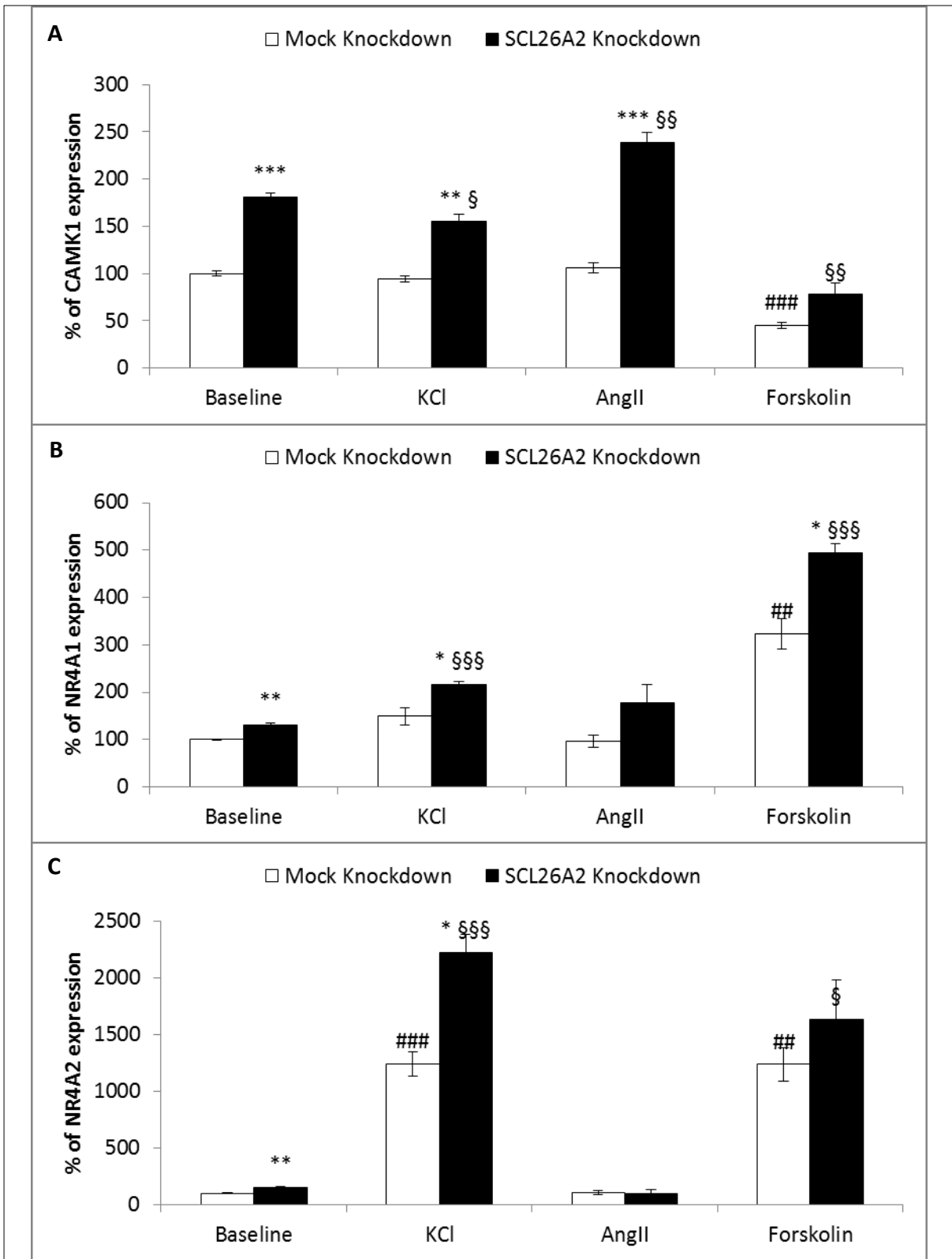
Figure 3.30: CAM kinase cascade in SLC26A2 knockdown cells. Expression levels of CAMK1 in knockdown cells were higher than in control cells in baseline and stimulating conditions (**A**). Transcription factors NGFIB (NR4A1) (**B**) and NURR1 (NR4A2) (**C**) were also upregulated in the knockdown cells. * depicts significant differences between Mock and SLC26A2 Knockdown cells of the same treatment; # depicts significant differences between baseline and stimulated Mock Knockdown cells; § depicts significant differences between baseline and stimulated SLC26A2 Knockdown cells. For all groups, n=3.

NR4A2 expression in cells stimulated with AngII, a difference between control and knockdown cells was not observed (107.2±16.9 vs 102.0±29.6 %, *P*=0.885).

A western blot analysis was conducted to deduce changes in phosphorytation levels of CREB1, a CAMK1 activated transcription factor which binds to cAMP response elements upstream of CYP11B2. 20 µg of total protein from lysates of control and knockdown cells under baseline and stimulating conditions were loaded on the gels. Upon application of antibodies against phosphorylated CREB1 and beta actin and subsequent visualization of peroxidase activity, increases in phosphorylated CREB1 levels in knockdown cells were observed in baseline (100 vs 133 %), AngII (78 vs 151 %) and forskolin (140 vs 181 %) treatments (Fig. 3.31A&B).

Figure 3.31: Phosphorylated CREB1 levels of SLC26A2 knockdown cells. **A**, Western blot analysis reveals increased intensity of phosporylated CREB1 bands in knockdown cells under baseline condition and AngII or forskolin stimulation. **B**, Quantification of band intensities and normalization with β-actin levels are plotted. For all groups, n=1.
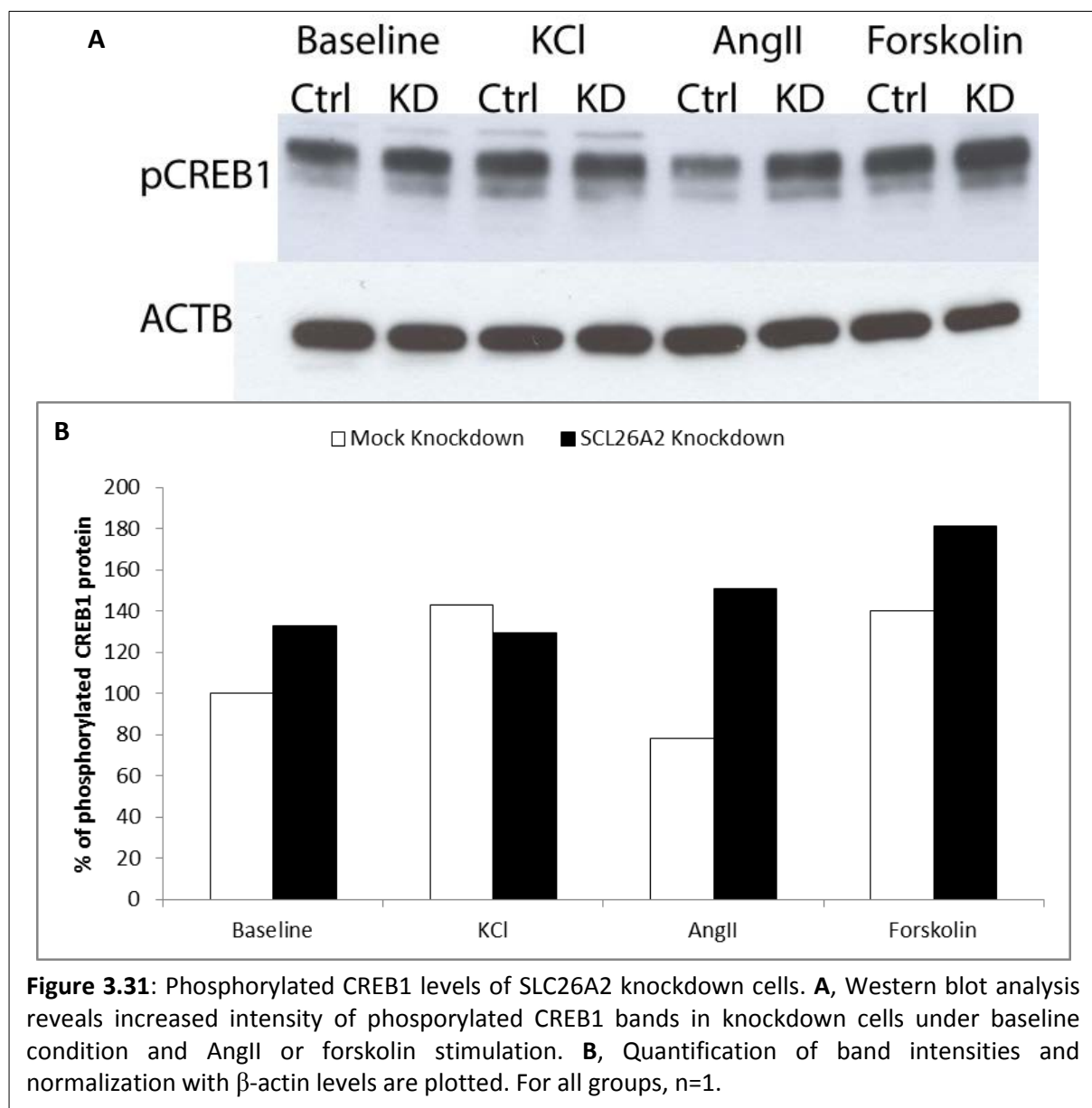
3.7.4. Intracellular Ion Content

The expression changes in the components of calcium signalling cascade led to investigation of intracellular Ca^{2+} levels. Mean fluorecense ratios (mfr) were calculated for control and knockdown cells using the radiometric Ca^{2+} indicator Fura-2-AM with Ringer's type or increased Ca^{2+} and K^+ extracellular solution. Intracellular calcium levels were significantly elevated in SLC26A2 knockdown cells compared to controls (Ringer's: 1.262±0.014 vs 1.334±0.013 mfr, P<0.001; Ca^{2+}: 1.387±0.02 vs 1.509±0.021 mfr, P<0.001; KCl: 1.365±0.026 vs 1.452±0.016 mfr, P<0.001) (Fig. 3.32). Investigating levels of the electrolytes Na^+ (WT: 21.0±1.6, mock: 17.4±1.2, KD: 22.9±2.0 mmol/kg) (Fig. 3.33A), Cl^- (WT: 36.9±2.3, mock: 32.7±1.2, KD: 35.1±1.7 mmol/kg) (Fig. 3.33B) and K^+ (WT: 132.2±6.4, mock: 118.8±3.8, KD: 130±2.9 mmol/kg) (Fig. 3.33C) by electron microprobe analysis revealed a decreasing effect of lentiviral transduction and a slight increase in knockdown cells compared to controls.
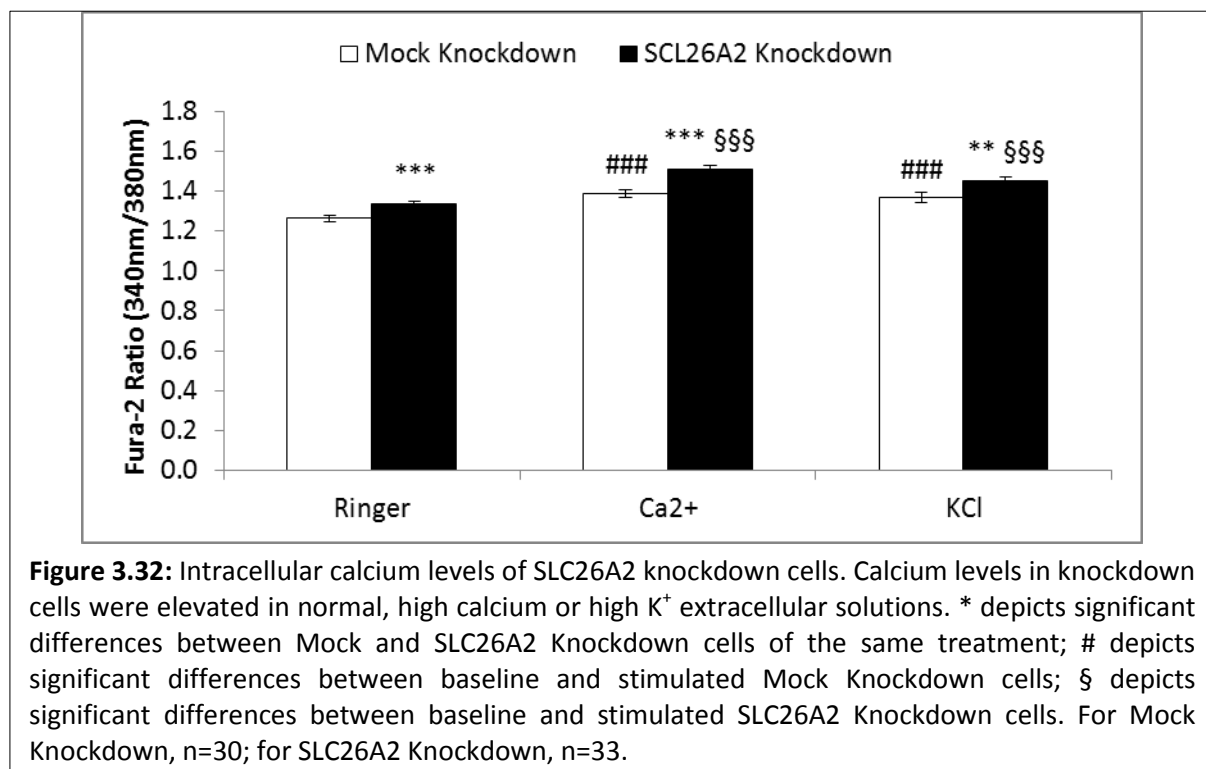
Figure 3.32: Intracellular calcium levels of SLC26A2 knockdown cells. Calcium levels in knockdown cells were elevated in normal, high calcium or high K^+ extracellular solutions. * depicts significant differences between Mock and SLC26A2 Knockdown cells of the same treatment; # depicts significant differences between baseline and stimulated Mock Knockdown cells; § depicts significant differences between baseline and stimulated SLC26A2 Knockdown cells. For Mock Knockdown, n=30; for SLC26A2 Knockdown, n=33.

3.7.5. Pharmacological Inhibition

As chronic response to agonists of aldosterone production in ZG cells is achieved by upregulation of CYP11B2 expression, mediated by Ca^{2+}/CaM dependent kinases, increased expression of CAMK1 and related nuclear factors in SLC26A2 knockdown cells necessitated further investigation of calcium signalling events. Effects of intracellular Ca^{2+} are beared to Ca^{2+} dependent enzymes via the ubiquitous calcium binding protein calmodulin. Using the CaM inhibitor calmidazolium, the elevating effect of knockdown on the aldosterone production of cells (100±12.9 vs 151.5±7.5 %, *P*=0.026) were

reduced to levels below statistical significance (74.6±9.6 vs 90.7±4.1 %, P=0.197) (Fig. 3.34). Furthermore, competitive inhibition of Ca^{2+}/CaM dependent protein kinases against calmodulin by the compound KN-93 completely nullified the phenomenon of increased aldosterone production in response to SLC26A2 knockdown (34.6±2.4 vs 22.7±1.4 %, P=0.013).
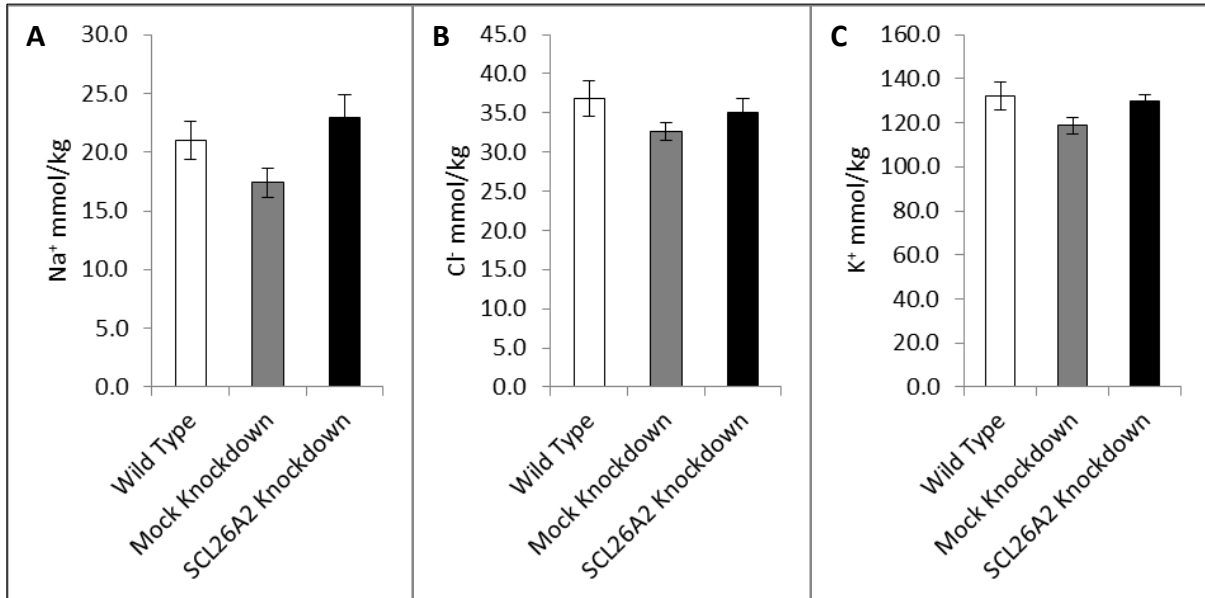
Figure 3.33: Sodium (**A**), chloride (**B**) and K^+ (**C**) contents of SLC26A2 knockdown NCI-H295R cells. Lentiviral transduction had a lowering effect on these ions; with SLC26A2 suppression elevating them to wild type levels. However, these differences were not statistically significant. For all groups, n=3.
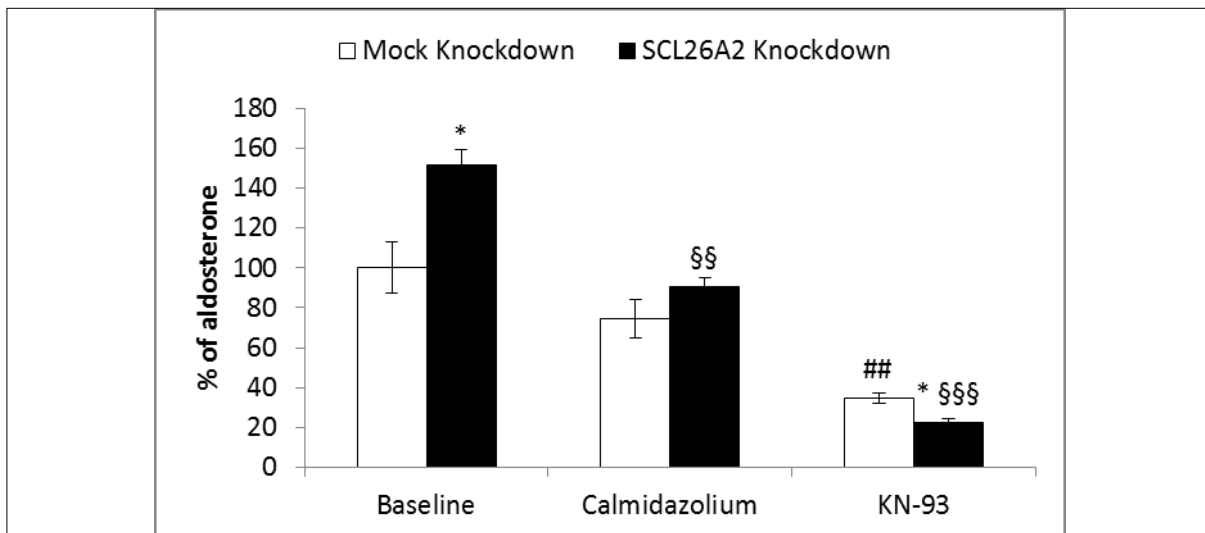
Figure 3.34: Pharmacological inhibition of CAM kinase cascade. The SLC26A2 suppression induced increase of aldosterone production was reduced by inhibition of calmodulin with the drug calmidazolium and completely negated by arresting the activation of CAM kinases with the inhibitor KN-93. * depicts significant differences between Mock and SLC26A2 Knockdown cells of the same treatment; # depicts significant differences between baseline and stimulated Mock Knockdown cells; § depicts significant differences between baseline and stimulated SLC26A2 Knockdown cells. For all groups, n=3.

3.7.6. Gene Expression Analysis

Investigation of the mechanisms by which the SLC26A2 knockdown affects calcium signaling cascade to effect increased aldosterone production was carried on by microarray whole transcriptome expression profiling on Affymetrix Human Gene 1.0 ST Arrays. Preparations from control and SLC26A2 knockdown NCI-H295R total RNA extracts were hybridized to arrays, with three separately handled samples per group. Fold-change calculations revealed that 58 genes were above the 2-fold change cutoff, with 20 being up-regulated and 38 being down-regulated in knockdown cells (Table 3.1).

The microarray data set was validated for the genes CYP11B2, CAMK1 and MC2R by RT-PCR. The array data for these genes yielded 1.17-fold, 1.23-fold and 2.82 fold increase in knockdown samples, respectively. Validation by RT-PCR using the same RNA samples, however, yielded 4-fold increase for CYP11B2 (100.0 ± 14.7 vs 414.4 ± 27.8 %, $P<0.001$), 1.5-fold increase for CAMK1 (100.0 ± 4.2 vs 153.7 ± 2.7 %, $P<0.001$) and 3.6-fold increase for MC2R (100.0 ± 14.5 vs 364.4 ± 59.2 %, $P=0.012$) in knockdown cells (Fig. 3.35). The discrepancy between data from two methods indicates an underrepresentation of differential gene expression regulation by the microarray method.

The microarray data was used to analyze which pathways and processes were affected the most by the knockdown of SLC26A2. Functional annotation enrichment was applied on genes 2-fold up or down regulated. The meager number of genes passing this criterion indicated only two pathways (Table 3.2). Transmembrane transport of small molecules was enriched by upregulated genes, and integrin cell surface interactions were enriched by the downregulated genes. Upregulated genes also indicated the ontology process terms of organic acid transport, cytokine production, along with cellular compartment term plasma membrane and functional term amino acid transport. Downregulated genes enriched process terms cell surface receptor linked signal transduction and fatty acid metabolic process, as well as cellular compartment term plasma membrane, but no molecular function terms.

All of these pathways and ontology terms were weakly enriched by a small number of hits from the limited set of 2-fold regulated genes (Table 3.2). Using the whole transcriptome data, heat maps were generated for Gene Ontology terms [150] (Fig. 3.36A) and KEGG pathways [154] (Fig. 3.36B). Also a list of genes with relevance to aldosterone biosynthesis and function or to SLC26A2 was compiled (Table 3.3). Finally, the genes with significantly different expression levels between control and knockdown cells (P<0.05) were used to enrich Wikipathways [163] and Reactome pathways [159], using the Pathvisio pathway analysis program [156]. Top three scoring pathways were insuling signaling (Z score: 5.43), cardiac hypertrophic response (Z score: 5.05) and MAPK cascade (Z score:

HUGO Gene Symbol	Gene Description	Gene Accession	Knockdown vs Control Fold Change	Knockdown vs Control *P*-value
PDE3A	phosphodiesterase 3A, cGMP-inhibited	NM_000921	2.9348	3.91E-04
MC2R	melanocortin 2 receptor (adrenocorticotropic hormone)	NM_000529	2.8199	6.04E-05
PLK2	polo-like kinase 2	NM_006622	2.7618	4.51E-06
TSPAN8	tetraspanin 8	NM_004616	2.7081	4.93E-05
TRIB3	tribbles homolog 3 (Drosophila)	NM_021158	2.5743	1.23E-04
DPP4	dipeptidyl-peptidase 4	NM_001935	2.4798	4.53E-06
INHBE	inhibin, beta E	NM_031479	2.4134	1.19E-03
NFATC2	nuclear factor of activated T-cells, cytoplasmic, calcineurin-dependent 2	NM_012340	2.3926	1.47E-05
SLC16A6	solute carrier family 16, member 6 (monocarboxylic acid transporter 7)	NM_001174166	2.3549	1.39E-04
BEST1	bestrophin 1	NM_004183	2.2896	1.15E-03
SLC43A1	solute carrier family 43, member 1	NM_003627	2.2831	7.63E-05
ETV5	ets variant 5	NM_004454	2.2773	2.39E-05
TNFAIP3	tumor necrosis factor, alpha-induced protein 3	NM_006290	2.1585	2.54E-05
LPPR1	lipid phosphate phosphatase-related protein type 1	NM_207299	2.1339	1.56E-05
C9orf84	chromosome 9 open reading frame 84	NM_173521	2.1336	4.51E-06
CHAC1	ChaC, cation transport regulator homolog 1 (E. coli)	NM_024111	2.1202	4.84E-04
TNFSF4	tumor necrosis factor (ligand) superfamily, member 4	NM_003326	2.1023	3.19E-05
LOC644714	hypothetical LOC644714	BC047037	2.0756	2.26E-02
DDIT3	DNA-damage-inducible transcript 3	NM_001195053	2.0051	1.48E-04
SLC7A1	solute carrier family 7 (cationic amino acid transporter, y+ system), member 1	NM_003045	2.0016	1.34E-05
ZNF486	zinc finger protein 486	NM_052852	-2.0199	6.83E-04
FLJ38894	hypothetical protein LOC646029	AK096213	-2.0224	2.90E-06
PTPRZ1	protein tyrosine phosphatase, receptor-type, Z polypeptide 1	NM_002851	-2.0297	1.39E-05
INA	internexin neuronal intermediate filament protein, alpha	NM_032727	-2.0505	3.31E-04
GFRA2	GDNF family receptor alpha 2	NM_001495	-2.0619	1.93E-03
EPCAM	epithelial cell adhesion molecule	NM_002354	-2.0620	6.43E-05
SPP1	secreted phosphoprotein 1	NM_001040058	-2.0712	6.16E-05
HAVCR2	hepatitis A virus cellular receptor 2	NM_032782	-2.0748	1.93E-04
PLP1	proteolipid protein 1	NM_000533	-2.1305	2.28E-06
PCDH20	protocadherin 20	NM_022843	-2.1667	7.53E-05
LPPR4	lipid phosphate phosphatase-related protein type 4	NM_014839	-2.1709	3.23E-05
RALYL	RALY RNA binding protein-like	NM_173848	-2.1952	1.33E-04
AKR1C3	aldo-keto reductase family 1, member C3 (3-alpha hydroxysteroid dehydrogenase, type II)	NM_003739	-2.2265	1.75E-05
NDP	Norrie disease (pseudoglioma)	NM_000266	-2.2524	1.68E-05
PCDHB17	protocadherin beta 17 pseudogene	NR_001280	-2.2724	1.16E-03
ITGA8	integrin, alpha 8	NM_003638	-2.2859	4.55E-04
CADPS	Ca++-dependent secretion activator	NM_003716	-2.3034	3.52E-05
CNTN1	contactin 1	NM_001843	-2.3630	4.85E-04
GPR183	G protein-coupled receptor 183	NM_004951	-2.3844	1.01E-04
FGFR2	fibroblast growth factor receptor 2	NM_000141	-2.4042	1.91E-05
RAB3C	RAB3C, member RAS oncogene family	NM_138453	-2.4046	1.71E-06
SLC26A2	solute carrier family 26 (sulfate transporter), member 2	NM_000112	-2.4206	4.51E-06
SEZ6L	seizure related 6 homolog (mouse)-like	NM_021115	-2.4440	3.44E-05
C11orf92	chromosome 11 open reading frame 92	NR_034154	-2.5139	3.58E-05
ZNF737	zinc finger protein 737	NM_001159293	-2.5383	6.46E-04
FAM102B	family with sequence similarity 102, member B	NM_001010883	-2.5603	5.81E-06
MYOT	myotilin	NM_006790	-2.6300	1.06E-06
SLC36A2	solute carrier family 36 (proton/amino acid symporter), member 2	NM_181776	-2.6479	3.55E-05
ZNF676	zinc finger protein 676	NM_001001411	-2.6917	1.66E-03
SFRP1	secreted frizzled-related protein 1	NM_003012	-2.6919	1.13E-05
ELOVL2	elongation of very long chain fatty acids (FEN1/Elo2, SUR4/Elo3, yeast)-like 2	NM_017770	-2.7390	2.04E-04
CD109	CD109 molecule	NM_133493	-2.7587	2.29E-04
LMLN	leishmanolysin-like (metallopeptidase M8 family)	NM_001136049	-2.8253	6.66E-05
EPCAM	epithelial cell adhesion molecule	NM_002354	-3.2090	1.36E-03
CALB1	calbindin 1, 28kDa	NM_004929	-3.4670	2.12E-06
PRUNE2	prune homolog 2 (Drosophila)	NM_015225	-3.7422	7.41E-05
NPY1R	neuropeptide Y receptor Y1	NM_000909	-4.8297	3.72E-06
GABRG1	gamma-aminobutyric acid (GABA) A receptor, gamma 1	NM_173536	-6.5800	5.64E-07

Table 3.1: List of genes with over 2-fold change in expression between control and SLC26A2 knockdown NCI-H295R cells.

4.6). Of these, the regulation of Map kinase components were plotted on a pathway map with knockdown vs control cell expression fold changes depicted in values and a color gradient (Fig. 3.37).
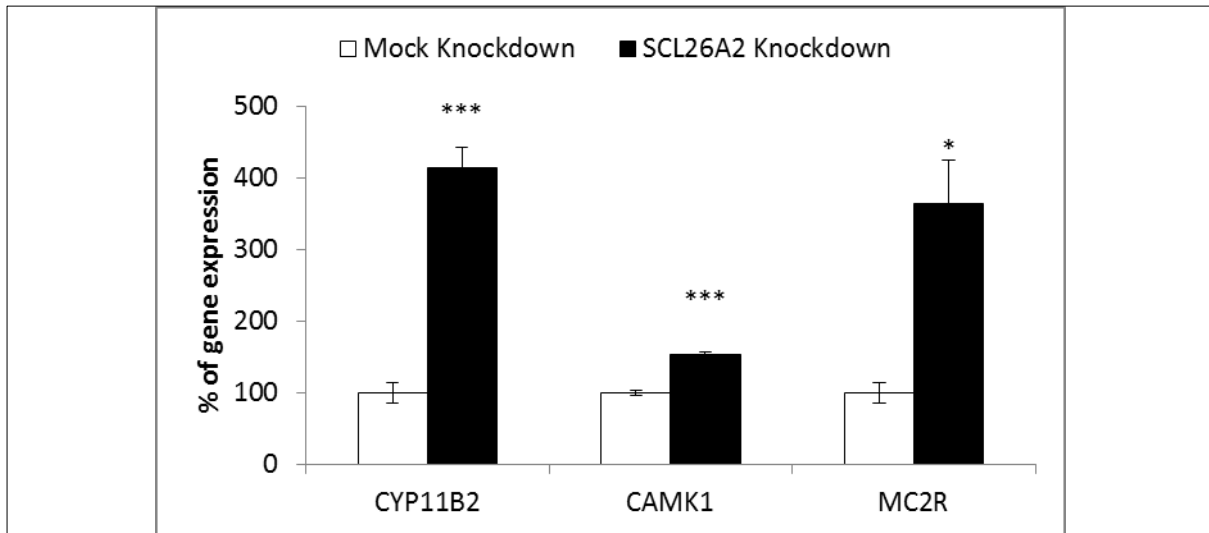
Figure 3.35: Validation of microarray gene expression analysis by RT-PCR. Quantification of CYP11B2, CAMK1 ad MC2R expression with PCR presented a higher level of change between knockdown and control cells compared to microarray analysis. * depicts significant differences between Mock and SLC26A2 Knockdown cells. For all groups, n=3.
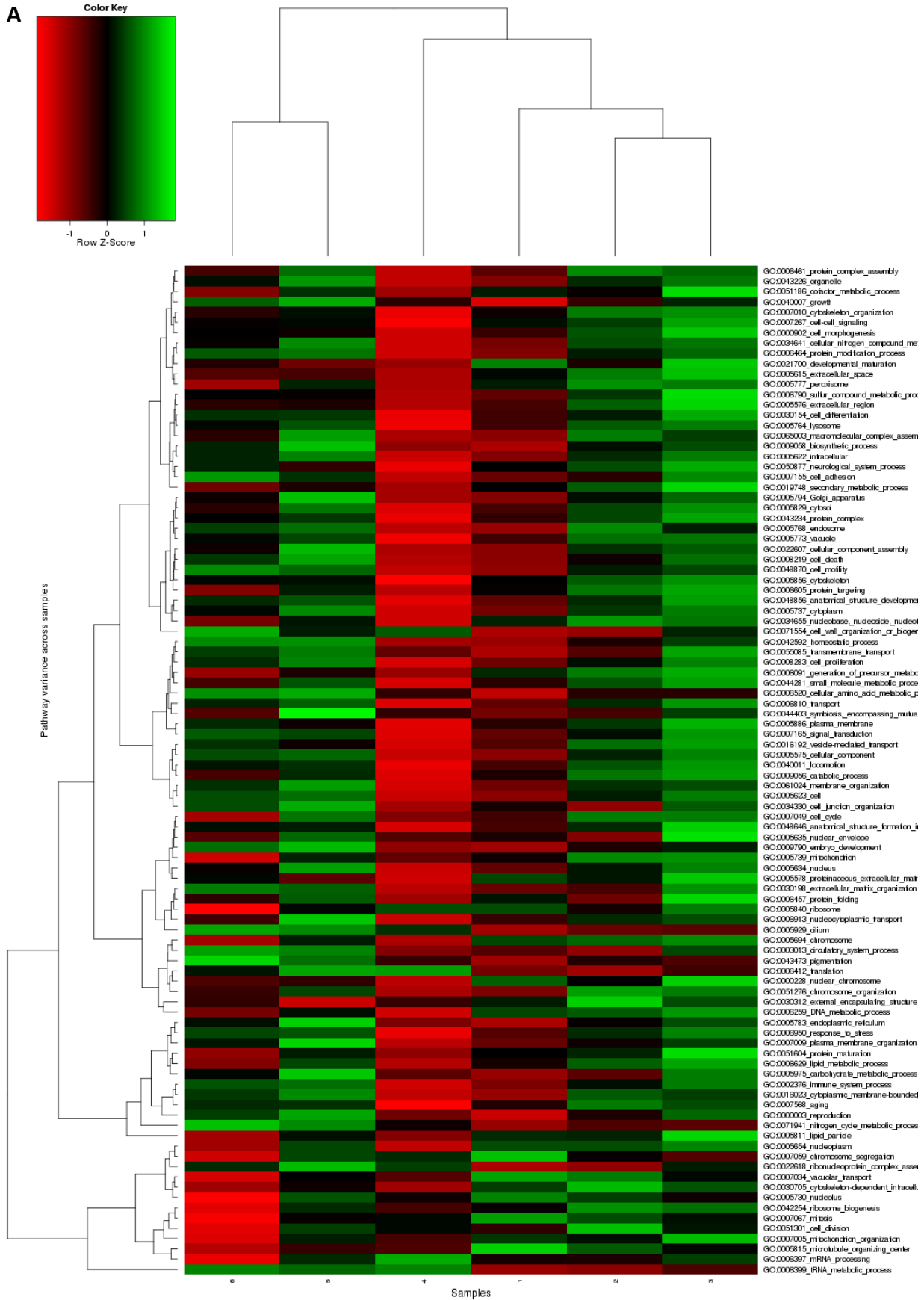
Enrichment of genes with over 2-fold upregulation in SLC26A2 knockdown cells

Category	Term	Genes	Count	%	P Value	Benjamini
REACTOME_PATHWAY	REACT_15518:Transmembrane transport of small molecules		2	10.0	4.9E 2	2.6E 1

Category	Term	Genes	Count	%	P Value	Benjamini
GOTERM_BP_FAT	carboxylic acid transport		3	15.0	9.8E 3	9.0E 1
GOTERM_BP_FAT	organic acid transport		3	15.0	9.9E 3	6.8E 1
GOTERM_BP_FAT	negative regulation of molecular function		3	15.0	4.5E 2	9.7E 1
GOTERM_BP_FAT	negative regulation of transcription factor activity		2	10.0	4.6E 2	9.3E 1
GOTERM_BP_FAT	cytokine production		2	10.0	4.7E 2	8.9E 1
GOTERM_BP_FAT	negative regulation of DNA binding		2	10.0	5.2E 2	8.7E 1
GOTERM_BP_FAT	negative regulation of binding		2	10.0	5.9E 2	8.7E 1
GOTERM_BP_FAT	amino acid transport		2	10.0	8.9E 2	9.3E 1
GOTERM_BP_FAT	regulation of immune effector process		2	10.0	1.0E 1	9.3E 1

Category	Term	Genes	Count	%	P Value	Benjamini
GOTERM_CC_FAT	plasma membrane part		7	35.0	1.5E 2	4.6E 1
GOTERM_CC_FAT	integral to plasma membrane		5	25.0	2.7E 2	4.3E 1
GOTERM_CC_FAT	intrinsic to plasma membrane		5	25.0	2.9E 2	3.3E 1
GOTERM_CC_FAT	insoluble fraction		4	20.0	4.9E 2	4.0E 1
GOTERM_CC_FAT	cell fraction		4	20.0	9.1E 2	5.4E 1

Category	Term	Genes	Count	%	P Value	Benjamini
GOTERM_MF_FAT	L amino acid transmembrane transporter activity		2	10.0	4.0E 2	9.7E 1
GOTERM_MF_FAT	amino acid transmembrane transporter activity		2	10.0	6.2E 2	9.4E 1
GOTERM_MF_FAT	amine transmembrane transporter activity		2	10.0	7.7E 2	9.1E 1

Enrichment of genes with over 2-fold downregulation in SLC26A2 knockdown cells

Category	Term	Genes	Count	%	P Value	Benjamini
REACTOME_PATHWAY	REACT_13552:Integrin cell surface interactions		2	5.6	9.2E 2	4.4E 1

Category	Term	Genes	Count	%	P Value	Benjamini
GOTERM_BP_FAT	cell surface receptor linked signal transduction		10	27.8	1.0E 2	9.7E 1
GOTERM_BP_FAT	cell adhesion		6	16.7	1.3E 2	9.0E 1
GOTERM_BP_FAT	biological adhesion		6	16.7	1.3E 2	7.8E 1
GOTERM_BP_FAT	fatty acid metabolic process		3	8.3	6.3E 2	1.0E0
GOTERM_BP_FAT	neurological system process		6	16.7	1.0E 1	1.0E0

Category	Term	Genes	Count	%	P Value	Benjamini
GOTERM_CC_FAT	plasma membrane		17	47.2	1.2E 3	8.8E 2
GOTERM_CC_FAT	intrinsic to membrane		20	55.6	3.6E 3	1.3E 1
GOTERM_CC_FAT	synapse		5	13.9	6.2E 3	1.4E 1
GOTERM_CC_FAT	plasma membrane part		11	30.6	1.1E 2	1.9E 1
GOTERM_CC_FAT	synapse part		4	11.1	1.5E 2	2.0E 1
GOTERM_CC_FAT	integral to membrane		17	47.2	4.7E 2	4.5E 1
GOTERM_CC_FAT	apical part of cell		3	8.3	5.4E 2	4.5E 1
GOTERM_CC_FAT	anchored to membrane		3	8.3	7.8E 2	5.3E 1
GOTERM_CC_FAT	integral to plasma membrane		6	16.7	1.0E 1	5.8E 1

Table 3.2: Reactome pathway and Gene Ontology term enrichment scores for genes with over 2-fold expression difference between control and SLC26A2 knockdown cells. Count of involved genes per term, % of involved genes / total genes, modified Fisher Exact *P* value and Benjamini scores are listed.

Figure 3.36: Gene expression microarray data heat maps for Gene Ontology terms **(A)** and KEGG pathways **(B)**. Samples 1,2 and 3 are control cells; 4,5 and 6 are SLC26A2 knockdown cells.
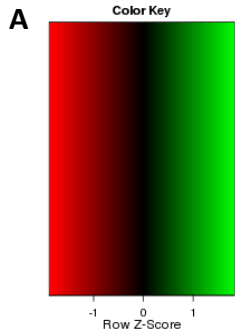
Table 3.3 (rotated landscape table). Columns grouped in three sets, each with: Aldosterone & SLC26A2 Relevance | HUGO Gene Symbol | Knock-down vs Control Fold Change | Knock-down vs Control P-value.

Relevance (set 1)	Gene	Fold Change	P-value	Relevance (set 2)	Gene	Fold Change	P-value	Relevance (set 3)	Gene	Fold Change	P-value
somatic APA mutations found	PLCL2	1.180	0.008	somatic APA mutations found	ATP1A1	-1.130	0.000	MAP kinases	MAPK1	-1.014	0.020
	PLCE1	1.152	0.007		CACNA1D	-1.217	0.000		MAPK10	-1.015	0.618
mouse models of PA	PLCL1	1.087	0.358	mouse models of PA	KCNK9	1.237	0.010		MAPK8IP1	-1.016	0.466
	PLCD4	1.073	0.383		KCNK3	1.055	0.071		MAPK14	-1.019	0.347
	PLCH1	1.069	0.468		CRY2	1.013	0.710		MAPKBP1	-1.022	0.649
	PLCB1	1.036	0.217		CRY1	-1.003	0.825		MAPK12	-1.025	0.462
phospho-lipase C	PLCD1	1.017	0.711	calcium signalling	CAMK1	1.230	0.025		MAPK8IP2	-1.041	0.456
	PLCZ1	1.014	0.309		PPP3R1	1.168	0.003		MAPKSP1	-1.042	0.386
	PLCG1	1.012	0.630		PPP3CC	1.148	0.026		MAPK8IP1	-1.043	0.292
	PLCG2	1.008	0.890		CAMK2A	1.082	0.051		MAPK8IP3	-1.049	0.094
	PLCD3	-1.009	0.679		PPP3R2	-1.012	0.888		MAPK11	-1.056	0.340
	PLCH2	-1.030	0.158		CAMKK1	-1.033	0.558		MAPKAP1	-1.056	0.011
	PLCB4	-1.034	0.487		CALM2	-1.037	0.105		MAPKAPK2	-1.058	0.147
	PLCB2	-1.040	0.190		CALM2	-1.037	0.105		MAPK9	-1.072	0.097
	PLCXD3	-1.049	0.429		CAMK1G	-1.040	0.177		MAPK13	-1.144	0.066
	PLCXD1	-1.059	0.102		CAMK2N2	-1.047	0.021		MAPK8	-1.158	0.000
	PLCXD1	-1.059	0.093		CAMK1D	-1.048	0.274		MAPK3	-1.173	0.001
	PLCXD2	-1.061	0.375		CAMK2G	-1.068	0.048		MAPKAPK3	-1.176	0.006
	PLCB3	-1.278	0.003		CAMK2D	-1.082	0.022		MAPK4	-1.773	0.001
phospho-diesterase 3	PDE3A	2.935	0.000		CAMK2N1	-1.083	0.010	adrenocortical streoidogenic enzymes	CYP21A2	1.773	0.000
	PDE3B	-1.041	0.582		CAMKK2	-1.097	0.023		CYP11B1	1.257	0.027
protein kinase C	PRKCH	1.919	0.000		PPP3CA	-1.120	0.002		CYP11B2	1.170	0.203
	PRKCQ	1.184	0.004		PPP3CB	-1.123	0.038		STAR	-1.005	0.422
	PRKCG	1.071	0.457		CAMKV	-1.147	0.052		CYP11A1	-1.065	0.027
	PRKCSH	1.031	0.031		CAMK4	-1.281	0.016		CYP17A1	-1.386	0.000
	PRKCDBP	1.004	0.943		CALM1	-1.310	0.000	cholesterol uptake / synthesis	ACSS1	1.329	0.000
	PRKCB	-1.044	0.195		CAMK2B	-1.319	0.004		APOA1	-1.023	0.739
	PRKCZ	-1.057	0.067	steroidogenic transcription factors	CREBL2	1.291	0.000		APOA1	-1.027	0.682
	PRKCA	-1.098	0.058		CREB3L4	1.272	0.013		SCARB1	-1.105	0.004
	PRKCI	-1.114	0.007		CREB3L2	1.140	0.003		CETP	-1.124	0.218
	PRKCD	-1.205	0.004		NR5A1	1.093	0.010		LPL	-1.704	0.000
	PRKCE	-1.294	0.004		CREBBP	1.072	0.036	cardiac hypertrophic response	NFATC2	2.393	0.000
protein kinase A	PRKACA	1.010	0.445		CREBZF	1.044	0.318		FGF23	1.017	0.652
	PRKACB	-1.025	0.272		CREB3	1.031	0.154		FGF2	-1.143	0.001
	PRKACG	-1.062	0.102		NR4A1	1.029	0.086		FGFR2	-2.404	0.000
angiotensin II receptor	AGTR1	1.134	0.005		CREB3L1	1.011	0.860	ras signalling	NRAS	-1.004	0.867
	AGTRAP	1.066	0.293		CREB1	1.007	0.868		HRAS	-1.056	0.029
	AGTR2	-1.005	0.943		NR4A2	-1.017	0.758		KRAS	-1.097	0.024
ACTH receptor	MC2R	2.820	0.000		CREB3L3	-1.046	0.463	putative SLC26A2 interacting	LGALS8	1.469	0.001
	DAB2	1.108	0.015		CREB5	-1.050	0.441		LGALS3	1.069	0.060
ZG localized	NCAM1	1.067	0.020	MAP kinases	MAPKAPK5	1.119	0.006		VAPB	1.026	0.484
	DKK3	-1.249	0.000		MAPK6	1.094	0.193		ERGIC3	1.017	0.522
	DKK3	-1.027	0.510		MAPK7	1.006	0.852		MGAT4B	-1.025	0.416
somatic APA mutations found	KCNJ5	1.257	0.000		MAPK8IP1	1.003	0.890		UBC	-1.027	0.166
	CTNNB1	1.033	0.002		MAPK15	-1.007	0.908		FAM189A2	-1.044	0.326
	ATP2B3	-1.051	0.267		MAPK1IP1L	-1.013	0.549		NNT	-1.078	0.000

Table 3.3: SLC26A2 knockdown vs control expression fold change values and significance levels of genes related to SLC26A2 or aldosterone production and function.

Figure 3.37: SLC26A2 knockdown induced expression changes of MAP kinase pathway genes in NCI-H295R cells. Green depicts downregulation and red depicts supregulation of the gene in knockdown cells. Color intensity is proportional to fold-change of the gene. Fold change values are given to the left of each data node.

3.8. Targeting SLC26A2 *in vivo*

3.8.1. SLC26A2 Knock-In Mutant Mice

Ever since the demonstration of anthrax toxin's lethality changes depending whether it is obtained in culture or from an infection [**183**], complementing *in vitro* findings with *in vivo* studies has been consensus in the scientific community. Therefore, substantiation of the effects seen in NCI-H295R cells upon SLC26A2 knockdown by observations from live organisms was sought. To this purpose, an *Slc26a2* knock-in mutant mouse model was employed. These mice harbored A386V substitution in the *Slc26a2* gene, a mutation detected in a patient with non-lethal diastrophic dysplasia. Along with this mutation, the knock-in process caused impaired splicing of intron 2 of the gene. Homozygous animals had diminished sulfate uptake by chondrocytes, giving way to impaired growth and reduced body weight and motor function as well as sharply decreased lifespan.

In order to evaluate endocrine profile of the *Slc26a2* mutant mouse model, adrenal glands of wild type and mutant animals, along with plasma samples, were obtained. Formalin fixed-paraffin embedded adrenal gland samples were investigated by H&E staining. Comparison of wild-type and mutant samples from both sexes did not reveal any morphological differences (Fig. 3.38A-D).
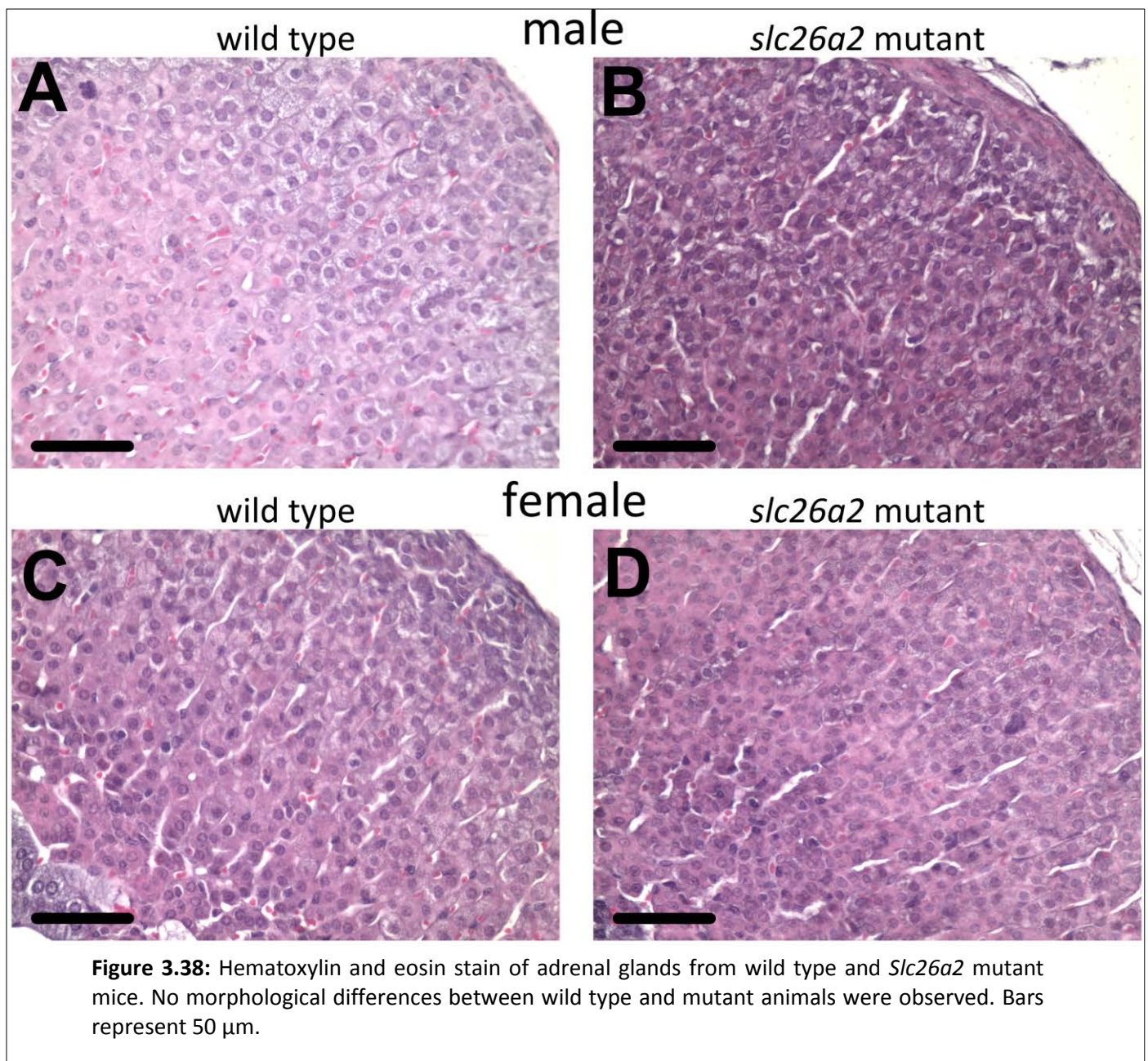
As the disease conditions these mice modelled did not contain a total eradication of *Slc26a2* expression, determination of the actual level of *Slc26a2* transcript present in the adrenal tissue was necessitated. The adrenal gland samples were obtained from 45 days old mice leading to a limitation on the size of the samples for RNA extraction, so both adrenals of the same animal were combined to produce the cDNA. The subsequent quantification of transcript levels revealed a marked decrease in *Slc26a2* in mutant animal adrenals (male: 100 ± 12.1 vs 17.4 ± 2.9 %, $P<0.001$; female: 177.8 ± 21.1 vs 11.9 ± 1.4 %, $P=0.001$) (Fig. 3.39).

The severe decrease in *Slc26a2* mRNA levels in mutant mice were confirmed also on the protein level. Staining of adrenal tissue sections from wild type and mutant animals with an antibody raised against *Slc26a2* reveal lessened chromogenic intensity in mutants throughout the adrenal cortex. As the antibodies specificity for *Slc26a2* could not be confirmed with certainty, partial immunopositivity in the medullary regions were also observed (Fig. 3.40A-D).

3.8.2. Steroidogenic Gene Expression Profile

After establishing the *Slc26a2* reduction in the adrenals, the cDNA from the samples were used to quantify components of steroidogenic apparatus. In male animals, there was an increase of *Cyp11b2* expression in mutants compared to wild type. A less pronounced similar trend was also observed for females, but in both sexes, intragroup variability and small samples sizes denied this difference

Figure 3.38: Hematoxylin and eosin stain of adrenal glands from wild type and *Slc26a2* mutant mice. No morphological differences between wild type and mutant animals were observed. Bars represent 50 μm.

statistical significance (male: 100±14.5 vs 215.7±64.4 %, *P*=0.182; female: 106.6±14.0 vs 120.5±42.4 %, *P*=0.687) (Fig. 3.41).

3β-hsd expression levels of the mutant adrenals were quantified; showing that the isozyme functional in aldosterone production, *Hsd3b6* [**184**], had increased levels in mutant adrenals compared to wild type in both males (100±19.2 vs 173.5±19.6 %, *P*=0.025) and females (75.5±8.3 vs 152.6±35.9 %, *P*=0.009) (Fig. 3.42A). The isozyme *Hsd3b1*, broadly expressed in the adrenal rather than being ZG specific, was either unaffected, as in the case of males (100±8.4 vs 90.3±7.9 %, *P*=0.431), or decreased, as observed in females (132.9±11.4 vs 81.9±1.4 %, *P*=0.032) (Fig. 3.42B).

Investigation of the enzymes acting at the rate limiting step of adrenocortical steroidogenesis,

Figure 3.39: Expression level of *Slc26a2* was significantly lower in *Slc26a2* mutant adrenals in both male and female animals, with a more profound decrase in females due to their increased wild type *Slc26a2* expression (*P*= 0.01). * depicts significant differences between wild type and *Slc26a2* mutant mice of the same sex; # depicts significant differences between male and female wild type mice. Male wild type, n=7; male mutant, n=11; female wild type, n=9; female mutant, n=3.

cholesterol side chain cleavage, was performed next. In both side chain cleaving enzyme *Cyp11a1* (Fig. 3.43A) and the cholesterol transporting *Star* (Fig. 3.43B), a reduction in mutants was observed, falling short of statistical significance only in the case of *Star* in females (*Cyp11a1*, male: 100±8.6 vs 70.8±3.3 %, *P*=0.002; female: 93.9±7.2 vs 50.2±4.5 %, *P*=0.007; *Star*, male: 100±9.3 vs 66.2±8.9 %, *P*=0.023; female: 86.4±9.5 vs 71.2±2.6 %, *P*=0.393).

3.8.3. Renin-Angiotensin-Aldosterone System

After discerning that the expression profiles of the components of adrenal steroidogenic apparatus were modified in the mutant line in an aldosterone favoring manner, circulating aldosterone levels were quantified using plasma samples. A major elevation in aldosterone levels were witnessed in female muntant animals compared to wild types (22.5±2.0 vs 242.2±57.8 pg/ml, *P*=0.005) (Fig. 3.44). However, in male animals, although an increase in mutants was also observed, it was of lesser magnitude and not statistically significant (62.2±11.2 vs 84.9±10.6 pg/ml, *P*=0.191).

Inasmuch as the *in vitro* observations in NCI-H295R cells established a causality between low SLC26A2 expression and elevated aldosterone synthesis, in a living system, aldosterone levels cannot be evaluated independently from circulating renin. Accordingly, renin activity in the plasma samples were evaluated. An elevation in average renin activity in samples from mutant animals was observed, albeit with a large variability between mutant animals (male: 3±1.6 vs 22.9±14.8 ng/(ml*hour), *P*=0.172; female: 0.7±0.2 vs 4.9±1.7 ng/(ml*hour), *P*=0.04) (Fig. 3.45).
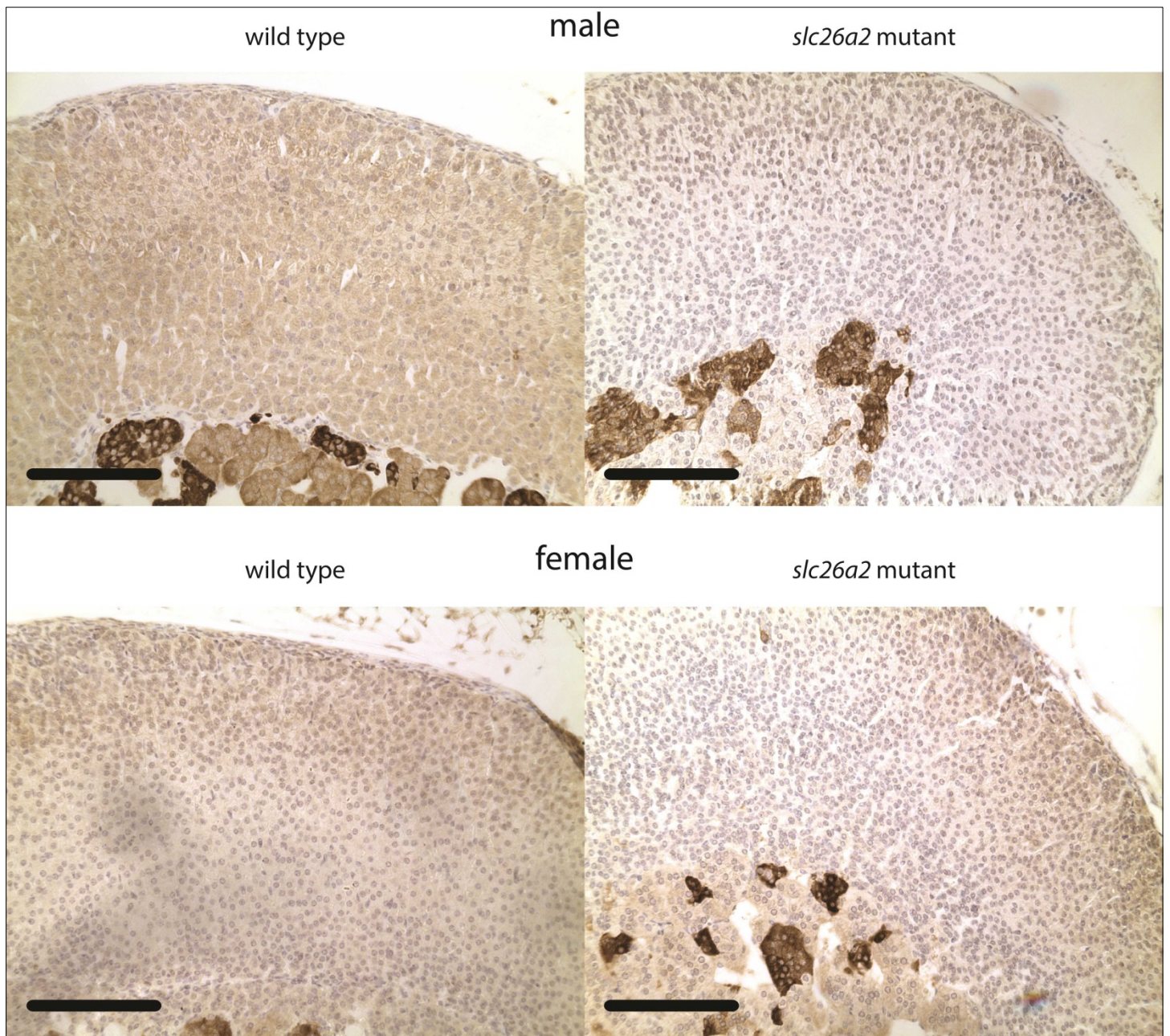
Figure 3.40: Immunohistologocal detection of *Slc26a2* in wild type and *Slc26a2* mutant mice adrenals. Mutant adrenals from both sexes stained against *Slc26a2* with less intensity throughout the cortex. Bars represent 125 μm.

Quantification of plasma renin activity and aldosterone concentration enables the calcutation of aldosterone to renin ratio, an important screening tool for primary aldosteronism. The overall mean of the ratio for each group depict an increase for mutant animals in both males (37.3±9.5 vs 159.5±139.9 pg/ml per ng/(ml*hour), *P*=0.355) and females (53.5±19.2 vs 825.5±772.4 pg/ml per ng/(ml*hour), *P*=0.347) (Fig. 3.46). However, the plasma renin activity values, which are the covariants in ARR with a dominating effect on the ratio [**95**], having very large margins of variability, prevented the data from presenting a definitive conclusion.

In order to attain a more complete picture of the endocrine phenotype of the mutant animals, their stress levels as a function of hypothalamic–pituitary–adrenal axis activation were investigated by quantifying corticosterone levels in plasma samples. Quantification by enzyme immoassay revealed highly elevated corticosterone levels in mutant animals, but no significant sex specific differences (male: 151.5±21.1 vs 645.3±154.4 ng/ml, *P*=0.009; female: 158.8±44.2 vs 810.7±112.9 ng/ml, *P*<0.001) (Fig. 3.47).
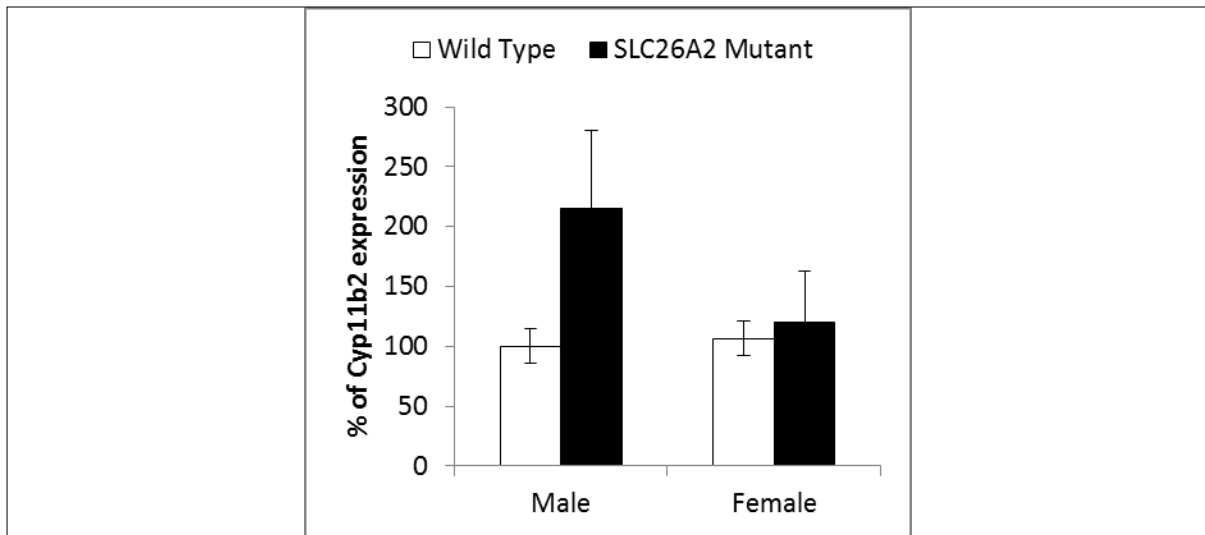
Figure 3.41: Adrenal expression level of *Cyp11b2* in wild type and *Slc26a2* mutant mice. An increase below significance levels was observed in male mutants. Male wild type, n=7; male mutant, n=11; female wild type, n=9; female mutant, n=3.
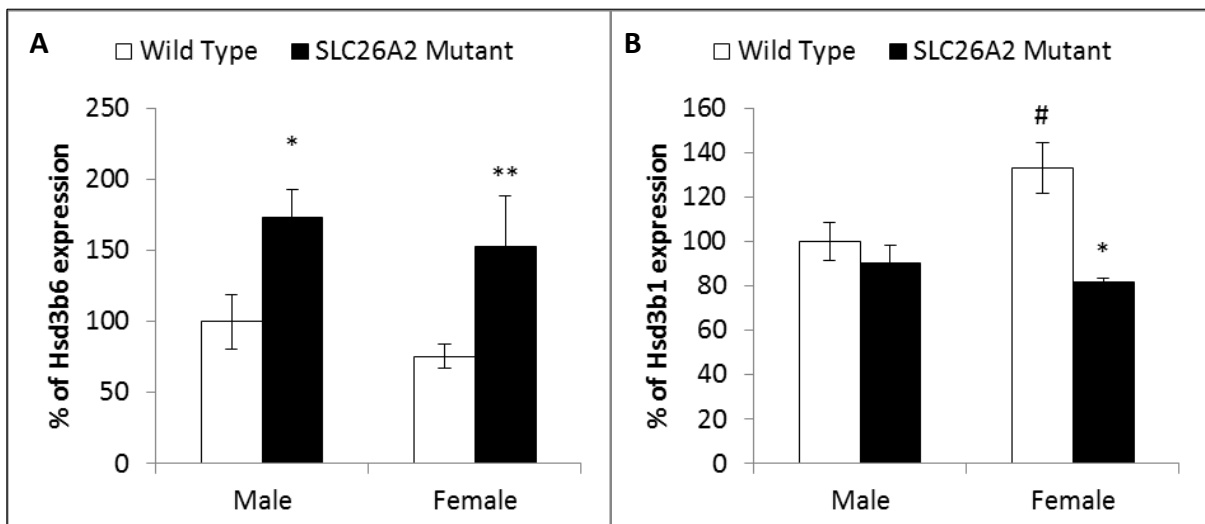
Figure 3.42: Adrenal expression level of 3β-HSD isozymes in wild type and *Slc26a2* mutant mice. In mutant animals *Hsd3b6* was increased (**A**), in contrast of lowered *Hsd3b1* transcription (**B**). * depicts significant differences between wild type and *Slc26a2* mutant mice of the same sex; # depicts significant differences between male and female wild type mice. Male wild type, n=7; male mutant, n=11; female wild type, n=9; female mutant, n=3.
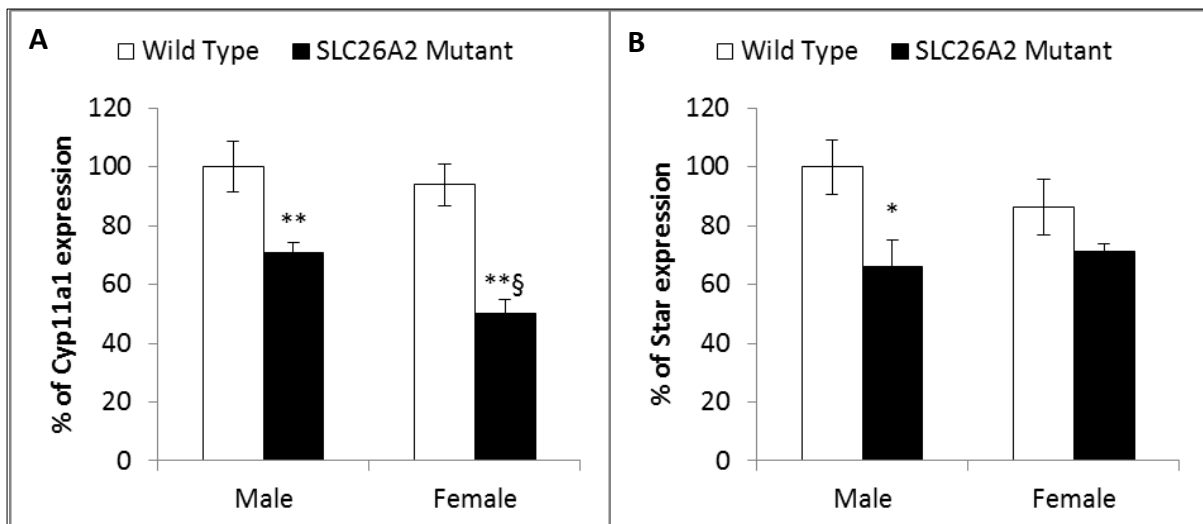
Figure 3.43: Adrenal expression level of cholesterol sidechain cleavage components *Cyp11a1* (**A**) and *Star* (**B**) in wild type and *Slc26a2* mutant mice. Expression of both enzymes were downregulated in knockdown animals. * depicts significant differences between wild type and *Slc26a2* mutant mice of the same sex; § depicts significant differences between male and female mutant mice. Male wild type, n=7; male mutant, n=11; female wild type, n=9; female mutant, n=3.
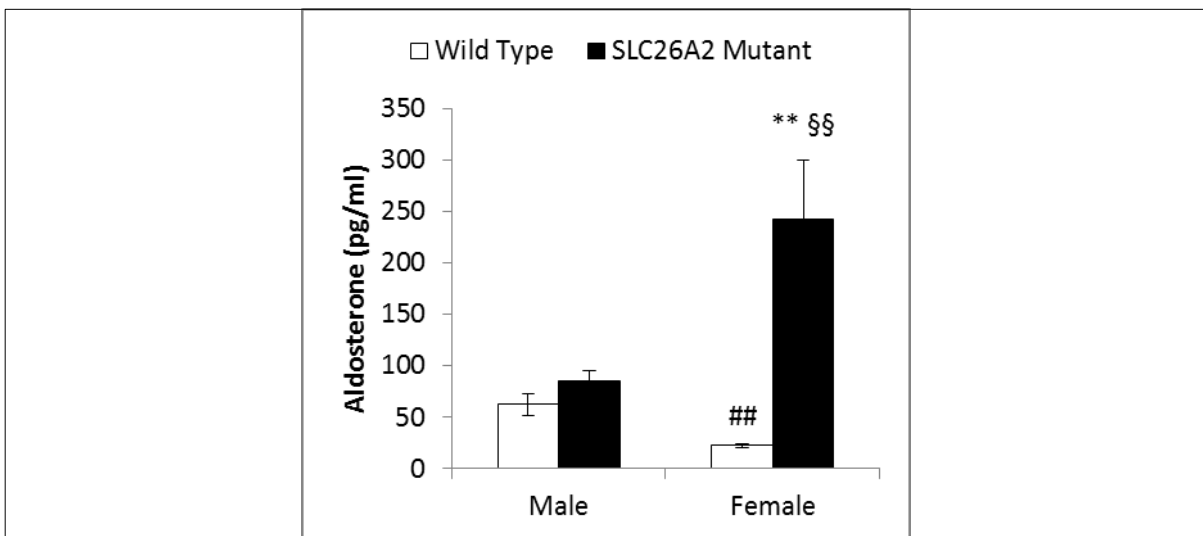
Figure 3.44: Plasma aldosterone concentration of wild type and *Slc26a2* mutant mice. Female mutants had a profound increase in circulating aldosterone levels, along with observed sex-dependent differences in wild type animals. * depicts significant differences between wild type and *Slc26a2* mutant mice of the same sex; # depicts significant differences between male and female wild type mice; § depicts significant differences between male and female mutant mice. Male wild type, n=5; male mutant, n=4; female wild type, n=5; female mutant, n=5.
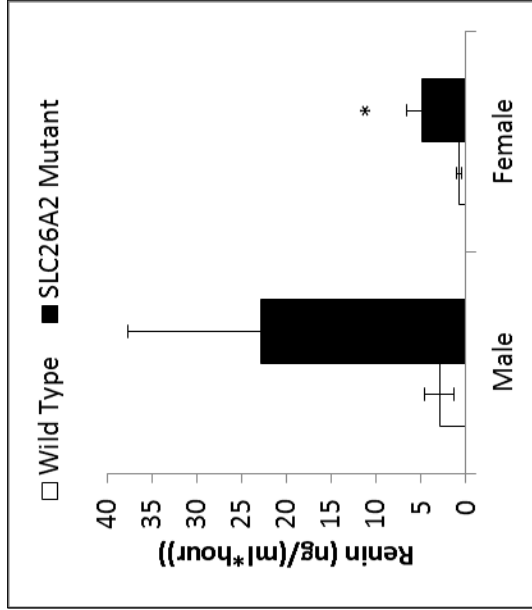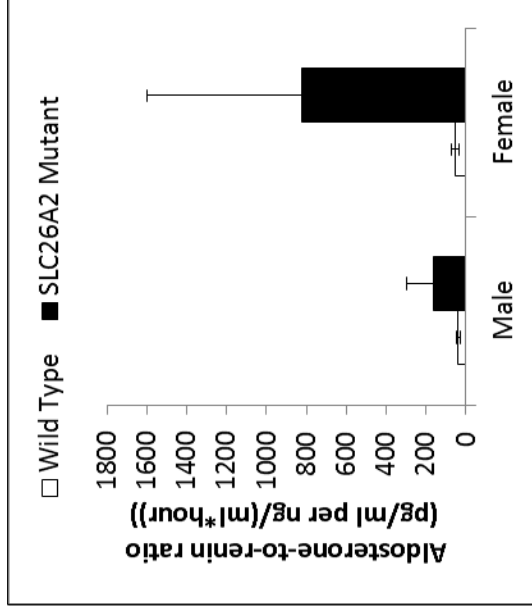
Figure 3.45: Plasma renin activity of wild type and *Slc26a2* mutant mice. Mean renin activity in mutants were higher than wild types, although a large intragroup variation was observed. * depicts significant differences between wild type and *Slc26a2* mutant mice of the same sex. Male wild type, n=5; male mutant, n=4; female wild type, n=5; female mutant, n=5.

Figure 3.46: Aldosterone-to-renin ratio of wild type and SLC26A2 mutant mice. The ratio was higher in mutant animals, with a large margin of error due to the intragroup variation of the renin denominator. Male wild type, n=5; male mutant, n=4; female wild type, n=5; female mutant, n=5.
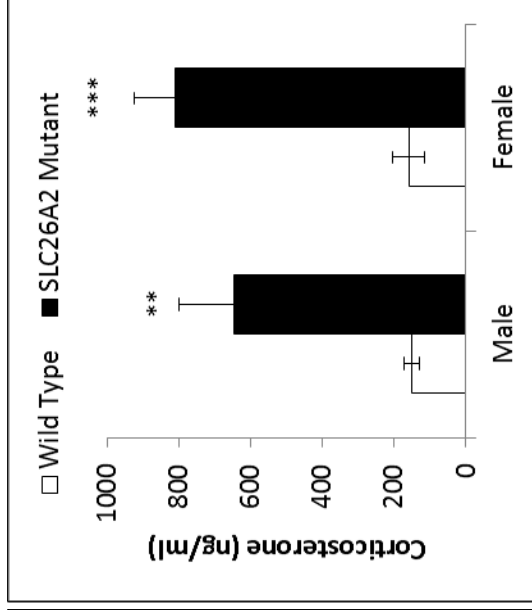
Figure 3.47: Plasma corticosterone levels of wild type and SLC26A2 mutant mice. Corticosterone concentration was elevated in mutant animals, with no significant differences being evident between sexes. * depicts significant differences between wild type and *Slc26a2* mutant mice of the same sex. Male wild type, n=5; male mutant, n=4; female wild type, n=5; female mutant, n=5.

85

4. Discussion

Ever since the realization that a steroid other than cortisol is responsible for the main mineralocorticoid activity [**185**], and costly extraction and crystallization of electrocortin (21 mg from 500 kg of beef adrenals) by the Taits-Reichstein collaboration [**186**], much research has been devoted to elucidation of aldosterone synthesis and function [**61; 187**] especially in regard to its essential role in the pathogenesis of Conn's Syndrome [**188**]. Identification of familial forms of primary hyperaldosteronism and their causative genetics illuminated many aspects of aldosterone regulation [**84; 189; 190**]. Although initially considered as a minor contributor to hypertension due to diagnosis based on hypokalemia [**191**], the syndrome received renewed attention as increasing utilization of plasma aldosterone concentration to plasma renin activity ratio as a case finding tool verified [**192**] Dr. Conn's claims of higher incidence within hypertensive population [**193**]. This, as a result, brought about major breakthroughs in the identification of somatic mutations in potassium channel KCNJ5 [**86**] and cation transport ATPases [**87**] with high prevalence in aldosterone producing adenomas [**111**], establishing crucial role of ion homeostasis of zona glomerulosa cells in regulation of aldosterone biosynthesis. In this study, using the hypothesis-free approach of genome-wide association studies [**194**], a locus associated with high aldosterone to renin ratio in a well-phenotyped population [**166**], hosting an anion carrier with previously unknown but strongly evidenced role in regulation of aldosterone biosynthesis. In this section the relevance of the methodology and obtained evidence to the conclusion that SLC26A2 plays a role in aldosterone regulation is discussed under several topics.

4.1. Genome-Wide Association Study

As of present, GWA studies are the most wide-spread and successfully used technique in genetic epidemiology [**133**]. However seven years of intense utilization of these studies identified a substantial amount of pitfalls and shortcomings as well [**144**], with critics questioning the justification of hundreds of million dollars spent on funding [**195**]. Most prominent of these problems is the "missing heritability" phenomenon [**145**], after the fact that the massive amount of SNP-trait associations identified so far accounts for only a fraction of the estimated heritability of the phenotypes by classical methods such as twin studies. In the attempts to address this issue, many hypotheses were put forth, seeking the unaccounted heritability in low frequency-high effect variations [**196**], false-negative associations of small effect-common variants [**197**], epistasis due to rare combinations of common variants [**198**], gene-environment interactions [**199**], structural polymorphisms such as copy number variations [**146**], transgenerational epigenetic inheritance [**112**]; as well as even challenging the methods of heritability estimation [**200**]. Novel statistical

approaches on interpretation of GWAS data that take multi-trait association into account are also emerging [201-203]. It should also be noted that up until present, most GWA studies, including the one presented in this study, were conducted with SNP arrays of 1000K or less [133], and genotype imputation methods used the HapMap repository of a meagre 3.1 million variations [152] compared to more recent repositories of 38 million SNPs and more than a million other types of variation [204]. In any case, taking a snapshot of the genome by SNP arrays may soon be rendered irrelevant in the face of exponential development rate of next generation sequencing, which has already brought down the cost of a whole-genome sequencing run to an affordable thousand dollars [205]. Whether technological innovation will suffice to brute-force through this problem, or a fundamental change in the current understanding of genetic epidemiology is required remains to be seen.

The primary use for GWA studies is investigation of biologic pathways of disease causation [144], as in the case of this study. In this regard, it is manifest that GWA studies will attain their full potential through combined-arms approach of follow-up functional studies. Therefore, design and implementation of GWA studies is of utmost importance. Most critical issues hereof are size and composition of sample population and considerations on phenotype suitability and quality.

Earliest GWA studies had small sample sizes in the hundreds [139]. Later studies comprised of thousands [206], and meta analyses reached to over 100000 participants [207]. Successful associations from studies employing a gradient of sample size are due to the spectrum of effect sizes and variant frequencies [146], as detection of rarer or less effective associations necessitating a larger assembly of participants. Given that the median sample size in the association studies of quantitative traits listed in The NHGRI GWAS Catalog is 1345 as of present [208], the population of the GWAS presented here is in the typical range. For a minor allele frequency of 10 %, this sample size has power to detect associations of variants with a genotypic relative risk above 1.3 [209].

Population stratification may cause bias in interpretation of association studies [144]. In the present study, several factors abate the confounding effects of population structure. Chief among them is the standardized statistical genomic control tests applied by the genetic epidemiology team of the KORAgen platform [210], by whom the association analysis was carried out. Furthermore, the population of the KORA biobank, from the region surrounding Augsburg with 600000 inhabitants, reduces apprehensiveness over the topic due to its largely Caucasian ethnic composition with no detectable substructures within population [211], especially when taken together with the fact that the magnitude of the bias comprised from stratification itself is a debated issue [212].

GWA studies of quantitative traits usually follow a whole-spectrum focused approach, in contrast to case-control methodology based on arbitrary cutoffs [213-215]. In most cases, the latter approach

may simply be impossible, as with traits such as height [216] or body-mass index [217]. In accordance with these precepts, in this study association of genotypes to a whole spectrum of ARR was analyzed. Furthermore, the epidemiology focused design of the study did not allow confirmatory tests on subjects for hypertensiveness or presence of bilateral adrenal hyperplasia. In fact, epidemiological investigation into complex diseases via association studies with immediate endophenotypes is a trending approach among researchers [218].

In the case of primary hyperaldosteronism, ARR is the most feasible clinical marker [219], despite a number of criticisms directed against it. Although it is established that plasma aldosterone concentration is increased and plasma renin activity is decreased in primary aldosteronism, ARR itself is not of absolute reliability as the ratio is dependent on plasma renin activity [95]. This dependence may also lead to ARR levels being considered above cutoff values due to very low plasma renin activity, even though aldosterone levels are also too low for PA [220]. On the other hand, a novel understanding that PA and low renin hypertension is a continuum [221] is emerging, with redefinition of normal aldosterone levels [222] suggesting autonomous aldosterone secretion in low renin hypertension [221]. Even as understanding of aldosterone-renin interplay is improving, clinical guidelines still suggest employment of ARR as a screening tool [76; 90], providing justification for its use as the phenotype parameter in a GWAS for PA and RAAS.

Further support for ARR as the choice determinant value for GWA study comes from the estimated heritabilities of RAAS components. Despite an early twin study asserted strong heritable components of basal state PAC and PRA [223], later studies contrasted these findings very low estimates for PAC heritability [116; 224]. PRA estimates varied, with a twin study estimating 66 % (h^2) only in males [225], and a sib-pair study estimating similar levels (PRA h^2, supine: 0.46, standing 0.69) [224], the disparity between studies being possibly due to varying controls for salt intake and posture. A more recent estimate by the Framingham study showed substantial heritability for ARR (40 %), along with relatively lower heritabilities of PAC (11 %) and PRC (22 %) [77]. Similar results (ARR: 38.1 % PAC: 28.7 % PRC: 27.4 %) obtained by a group from University of Glasgow [143] consolidated the significantly higher estimated heritability of ARR compared to its constituent biomarkers. Taken together, these findings explain the logic of conducting a GWAS for ARR rather than only for PAC or PRC.

One of the main justifications for the immense cost of undertaking GWA studies and the necessary infrastructure is the potential to identify susceptibility alleles, which would directly translate to advances clinical care and risk management [226]. In this regard, associations found in a discovery cohort should be replicated in an unrelated cohort [144]. Replication is indeed a litmus test for

GWAS [**124**] when the aim is identifying risk alleles [**146**]. Many prominent GWA studies used this approach [**206**], as well as complete replication of studies in other cohorts [**227; 228**] for traits that can be phenotyped with uniform clinical standards providing high replicability across research centers and clinics. Other GWAS studies with the KORA F4 cohort employs this method of statistical assurance as well [**136**]. In the case of RAAS components renin and angiotensin, however, such replicability is mostly out of reach, as wide range of inter-laboratory variations in absolute values has been demonstrated [**229-231**]. This predicament is further intensified by the variability of results depending on the conditions of sample retrieval from the subjects such as posture and fasting state. Ensuring intraassay consistency for all these parameters provides a measure of reliability in the GWAS findings. Moreover, in the time frame of this study, only one other GWAS for ARR was encountered in the public databases [**232**]. In this study, the authors report utilization of a replication cohort after initial analysis in a discovery cohort of 936 individuals. However, the replication cohort was not phenotyped for either PAC or PRA, presumably due to the same kind of confounding factors. Only recently the first ever meta-analysis of RAAS components was published, incorporating data from multiple European cohorts, including KORA-F4 [**233**]. As this study did not test for association to ARR, replicating the top ARR associated SNPs in KORA-F4 in the cohort would be most enticing; even more so when considering other highly significant loci at chromosomes 4, 8 and 20 (Fig 3.1A). Indeed, when investigating their Manhattan plots for PRC association, the same locus at chromosome 5 seems to have high, though not genome-wide, significance. Regardless, the quality of data in the GWAS presented here certainly suffices to spotlight associated loci for further functional studies, as supported by the substantial body of evidence for functional implications reported in this study.

4.2. Genes in Linkage Disequilibrium

The GWAS data presented genome-wide significant association of ARR with the polymorphism *rs1433010*. Other variations in LD with this SNP indicated a locus containing the genes SLC26A2, TIGD6 and HMGXB3. Imputed SNPs, taken together with HapMap recombination rates, extended possible LD to include CSF1R as well.

4.2.1. Tigger Transposable Element Derived 6 (TIGD6)

Tigger transposable element derived 6 is a member of the tigger family of DNA-mediated transposons that encode a terminal inverted repeat binding transposase [**234**]. This family has been put for as putative redundant paralogs of centromere protein B, a presumably important yet functionally uncharacterized centromere-associated protein; the hypothesis was experimentally refuted in mammalians [**235**]. No other functional information on this particular transposon is

obtainable from the literature as of present, therefore this gene was excluded from further functional investigations.

4.2.2. HMG Box Domain Containing 3 (HMGXB3)

This gene belongs to the high mobility group box family. Members of this family have DNA binding ability by virtue of their HMG-box motifs, and manipulate chromatin structure, participating in nuclear processes of DNA repair, recombination and transcription [236]. HMGXB3 has also been shown to play a role in innate immune responses by nucleic acids mediated by the transmembrane Toll-like receptors and cytosolic receptors [237]. This protein was detected as a surface in pancreatic islet cells, colocalizing with insulin to some degree [238]. The lack of further functional knowledge, or of any particular relevance to the adrenal function inferred from publicly available Gene Atlas expression dataset [151] ruled out any rationale in carrying out functional investigation of this gene.

4.2.3. Colony Stimulating Factor 1 Receptor (CSF1R)

The protein product of CSF1R gene, the most extensively studied in the associated locus, is a transmembrane receptor tyrosine kinase with affinity to the cytokine colony stimulating factor 1 [239]. Its expression was observed in several cell types, of immune system and others [240]. Primarily, CSF1R regulates mononuclear phagocyte production [241]. CSF1R dependent regulation was also evident in the female reproductive tract and fertility [242]. Mutations in the protein kinase domain of the gene are associated with gastrointestinal tumors and acute myeloid leukemia [243; 244]. Myeloid malignancies presented overexpression of CSF1R [245].

In the context of the genome-wide association of the locus containing CSF1R gene to ARR, potential uncharacterized steroidogenic effects of this receptor were investigated. The adrenal steroidogenic model cell line NCI-H295R showed trace levels of expression of the gene, compared to more abundant mRNA levels from adrenal tissue samples. Unsurprisingly, application of transient gene silencing on this cell line yielded no observable effects on baseline aldosterone productivity. Induction of the receptor by its ligand, M-CSF, in H295R or primary adrenal cells also had no effect on aldosterone production. These findings suggest a lack of direct regulatory function of CSF1R on aldosterone production in adrenocortical cells.

Before complete dismissal of a putative CSF1R modulated effect on adrenal steroidogenesis, it would be prudent to recall that resident testicular macrophages stimulate steroidogenesis in Leydig cells by supplying a StAR independent substrate (25-hydroxycholesterol) for pregnenolone production [246]. As the effects of CSF1R impairment include lowered resident mononuclear phagocyte density in a variety of cells [240], resident adrenal macrophages should be further investigated in respect to their

contribution to aldosterone production and the modulation of their generation via CSF1R.

4.2.4. Solute Carrier Family 26 (Anion Exchanger), Member 2 (SLC26A2)

The diastrophic dysplasia sulfate transporter gene encodes a transmembrane glycoprotein with electroneutral $SO_4^{2-}/2OH^-$, $SO_4^{2-}/2Cl^-$, $SO_4^{2-}/OH^-/Cl^-$ anion exchanger functions in an extracellular Cl^- dependent manner, along with ability to exchange Cl^- for I^-, Br^- or NO_3^- [247]. Furthermore, it mediates bidirectional oxalate / SO_4^{2-} exchange [248]. It was first identified as the gene causing diastrophic dysplasia [249]. A mouse model with a DTD mutation knock-in mimicked the disease phenotype, with impaired SO_4^{2-} uptake in chondrocytes, resulting in proteoglycan undersulfation in the extracellular matrix [171; 250]. Additionally, cultured colon cancer cells had a lowered expression of SLC26A2, and suppression of SLC26A2 expression enhanced growth rate of cancer cells [251]. Expression of SLC26A2 was detected in cartilage along with a variety of tissues, including placenta [179], where it is one of the main sulfate providers to the embryo [252].

In addition to the strong linkage to the lead SNP of the GWA study and demonstration of its pathophysiological role in human disease, this gene also drew attention by the merit of its high level of expression in adrenal gland and cortex in the Gene Atlas dataset [151]. After confirmation of this phenomenon by RT-PCR, evidence of its co-regulation with aldosterone production *in vitro* and *in vivo* was found. Through its knockdown, modulatory effect of SLC26A2 on aldosterone was shown and backtracked to calcium signaling pathway. A germline *in vivo* knock-in model showed increased aldosterone production in female mutants, as well as upregulation of enzymes specific to aldosterone pathway.

4.3. Zonal Localization SLC26A2 within the Adrenal Gland

The coregulation of aldosterone production and SLC26A2 by potassium and AngII leads to an instinctive hypothetization of their colocalization in the adrenal as well. Initially, this hypothesis was not testable due to lack of a properly functioning immunohistochemistry suitable antibodies for either protein. Isolation of the zona glomerulosa also fell out of the technical scope of the project. As more precise antibodies became available, adrenal cortex sections were stained with both antibodies, revealing scattered and clustered CYP11B2 positive cells in the cortex and a ubiquitous immunopositivity to SLC26A2 throughout the cortical zones, with a slight emphasis on the zona fasciculata.

Of the enzymes that have a direct effect on aldosterone synthesis, 3βHSD is the most disputed one in regards isoform specificity to zona glomerulosa. The second isoform was held responsible for steroidogenesis in the adrenal cortex [253] until homology inferred from a knockout mouse model

postulated zona glomerulosa specificity of HSD3B1 [**184**]. Subsequently this was verified by subtype specific antibodies [**58**] as well as demonstration of a NGFIB responsive element in HSD3B1 promoter [**67**]. However, the same study demonstrated near exclusive presence of HSD3B2 in expense of HSD3B1 in APAs. Another study utilized immunostains of CYP11B1, CYP11B2 and 3βHSD, without distinguishing between 3βHSD isozymes; observing intense CYP11B2 and 3βHSD staining in APAs. Taken together, while aldosterone production in healthy adrenal is driven by HSD3B1, in pathological conditions HSD3B2 is the dominant isozyme. The only evidence to the contrary comes from colocalization of HSD3B1 and CYP11B2 in the same APA cells in one study [**59**], even as in this study HSD3B2 is more prevalent across the APA, and the aldosterone synthase staining is weaker compared to the prior studies as well as the staining in this study using the same antibodies provided by Gomez-Sanchez group [**55**].

Considering the example set by the 3βHSD isoforms, exclusive colocalization of aldosterone synthase and SLC26A2 may not be necessary for development of pathological conditions when the expression of the latter is suppressed. Indeed, a marked decrease in the intensity of SLC26A2 expression is readily observable in CYP11B2 positive APA in comparison to normal adrenal. This is also in accordance with the *in vitro* observation of increased aldosterone production in response to SLC26A2 knockdown in NCI-H295R cells and decreased SLC26A2 mRNA expression in APAs compared to control adrenals. Nevertheless, application of additional techniques may help clear the contention in the issue. *In situ* hybridization may provide a quick answer on the transcriptome level. A more definitive solution might be surface protein biotinylation and subsequent probing of the membrane proteins recovered by streptavidin for SLC26A2 immunopositivity in freshly isolated CD56 expressing zona glomerulosa cells [**254**].

4.4. Linking SLC26A2 to Aldosterone Regulation – *in vitro*

Zona glomerulosa cell is hyperpolarized in its resting state, and this membrane potential is what keeps the cell steroidogenically inactive. Importance of cation currents in maintenance of resting membrane potential in zona glomerulosa cells had already been appreciated [**61**] when recent exome sequencing studies of APAs showed that disruption of this homeostasis leads to pathological aldosterone production [**255**]. Initial finding of mutations in KCNJ5 leads to a sodium leakage, perturbing the exclusivity of background potassium conductance [**256**]. Further mutations found in membrane sodium potassium pump ATP1A1, which also ultimately leads to sodium leakage into the cell [**89**]. These mutations therefore impair the polarized state of the membrane, which mimics the effects of AngII and potassium stimulation where membrane depolarization leads to calcium influx to the cytosol. Mutations found on ATP2B3, a membrane Ca^{2+} pump, presumably stops calcium

disposal to extracellular space and an accumulation of cytosolic calcium [87]. Finally, CACNA1D mutations hampering the L-type voltage gated potassium channel reduces the necessary activating voltage, and triggering the activation of L-type calcium influx [88], which normally reserved for supraphysiological extracellular potassium concentrations, or reinforcement of steroidogenic RAAS signal by ACTH in severe volume loss [45].

The emphasis on the role on cation homeostasis in aldosterone producing cells arguably stands on one leg, as any detailed characterization of anion balance is lacking. Epithelial anion transporters were extensively characterized in the last two decades of the last century, partially due to the interest generated by their role in cystic fibrosis etiology [257]. Findings from this era establish that chloride channels are important in maintaining membrane potential stability. In heart cells, chloride efflux results in activation of calcium channels. It was also observed in Leydig cells that Cl^- efflux led to membrane depolarization and subsequent steroidogenesis [46] and Cl^- channels were present in rat adrenal zona glomerulosa, with ACTH modulated cAMP independent early Cl^- currents through Ras activation was shown [258].

SLC26A2 functions as a anion transporter, primarily a sulfate uptaker, and apparently the predominant mediator of this function, as severe forms of dysfunction in this gene is extremely damaging and even lethal [171]. It is also ubiquitously expressed throughout epithelia, on the apical membranes of various tissues [179]. Thus, SLC26A2 has to mediate sulfate uptake from both acidic and alkaline luminal environments. A recent study on SLC26A2 expressing xenopus oocytes demonstrated how this can be accomplished. Under acidic extracellular conditions, extracellular sulphate is exchanged for intracellular hydroxide, whereas under alkaline conditions of most endocrine glands, this uptake is via exchange of intracellular chloride [247]. Serum acidosis is a trigger of aldosterone production [259] and aldosterone action shifts the pH to more alkaline levels. In the normal physiological conditions, SLC26A2 may mediate activation of chloride efflux as extracellular pH increases as a result of aldosterone action, participating in homeostasis of chloride currents. Unlike the collecting duct cells, where its functionality and expression is disputed [260], SLC26A2 knockdown led an intracellular chloride built-up in H295R cells. Therefore repression of SLC26A2 expression may well deprive the cells from a negative feed-back mechanism for aldosterone production.

NCI-H295R is a predominantly cortisol producing cell line with low levels of baseline aldosterone production when grown as a monolayer, even though it displays the zona glomerulosa specific potassium sensitivity as well [181]. In contrast the predominance of cortisol production, the NCI-H295 cells have little or no ACTH response [182], which is the driving rationale behind development

of new adrenocortical cell lines such as HAC-15. As a further confirmation of this observation, in the results of this study, although SLC26A2 expression in wild type H295R cells were markedly upregulated by cAMP through forskolin stimulation, ACTH displayed no such modulation. H295R cells are very sensitive for potassium and spheroidal growth of the cells induces a potent increase in the aldosterone production. In the experiments carried out in this study, special care was taken to the growth of H295R cells as uniform monolayer, assisted by poly-d-lysine coating of culture surfaces. The potent increase of baseline aldosterone production of the cells by SLC26A2 knockdown mimics the spheroidal growth of wild-type cells, along with further similarity of elevated ACTH receptor (MC2R) expression. If this similarity of SLC26A2 KD and spheroidal H295R cells are valid, it may also explain the less potent increases in cortisol production of knockdowns cells, via decreased CYP17A1 expression.

ACTH activates a Ras mediated calcium current in early stages independent of cAMP production [**258**]. Transcription of human Ras family members, NRAS, HRAS and KRAS were not significantly regulated by SLC26A2 knockdown. However, as the model cell line is derived from an adrenal carcinoma, a constitutively active Ras indigenous to the cell line might not necessitate an upregulation, and enzymatic activation of Ras pathway was not determined. Angiotensin II also may participate here, as it activates Src tyrosine kinase [**261**], presumably resulting in subsequent Ras activation. This pathway of Ras mediated chloride efflux leading to depolarization is an additional candidate through which SLC26A2 knockdown exerts its effects.

In the lacking of any exome mutations [**176**], SLC26A2, as a putative pathogenic gene in PA, should modulate its effects on the plasma membrane potential and ion homeostasis, not through a gain of function mutation as in recently observed cation channels and pumps, but rather through regulatory changes leading to its transcriptional downregulation. A case of ion leakage due to functional site mutations is further unlikely because of its already established bidirectional transport capability and affinity to a variety of anions. Regardless of the exact effect of SLC26A2 knockdown on the ion homeostasis of the cell, this study demonstrates that aldosterone overexpression is mediated via intracellular calcium induced activation of CAM kinase pathway. Calcium influx is indeed a common convergence point of the effects of recently identified APA mutations in KCNJ5, ATP1A1, ATP2B3 and CACNA1D [**85; 256**]. Although available exome sequencing data from APA sets does not reveal any mutations in the SLC26A2 gene, the possibility of this gene's role in PA pathogenesis cannot be readily dismissed. As this study demonstrated, a reduction of SLC26A2 expression may give rise to the PA phenotype, which could result from non-exomic regulatory sequence mutations. Furthermore epigenetic modifications might result in a similar repression: The upstream CpG island

of SLC26A2 gene was found to be partially methylated in HeLa-S3 cells in the Encode project [**149**]. Two non-synonymous common SNPs (*rs76784312* and *rs35919114*) exist in the coding sequence of the first exon. The microRNA hsa-miR-9 expression is observed in both adrenal gland and kidney [**262**], and several hsa-miR-9 target sites has been predicted on the 3' UTR of SLC26A2 by TargetScan [**161**], with one of them validated by immunoprecipitation [**263**] and one with a rare SNP nearby (*rs180966130*). Taken together with the large void in the knowledge of idiopathic hyperaldosteronism pathophysiology, even slight epigenetic and regulatory variations of SLC26A2 may very well contribute to PA pathogenesis.

In the attempt to further elucidate the downstream effects of SLC26A2 knockdown, a whole transcriptome expression analysis was carried out. This approach is very illuminating as it reveals a snapshot of the cell's mRNA levels, but not sufficient to reveal every aspect of expression in the lacking of proteomics and metabolomics data. In the microarray results, two confounding factors are immediately obvious: the small number of differentially expressed genes, and the lack of correlation between microarray and RT-PCR results. The prior impedes ontology enrichment analyses greatly, which could otherwise be informative about the knockdown targeted processes and pathways. The latter, when evaluated together with the RT-PCR's status as the gold standard for expression analysis, renders the cutoffs for differential expression arbitrary. For example, even though the aldosterone production and CYP11B2 upregulation in knockdown cells have been repeatedly confirmed by low-throughput methods; aldosterone synthase upregulation would be missed by even the most modest of cutoffs in microarray analysis. Nonetheless, the even though the magnitude of regulation differs between methods, its direction is essentially the same. This fact provides a wealth of information to be derived from the experiment.

The modest number of highly regulated (2-fold or more) genes immediately reveal events at the cell membrane, as related ontology terms are enriched by both upregulated (carboxylic acid transport, L-amino acid transport) and downregulated genes (cell adhesion, surface regulated signal transduction). Indeed, only two pathways are significantly enriched: transmembrane transport of small molecules is upregulated and integrin cell surface interactions are downregulated; in accordance of membrane localization and function of SLC26A2. SLC is originally implicated in extracellular matrix proteoglycan sulphation. The ~1.5-fold galectin-8 (LGALS8) upregulation, which implicated in matrix interaction [**264**] and a putative SLC26A2 interactant [**265**] is possibly related to these changes. Therefore, aldosterone producing phenotype of SLC26A2 knockdown cells may be the result of a simulation of cell-to-cell signaling characteristics of spheroidal H295R cell growth.

The microarray data readily reveals that SLC26A2 knockdown puts the cells in stress conditions.

There seems to be an unfolded protein response and DNA damage induction outlined by GADD45A activated p38MAP Kinase [**266**], leading to upregulation of DDIT3, CHAC1 and polo-like kinase (PLK2) stress response proteins. As the knockdown cells were properly controlled for viral transduction and shRNA expression, these could be direct effects of the SLC26A2 repression. On the other hand, control cell, while expressing non-targeting shRNA, does not lead to RNA-induced silencing complex turnover, thus unavailing the elimination of the stress response as a secondary effect of RNA interference.

Gene regulations with more direct relevance to aldosterone production include the significantly differentially-regulated MAP Kinase cascade. Upregulation of MAPK phosphatases are observed along with a repression of p44/42 MAPK expression. The upregulation of p38 path seems to be a DNA damage stress effect. Instead of MAPK driven aldosterone production, protein kinase C mediated effects are more likely, in consideration of strong PKCη subunit upregulation and upregulated FOS and JUN transcription factors without any apparent changes in their MAPK modulators [**267**]. The observed increases in intracellular calcium may be the driving force behind a likely enzymatic PLC activation (but not upregulation) and increase in DAG levels. These observations suggest a primary relevance of increased $[Ca^{2+}]_i$ in SLC26A2 knockdown cells, rather than it being a secondary, enhancing effect of some other pathway.

Historically, surgically removed aldosterone producing adenomas are known for their zona fasciculata like appearance. Improved detection methods now reveal that a spectrum of APA cell morphology exists [**268**], with APAs consisting predominantly of zona glomerulosa-like cells tending to be smaller and harder to detect, arguably lessening their availability in bio-bank repositories. Aldosterone producing H295R cells showed upregulated ACTH receptors [**181**], as did the SLC26A2 knockdown cells, in contrast of the modest increase of AngII receptor. Although intense phosphodiesterase 3A (PDE3A) upregulation also inclines toward an ACTH responsive cAMP mediated aldosterone upregulation in knockdown cells, in which ACTH indeed effects a more pronounced response; DAG induced PKC upregulation, rather than cAMP responsive PKA, seems to be the prime mover of aldosterone production. Furthermore, ZG specific markers DKK3, DAB2, and CD56 expression profiles mimic that of stimulated ZG cells [**254; 269; 270**]. Although without statistical significance, non KCNJ5 mutant APA had a lower median SLC26A2 expression level. More importantly, a ZG-like APA feature, *i.e.* contrasting decrease of CYP17A1 and increase of KCNJ5, was observed in the knockdown cells. CYP21A2 upregulation possibly further leads cells toward an emphasis on aldosterone production. The substrate for this increased steroidogenic activity might be *de novo* cholesterol biosynthesis as opposed to normal HDL uptake [**56**], as indicated by the changes

in transcript levels of the relevant statin pathway genes (LPL, CETP, APOA1, SCARB1, ACSS1).

The convergence of observations from low and high-throughput assays in this study suggests that SLC26A2, hitherto without a known adrenal of steroidogenic role, may act as a regulator of membrane potential and cell polarity. It is observable that SLC26A2 modulates anion and, indirectly, cation homeostasis of the cell. Repression of SLC26A2 expression leads to aldosterone overproduction *in vitro* through a ZG-like pattern of events. Substantiation of these potential mechanisms necessitates further experimentation, especially in the membrane transport kinetics and proteomics of SLC26A2 knockdown cells, ideally in a primary adrenal culture with enriched ZG population.

4.5. Linking SLC26A2 to Aldosterone Regulation – *in vivo*

SLC26A2 expression in the adrenal gland was not detected on the mRNA or protein level hitherto this study, except for microarray based transcriptome screenings. Confirmation of this expression in human tissue and corresponding expression profile in female C3HeB/FeJ murine tissues established mouse as a model organism fit for this investigation. Aldosterone biosynthesis regulation by secretagogues potassium and angiotensin II also regulated adrenal SLC26A2 expression *in vivo*, further confirming the initial hypothesis of a relation between the hormone and the gene.

Regulation of aldosterone production in healthy mice and adrenocortical tumor cells are found to be contrasting each other. The stimulants AngII and KCl caused adrenal SLC26A2 down regulation, in accordance with the phenomenon of SLC26A2 repression associated with aldosterone production. In the model cell line, only potassium had an effect of upregulation. This contradiction can be attributed to potassium hypersensitivity of NCI-H295R cells, along with the supraphysiological potassium concentration applied. A more intuitive explanation would be the essential differences between *in vivo* and *in vitro* systems. Murine adrenal glands are comprised of both medulla and the whole cortex, and only a small proportion of the cells are expected to be aldosterone producing, in contrast with the uniformity in an NCI-H295R culture. Moreover, wild-type mice used for co-regulation experiments have an intact endocrine and paracrine system, with real-time modulation of the adrenal interstitial fluid composition; whereas only autocrine effects are active *in vitro*. Primary culture of adrenal cells, from outer cortical zones after an adrenalectomy, showed similar SLC26A2 expression profile with the H295R cells, further evidencing this line of articulation.

Mouse mutant models of genes with suspected pathophysiological roles in aldosterone biosynthesis have been previously employed, successfully elucidating physiological mechanisms. The targeted genes so far were the potassium channels Task1 (Kcnk3), Task3 (Kcnk9) [101-104] and Kcnma1 (BK)

[105], the Wnt signaling component Dkk3 [269] and the circadian clock regulators cryptochrome 1 (Cry1) and 2 (Cry2) [184]. The mutant mice showed varying degrees of autonomous aldosterone producing phenotype, depending on diet and sex. Task1$^{-/-}$ mice showed exhibited salt intake independent primary (low renin and hypokalemic) hyperaldosteronism in females but not in males. This was found to be ZF localized CYP11B2 expression in females [101; 259], rendering the effects glucocorticoid remediable, although in a different mechanism than human FH1 patients, whose CYP11B2 production is under CYP11B1 promoter control. The ectopic CYP11B2 expression of the mice was also age dependent, as pre-puberty male mice also showed CYP11B2 expression in the ZF. Extension of the hyperaldosteronic phenotype to males was achieved by targeting Wnt signaling in Task1$^{-/-}$ mice by generating double Task1$^{-/-}$/Dkk3$^{-/-}$ mice [269]. These animals showed primary hyperaldosteronism with normal adrenal zonation in males. Such sex and age dependent variations in penetrance were observed in other mutant mice as well. A double knockout of Task1$^{-/-}$/Task3$^{-/-}$ male mice, although with normal adrenal zonation, exhibited renin independent hyperaldosteronism by virtue of their depolarized ZG cells [102]. Germline Task3$^{-/-}$ mice did not display the hyperaldosteronism of Task1$^{-/-}$ and Task1$^{-/-}$/Task3$^{-/-}$ mice, but their ARR was elevated due to low renin levels in both sexes [104], albeit to a lesser degree than double knockouts as shown by males of a another Task3$^{-/-}$ strain [103], providing a model for low renin essential hypertension side of the PA/LREH spectrum. BK channel α subunit deficient mice of both sexes had increased aldosterone production without corresponding increase in renin activity [105]. A further model of hyperaldosteronism resulted from circadian clock dysregulation in Cry1$^{-/-}$/Cry2$^{-/-}$ double mutant male mice, with chronic Hsd3b6 overexpression in the ZG. Finally, another gene of interest in PA, disabled-2 (Dab2) [270], shows sex dependent effects on embryonic lethality in on Dab2$^{+/-}$/p53$^{-/-}$ heterozygotes [271].

The sex and age specific penetrance of the mouse models are in accordance with the studies that establish dependence of adrenocortical development [272; 273] and RAAS parameters [274] on the same factors. Females of NMRI - C57BL/6 crossbred strain mice showed increased adrenal weight along with adrenocortical and ZG volume in comparison to males after 7 weeks of age [272], seemingly due to differential of p38 and p44/42 MAPK activation levels between sexes [273]. Regardless of the adrenocortical size, the components of RAA system were higher in males of pure and crossbred C57BL/6J and C3HeB/FeJ mice strains [274]. It was also observed that, although female adrenals had more volume, male ZG comprised larger percentage of the adrenal glands. The greater extent of paternal black-6 heritage yielded higher aldosterone levels in both sexes. For renin activity, females did not show strain dependent changes, but males with greater extent of paternal black-6 heritage had higher levels. As a resulting black 6 heritage conferred similar ARR levels

between sexes, whereas C3HeB/FeJ heritage reduced ARR of females.

The sex dependent differences of aldosterone regulation and production are also evident in humans. The Framingham study reveals that higher blood pressure and PRC in men, and higher PAC and ARR in women [77]. ARR was also shown to be positively correlated with female sex in another cohort as well [143]. Old age and female sex have shown a tendency for higher PAC and ARR values in the KORA F4 survey [166], from which the cohort of this study was derived. These findings are in agreement with higher prevalence of the newly identified pathogenic somatic APA mutations of KCNJ5 in women and at younger age [110; 275]. ATP1A1,ATP2B3 and CACNA1D mutations either did not show this female bias [88; 111] or had a male predominance [87; 276], as well as presenting increased age of diagnosis and smaller adenoma diameter [89]. Given these findings it is tempting to speculate on a protective role of androgens against hyperaldosteronism, especially in light of castrated male Task1$^{-/-}$ mice showing the female specific dezonation and rescuing effect of testosterone treatment in females [101; 259].

Given the significant sex related differences in aldosterone and ARR values in both humans and mice, the SLC26A2 knock in mice with black-6 background [171] unsurprisingly showed differential steroidogenic gene expression and hormone production, with more pronounced effects in female mutants. When the steroidogenic genes in the adrenal are categorized by their focus on ZG / aldosterone production or ZF / early steroidogenesis, the prior group showed overexpression in a sex dependent manner, whereas the latter group was downregulated. The most striking example of this comes from 3βHSD isozymes, where the ZG specific Hsd3b6 is elevated in knockdown animals, as opposed to the downregulated Hsd3b1. The rate limiting enzyme of aldosterone production was significantly elevated in male mutants, with no difference in wild type sexes. In contrast, the increase in aldosterone was most emphasized in female mutants, with lower female wild type levels in accordance with the earlier work described above [274]. Renin levels were found to be higher in male vs female and mutant vs wild type comparisons. However, the standard deviation of the renin activity measurements proved to be too high, even among wild type animals, to derive definitive conclusions from. As a direct result of this confounding factor, ARR measurements, in which the renin activity is the covariant, are also compromised.

The confounding results from renin activity measurements are most likely due to cryoactivation of prorenin during plasma storage and handling; as enzymatic assay internal controls did not suggest a discrepancy in that end. Such issues of renin cryoactivation has been observed in the past when the centers of collection and assaying are spatially distant [277]. There is also no evidence for differential stress levels in animals of the same group, as the corticosterone assay results presented similar

levels wild-type males and females low standard errors. However, it is obvious from the same assay that the mutant animals were under intense stress. This would be only natural, given their extreme disease condition of diastrophic dysplasia, causing increased morbidity and 50 % mortality by day 21 [171]. This mouse model was developed as a model for Mendelian diastrophic dysplasia syndrome, and as a result this setting poorly translates to studies of PA, a multifactorial, heterogeneous disease. The germline mutation of SLC26A2, in addition to the chondrodysplasia, may be especially impactful on developing embryo, as SLC26A2 is the main sulfate transporter responsible for supplying sulfate in the placenta [252]. The experience obtained in this study also indicates an increased lethality of homozygous females, which hampered availability of an adequate set of samples from this group for the endocrine characterization. Given the difficulties in endocrine phenotyping of SLC26A2 mutant mice, a tissue specific knockout model [106] through a ZG specific Cre deleter strain, similar to the promising model developed for studying mineralocorticoid target tissues [278], might be a great deal more illuminating for *in vivo* effects of SLC26A2 suppression, free from the many secondary effects seen on germline mutants.

4.6. SLC26A2 in the Kidney

Aldosterone acts through mineralocorticoid receptors found in many cell populations, but its primary target in ion and water homeostasis is the cortical collecting duct. In light of this knowledge, collecting duct cells were employed in investigating possible SLC26A2 interaction with aldosterone mediated renal function. SLC26A2 had been previously reported to be detected in the kidney [179], and RT-PCR confirmed its expression in the collecting duct cell line. Most functional studies described here presented mild and below-significant effects, with the exception of osmoprotective gene expression in SLC26A2 knockdown cells. A report published as this study was being conducted reported that SLC26A2 expression was exclusive to proximal tubule in the kidney [260]. Moreover, it was also reported that proximal tubule is an aldosterone target as well [15]. These publications presented compelling evidence against the use of collecting duct cells in this study, especially when combined with the results from aldosterone treated wild type or SLC26A2 knockdown cells. However, another explanation is also possible in that detection of membrane SLC26A2 is highly dependent on the epitope retrieval method used [179], with harsh heat induced epitope retrieval treatment of tissues yielding false negative results. The lack of collecting duct immunopositivity was reported after exactly that kind of tissue pretreatment, and therefore harboring a potential error. Using a method as described in section 5.3 for better elucidation of adrenal localization with surface protein immunoprecipitation of collecting duct cells would be more reliable. In the case that SLC26A2 expression indeed does not lead to protein synthesis and function in the collecting duct, an interesting possibility of post-transcriptional regulation by miRNAs would come to attention. Also, a

proximal tubule deficient in SLC26A2 may trigger RAAS signaling through detection of increased luminal sodium concentrations by the macula densa; as lack of SLC26A2 activity may force the nephron to over-reliant on sodium dependent sulfate uptake through SLC13A1 [**260; 279**]. It has also been proposed that SLC26A2 may take part in the Na^+, Cl^-, sulfate and oxalate recycling in the proximal tubule, and its repression may derail the interplay of these co-dependent exchange mechanisms, leading to higher sodium concentrations in the ascending limb lumen [**260; 280**]. These possibilities render a study of SLC26A2 on proximal tubule worthwhile from an aldosterone focused point of view.

4.7.   Perspectives

This study presents an application of genetic epidemiological methodology as a scout for biological functional studies, which are too often restricted by the current knowledge in their hypothesis driven approach. However, the findings of the experiments seemingly lead to more questions than answers. Future investigation into these loose ends can be summarized in three broad categories:

Renal SLC26A2 function: As discussed above, a definitive localization of the SLC26A2 within kidney is necessary to explain the collecting duct expression of the gene. Depending on the findings, nephrological studies could be carried out to elucidate the function of SLC26A2 in the kidney, either in the collecting duct or the proximal tubule of the nephron.

In vitro aldosterone overproduction via SLC26A2 repression: The main effort of this study in illumination of the links between SLC26A2 knockdown and aldosterone overproduction observed in adrenocortical carcinoma cells. Although it can be stated with reasonable confidence that the effect is carried through calcium signaling, how this is effected by the knockdown remains elusive. A thorough investigation of the electrophysiological properties of the knockdown cell membranes and the currents of ions that SLC26A2 has an affinity for would be most interesting. The confounding effects of a cortisol producing carcinoma cell line may even be overcome by replicating knockdown effects in a ZG enriched primary adrenal culture, providing more clear explanations into SLC26A2 – aldosterone interplay.

Slc26a2 knock-in mutation in black 6 mice showed a sex dependent hyperaldosteronism, but this finding was convoluted by the extremely morbid phenotype of the animals. It may be impossible to derive a better view of the adrenal effects from immediate post-natal animals, where their DTD symptoms are less pronounced, due to unattainably small adrenal size and blood volume, but the blood pressure measurements of older animals would be informative even in their distorted endocrine phenotype. As proposed in the previous section, a conditional or tissue specific knockout

animal would be a much more suitable model for studying SLC26A2-hyperaldosteronism relation.

Finally, one can always wish for the then impossible, only to see it come true by virtue of advances in biotechnology. Recent progress in "big data" generation may soon make scanning Conn's and IPA patients for genetic and epigenetic changes feasible, which may even identify SLC26A2 as a common culprit in development and progression of primary hyperaldosteronism, at least in subpopulations such as the KORA cohort.

Regardless of the outcomes of future studies, it is likely that current understanding of multifactorial diseases will be further challenged by technical innovation, reaffirming the notion that "life is complicated" [281]. This situation may well lead to a historical repetition of what transpired in the field of Newtonian physics over a century ago, bringing about another *annus mirabilis* in biology.

5. Summary

Arterial hypertension is the most prevalent risk factor for cardiovascular disorders. Most cases of hypertension are due to unknown etiology, with only 5-15 per cent being secondary effects. Primary aldosteronism (PA) is the single most prevalent form of secondary hypertension, and is defined by autonomous aldosterone secretion independent of the plasma renin activity. Routine usage of aldosterone to renin ratio (ARR) for screening PA has revealed greater prevalence of the disorder, especially in resistant or advanced forms of arterial hypertension. The two most common causes of PA are aldosterone producing adenomas (APA) and bilateral adrenal hyperplasia (BAH). Rare Mendelian forms of familial hyperaldosteronism are also described. Until recently, genetic background of only glucocorticoid-remediable familial PA was elucidated in detail. Utilization of the exome sequencing techniques since 2011 identified somatic mutations in the cation transporter genes KCNJ5, ATP1A1, ATP2B3 and CACNA1D as the causative factors for circa 50 % of APAs. The underlying genetic causes of BAH cases remain to be determined.

Genome-wide association studies (GWAS) have been the predominant methodology in genetic epidemiological research in the past ten years, under the hypothesis of "common disease – common variant". Its prevalent application identified many risk loci, containing targets for functional investigation. In this study ARR was used as a phenotypic parameter in a GWAS in the German KORA-F4 cohort of 1876 individuals, leading to genome-wide significance of a locus in chromosome 5q32. The four genes in this locus (SLC26A2, TIGD6, HMGXB3 and CSF1R) were evaluated by their known characteristics and functions, and functional studies investigating their relevance to aldosterone biosynthesis and function were carried out for SLC26A2 and CSF1R. SLC26A2, a ubiquitously expressed solute carrier with mainly sulfate, oxalate and chloride affinities, was found to be co-regulated with aldosterone production *in vivo* and *in vitro*. RNA interference in a model adrenocortical cell line resulted in significantly higher rate of aldosterone production and aldosterone synthase expression, as well as increased overall steroidogenic capacity. Subsequent studies identified calcium signaling dependent pathways as the mediator of this effect. A germline SLC26A2 knock-in mouse model also showed confirmatory endocrine and adrenal phenotype in a sex-specific manner, with elevated plasma aldosterone concentration and ARR in females. The evidence derived from these findings suggests a possible role of SLC26A2 function in the pathophysiology of PA, which requires further epidemiological and functional experiments to confirm and elucidate.

Zusammenfassung

Die arterielle Hypertonie gilt als wichtigster Risikofaktor für kardiovaskuläre Erkrankungen. Während in den meisten Fällen eine essentielle Hypertonie angenommen werden kann, liegt in 5-15 % der Patienten dem Bluthochdruck eine andere Erkrankung zugrunde. Mit dem Einsatz des Aldosteron-Renin-Quotienten (ARQ) konnte der primäre Hyperaldosteronismus als die häufigste Form des sekundären Bluthochdrucks eingeordnet werden. Die beiden häufigsten Ursachen des primären Hyperaldosteronismus sind das Aldosteron-produzierende Adenom (APA) und die beidseitige Nebennierenrindenhyperplasie (BAH). Monogenetische, familiäre Formen sind hingegen insgesamt sehr selten. Mit dem Einsatz moderner Sequenziertechniken konnten seit 2011 somatische Mutationen in Ionenkanälen und Transportern (KCNJ5, ATP1A1, ATP2B3 und CACNA1D) in etwa 50 % der APAs identifiziert werden. Die genetische Ursachen der BAH sind dagegen in der überwiegenden Mehrzahl der Fälle unbekannt.

Unter der "common disease – common variant" Hypothese sind Genomweite Assoziationsstudien (GWAS) in den letzten zehn Jahren zur vorherrschenden Methode der genetischen epidemiologischen Forschung geworden. Ihr weit verbreiteter Einsatz hat zur Identifizierung vieler genetischer Risiko-Loci geführt, die dann funktionellen Untersuchungen zugeführt werden konnten. In der vorliegenden Arbeit wurde der ARQ als phänotypische Parameter in einer GWAS der deutschen KORA-F4 Kohorte von 1.876 Personen verwendet. Hierdurch fand sich eine genomweite Signifikanz eines Locus auf Chromosom 5q32. Die vier in diesem Locus enthaltenen Gene (SLC26A2, TIGD6, HMGXB3 und CSF1R) wurden anhand bekannter Eigenschaften und Funktionen eingeordnet und weitergehende funktionelle Studien für SLC26A2 und CSF1R durchgeführt. Für SLC26A2 – einem Transporter mit bekannten Affinitäten zu Sulfat, Oxalat und Chlorid - konnte *in vivo* und *in vitro* eine gemeinsame Regulation der adrenalen Expression mit Aldosteron gefunden werden. Ein knock-down von SCL26A2 in einem *in vitro* Modell durch siRNA führte zu einer relevanten Erhöhung der Aldosteron-Sekretion und transkriptionellen Veränderungen des Steroidbiosynthese-Apparats. Weitergehenden Untersuchungen identifizierten vor allem Kalzium-abhängige Signalkaskaden als für diesen Effekt ursächliche Mechanismen. In einem *Slc26a2* knock-in Mausmodell konnten geschlechtsabhängig ein entsprechender endokriner Phänotyp mit einem erhöhten ARQ nachgewiesen werden. Zusammengenommen ergeben sich aus diesen Untersuchungen gute Hinweise für einen Einfluss von SLC26A2 in der Regulation der Aldosteronsekretion und in der Pathophysiologie des primären Hyperaldosteronismus. Weitere funktionelle, epidemiologische und genetische Untersuchungen werden notwendig sein, diese Ergebnisse weiter zu vertiefen und in ihrer potentiellen klinischen Wertigkeit einzuordnen.

6. References

1. Defoe D. *The Political History of the Devil*. Read Books; 1726..
2. Rosamond W, Flegal K, Furie K*, et al.* Heart disease and stroke statistics—2008 update: A report from the American Heart Association Statistics Committee and Stroke Statistics Subcommittee. *Circulation*. 2008;117:e25-e146.
3. Mancia G, Fagard R, Narkiewicz K*, et al. 2013 ESH/ESC Guidelines for the management of arterial hypertension*. 2013..
4. Carretero OA, Oparil S. Essential hypertension part I: definition and etiology. *Circulation*. 2000;101:329-335.
5. Schirpenbach C, Reincke M. Primary aldosteronism: current knowledge and controversies in Conn's syndrome. *Nat Clin Pract Endocrinol Metab*. 2007;3:220-227.
6. Conn JW. Presidential address. I. Painting background. II. Primary aldosteronism, a new clinical syndrome. *J Lab Clin Med*. 1955;45:3-17.
7. Biglieri EG, Schambelan M, Slaton PE, Stockigt JR. The intercurrent hypertension of primary aldosteronism. *Circ Res*. 1970;27:195-202.
8. Elsevier-Mosby. *Mosby's Medical Dictionary*. Elsevier Health Sciences; 2013..
9. Wikiquote Contributors. House (Season 1). 2014;2015.
10. Ashley-Ross MA, Hsieh ST, Gibb AC, Blob RW. Vertebrate land invasions—past, present, and future: An introduction to the symposium. *Integrative and Comparative Biology*. 2013.
11. Hu X, Funder JW. The evolution of mineralocorticoid receptors. *Mol Endocrinol*. 2006;20:1471-1478.
12. Baez J. Extinction. 2006;2015.
13. Thomas W, Harvey BJ. Mechanisms underlying rapid aldosterone effects in the kidney. *Annual review of physiology*. 2011;73:335-357.
14. Connell JM, Davies E. The new biology of aldosterone. *The Journal of endocrinology*. 2005;186:1-20.
15. Salyer SA, Parks J, Barati MT*, et al.* Aldosterone regulates Na+, K+ ATPase activity in human renal proximal tubule cells through mineralocorticoid receptor. *Biochimica et Biophysica Acta (BBA) - Molecular Cell Research*. 2013;1833:2143-2152.
16. Sheader E, Wargent E, Ashton N, Balment R. Rapid stimulation of cyclic AMP production by aldosterone in rat inner medullary collecting ducts. *Journal of Endocrinology*. 2002;175:343-347.
17. Kahle KT, MacGregor GG, Wilson FH*, et al.* Paracellular Cl-permeability is regulated by WNK4 kinase: insight into normal physiology and hypertension. *Proceedings of the National Academy of Sciences of the United States of America*. 2004;101:14877-14882.
18. Schrier RW, Cadnapaphornchai MA. Renal aquaporin water channels: from molecules to human disease. *Progress in Biophysics and Molecular Biology*. 2003;81:117-131.
19. Rogerson FM, Brennan FE, Fuller PJ. Mineralocorticoid receptor binding, structure and function. *Molecular and cellular endocrinology*. 2004;217:203-212.
20. Funder JW, Pearce PT, Smith R, Smith AI. Mineralocorticoid action: target tissue specificity is enzyme, not receptor, mediated. *Science*. 1988;242:583-585.
21. van Uum SH. Liquorice and hypertension. *Neth J Med*. 2005;63:119-120.
22. Soundararajan R, Pearce D, Ziera T. The role of the ENaC-regulatory complex in aldosterone-mediated sodium transport. *Molecular and cellular endocrinology*. 2012;350:242-247.
23. Yoo D, Kim BY, Campo C*, et al.* Cell surface expression of the ROMK (Kir 1.1) channel is regulated by the aldosterone-induced kinase, SGK-1, and protein kinase A. *The Journal of biological chemistry*. 2003;278:23066-23075.
24. Rozansky DJ, Cornwall T, Subramanya AR*, et al.* Aldosterone mediates activation of the thiazide-sensitive Na-Cl cotransporter through an SGK1 and WNK4 signaling pathway. *J Clin Invest*. 2009;119:2601-2612.
25. Verrey F, Summa V, Heitzmann D*, et al.* Short-term aldosterone action on Na,K-ATPase surface expression: role of aldosterone-induced SGK1? *Ann N Y Acad Sci*. 2003;986:554-561.
26. Gekle M, Golenhofen N, Oberleithner H, Silbernagl S. Rapid activation of Na+/H+ exchange by aldosterone in renal epithelial cells requires Ca2+ and stimulation of a plasma membrane proton conductance. *Proceedings of the National Academy of Sciences*. 1996;93:10500-10504.
27. McCormick JA, Bhalla V, Pao AC, Pearce D. *SGK1: A rapid aldosterone-induced regulator of renal sodium reabsorption*. 2005..
28. Hoorn EJ, Nelson JH, McCormick JA, Ellison DH. The WNK kinase network regulating sodium, potassium, and blood pressure. *Journal of the American Society of Nephrology*. 2011;22:605-614.

29.   Koppel H, Christ M, Yard B*, et al.* Nongenomic effects of aldosterone on human renal cells. *The Journal of Clinical Endocrinology & Metabolism*. 2003;88:1297-1302.

30.   Funder JW. The nongenomic actions of aldosterone. *Endocr Rev*. 2005;26:313-321.

31.   Booth RE, Johnson JP, Stockand JD. *Aldosterone*. 2002..

32.   Kim J, Kim YH, Cha JH*, et al.* Intercalated cell subtypes in connecting tubule and cortical collecting duct of rat and mouse. *J Am Soc Nephrol*. 1999;10:1-12.

33.   Wagner C, Devuyst O, Bourgeois S, Mohebbi N. Regulated acid–base transport in the collecting duct. *Pflügers Archiv - European Journal of Physiology*. 2009;458:137-156.

34.   Diaz R, Brown RW, Seckl JR. Distinct ontogeny of glucocorticoid and mineralocorticoid receptor and 11beta-hydroxysteroid dehydrogenase types I and II mRNAs in the fetal rat brain suggest a complex control of glucocorticoid actions. *J Neurosci*. 1998;18:2570-2580.

35.   Vallon V. Tubuloglomerular feedback and the control of glomerular filtration rate. *News in physiological sciences : an international journal of physiology produced jointly by the International Union of Physiological Sciences and the American Physiological Society*. 2003;18:169-174.

36.   Castrop H. Mediators of tubuloglomerular feedback regulation of glomerular filtration: ATP and adenosine. *Acta physiologica (Oxford, England)*. 2007;189:3-14.

37.   Atlas SA. The renin-angiotensin aldosterone system: pathophysiological role and pharmacologic inhibition. *Journal of managed care pharmacy : JMCP*. 2007;13:9-20.

38.   Erdos EG, Skidgel RA. The angiotensin I-converting enzyme. *Lab Invest*. 1987;56:345-348.

39.   Fuchs S, Xiao HD, Hubert C*, et al.* Angiotensin-converting enzyme C-terminal catalytic domain is the main site of angiotensin I cleavage in vivo. *Hypertension*. 2008;51:267-274.

40.   Carey RM, Siragy HM. Newly recognized components of the renin-angiotensin system: potential roles in cardiovascular and renal regulation. *Endocr Rev*. 2003;24:261-271.

41.   Reudelhuber TL. The renin–angiotensin system: peptides and enzymes beyond angiotensin II. *Current opinion in nephrology and hypertension*. 2005;14:155-159.

42.   Spyroglou A, Manolopoulou J, Wagner S*, et al.* Short term regulation of aldosterone secretion after stimulation and suppression experiments in mice. *Journal of molecular endocrinology*. 2009;42:407-413.

43.   Bali A, Jaggi AS. Angiotensin as stress mediator: role of its receptor and interrelationships among other stress mediators and receptors. *Pharmacological research : the official journal of the Italian Pharmacological Society*. 2013;76:49-57.

44.   Usberti M, Gargiulo A, Comberti E*, et al.* Effect of exogenous prostaglandin E2 on plasma antidiuretic hormone in normal man. Role of angiotension II. *American journal of nephrology*. 1989;9:285-290.

45.   Schoenenberg P, Kehrer P, Muller AF, Gaillard RC. Angiotensin II potentiates corticotropin-releasing activity of CRF41 in rat anterior pituitary cells: mechanism of action. *Neuroendocrinology*. 1987;45:86-90.

46.   Cooke BA. Signal transduction involving cyclic AMP-dependent and cyclic AMP-independent mechanisms in the control of steroidogenesis. *Molecular and cellular endocrinology*. 1999;151:25-35.

47.   Wilson JL, Miranda CA, Knepper MA. Vasopressin and the regulation of aquaporin-2. *Clinical and experimental nephrology*. 2013;17:751-764.

48.   Ayers CR, Katholi RE, Carey RM*, et al.* Acute and chronic intrarenal alpha-and beta-adrenergic receptor stimulation of renin release in the conscious dog. *Hypertension*. 1981;3:615-621.

49.   Herichova I, Szantoova K. Renin-angiotensin system: upgrade of recent knowledge and perspectives. *Endocr Regul*. 2013;47:39-45.

50.   Melmed S, Polonsky KS, Larsen PR, Kronenberg HM. *Williams Textbook of Endocrinology*. Elsevier Health Sciences; 2011..

51.   Mitani F. Functional zonation of the rat adrenal cortex: the development and maintenance. *Proc Jpn Acad Ser B Phys Biol Sci*. 2014;90:163-183.

52.   Nishimoto K. Adrenocortical zonation in humans under normal and pathological conditions. *J. Clin. Endocrinol. Metab.* 2010;95:2296-2305.

53.   Mitani F, Suzuki H, Hata J*, et al.* A novel cell layer without corticosteroid-synthesizing enzymes in rat adrenal cortex: histochemical detection and possible physiological role. *Endocrinology*. 1994;135:431-438.

54.   Nakamura Y, Felizola SJ, Satoh F*, et al.* Dissecting the molecular pathways of primary aldosteronism. *Pathol Int*. 2014;64:482-489.

55.   Gomez-Sanchez CE, Qi X, Velarde-Miranda C*, et al.* Development of monoclonal antibodies against human CYP11B1 and CYP11B2. *Molecular and cellular endocrinology*. 2014;383:111-117.

56.   Williams DL, Temel RE, Connelly MA. Roles of Scavenger Receptor Bi and APO A-I in Selective Uptake of Hdl Cholesterol by Adrenal Cells. *Endocr Res*. 2000;26:639-651.

57.   Penning TM. Molecular endocrinology of hydroxysteroid dehydrogenases 1. *Endocr Rev*. 1997;18:281-305.

58.   Doi M, Satoh F, Maekawa T*, et al.* Isoform-specific monoclonal antibodies against 3beta-hydroxysteroid dehydrogenase/isomerase family provide markers for subclassification of human primary aldosteronism. *The Journal of clinical endocrinology and metabolism*. 2014;99:E257-262.

59.   Konosu-Fukaya S, Nakamura Y, Satoh F*, et al.* 3β-hydroxysteroid dehydrogenase isoforms in human aldosterone-producing adenoma. *Molecular and cellular endocrinology*. 2014.

60.   Spät A. Glomerulosa cell—a unique sensor of extracellular K+ concentration. *Molecular and cellular endocrinology*. 2004;217:23-26.

61.   Spat A, Hunyady L. Control of aldosterone secretion: a model for convergence in cellular signaling pathways. *Physiol Rev*. 2004;84:489-539.

62.   Gu J, Wen Y, Mison A, Nadler JL. 12-lipoxygenase pathway increases aldosterone production, 3',5'-cyclic adenosine monophosphate response element-binding protein phosphorylation, and p38 mitogen-activated protein kinase activation in H295R human adrenocortical cells. *Endocrinology*. 2003;144:534-543.

63.   Chiu T, Santiskulvong C, Rozengurt E. *ANG II stimulates PKC-dependent ERK activation, DNA synthesis, and cell division in intestinal epithelial cells*. 2003..

64.   Condon JC, Pezzi V, Drummond BM*, et al.* Calmodulin-dependent kinase I regulates adrenal cell expression of aldosterone synthase. *Endocrinology*. 2002;143:3651-3657.

65.   Sackmann S, Lichtenauer U, Shapiro I*, et al.* Aldosterone producing adrenal adenomas are characterized by activation of calcium/calmodulin-dependent protein kinase (CaMK) dependent pathways. *Hormone and metabolic research = Hormon- und Stoffwechselforschung = Hormones et metabolisme*. 2011;43:106-111.

66.   Osman H, Murigande C, Nadakal A, Capponi AM. Repression of DAX-1 and induction of SF-1 expression. Two mechanisms contributing to the activation of aldosterone biosynthesis in adrenal glomerulosa cells. *The Journal of biological chemistry*. 2002;277:41259-41267.

67.   Ota T, Doi M, Yamazaki F*, et al.* Angiotensin II triggers expression of the adrenal gland zona glomerulosa-specific 3β-hydroxysteroid dehydrogenase isoenzyme through *de novo* protein synthesis of the orphan nuclear receptors NGFIB and NURR1. *Mol Cell Biol*. 2014;34:3880-3894.

68.   Bassett MH, Suzuki T, Sasano H*, et al.* The orphan nuclear receptor NGFIB regulates transcription of 3beta-hydroxysteroid dehydrogenase. implications for the control of adrenal functional zonation. *The Journal of biological chemistry*. 2004;279:37622-37630.

69.   Foster RH. Reciprocal influences between the signalling pathways regulating proliferation and steroidogenesis in adrenal glomerulosa cells. *Journal of molecular endocrinology*. 2004;32:893-902.

70.   Christenson LK, Strauss JF, 3rd. Steroidogenic acute regulatory protein: an update on its regulation and mechanism of action. *Arch Med Res*. 2001;32:576-586.

71.   Mitani F, Miyamoto H, Mukai K, Ishimura Y. Effects of long term stimulation of ACTH and angiotensin II-secretions on the rat adrenal cortex. *Endocr Res*. 1996;22:421-431.

72.   Azizan EA, Brown MJ. The genetics of primary aldosteronism. *Journal of Endocrinology and Metabolism*. 2015;4:19-30.

73.   Conn JW, Cohen EL, Rovner DR. Suppression of plasma renin activity in primary aldosteronism. *JAMA*. 1964;190:213-221.

74.   Young WF. Primary aldosteronism: renaissance of a syndrome. *Clinical Endocrinology*. 2007;66:607-618.

75.   Olivieri O, Ciacciarelli A, Signorelli D*, et al.* Aldosterone to renin ratio in a primary care setting: the Bussolengo study. *The Journal of clinical endocrinology and metabolism*. 2004;89:4221-4226.

76.   Funder JW, Carey RM, Fardella C*, et al.* Case detection, diagnosis, and treatment of patients with primary aldosteronism: an endocrine society clinical practice guideline. *The Journal of clinical endocrinology and metabolism*. 2008;93:3266-3281.

77.   Newton-Cheh C, Guo CY, Gona P*, et al.* Clinical and genetic correlates of aldosterone-to-renin ratio and relations to blood pressure in a community sample. *Hypertension*. 2007;49:846-856.

78.   Rossi GP, Bernini G, Desideri G*, et al.* Renal damage in primary aldosteronism: results of the PAPY Study. *Hypertension*. 2006;48:232-238.

79.   Petramala L, Pignatelli P, Carnevale R*, et al.* Oxidative stress in patients affected by primary aldosteronism. *Journal of Hypertension*. 2014;32:2022-2029 2010.1097/HJH.0000000000000284.

80. Venes D. *Taber's Cyclopedic Medical Dictionary*. F.A. Davis Company; 2013..

81. Mulatero P, Stowasser M, Loh KC*, et al.* Increased diagnosis of primary aldosteronism, including surgically correctable forms, in centers from five continents. *The Journal of clinical endocrinology and metabolism*. 2004;89:1045-1050.

82. Rossi GP, Bernini G, Caliumi C*, et al.* A prospective study of the prevalence of primary aldosteronism in 1,125 hypertensive patients. *J Am Coll Cardiol*. 2006;48:2293-2300.

83. Gazdar AF, Oie HK, Shackleton CH*, et al.* Establishment and characterization of a human adrenocortical carcinoma cell line that expresses multiple pathways of steroid biosynthesis. *Cancer research*. 1990;50:5488-5496.

84. Lifton RP, Dluhy RG, Powers M*, et al.* A chimaeric 11 beta-hydroxylase/aldosterone synthase gene causes glucocorticoid-remediable aldosteronism and human hypertension. *Nature*. 1992;355:262-265.

85. Fischer E, Beuschlein F. Novel genes in primary aldosteronism. *Current opinion in endocrinology, diabetes, and obesity*. 2014;21:154-158.

86. Choi M, Scholl UI, Yue P*, et al.* K+ channel mutations in adrenal aldosterone-producing adenomas and hereditary hypertension. *Science*. 2011;331:768-772.

87. Beuschlein F, Boulkroun S, Osswald A*, et al.* Somatic mutations in ATP1A1 and ATP2B3 lead to aldosterone-producing adenomas and secondary hypertension. *Nat Genet*. 2013;45:440-444.

88. Scholl UI, Goh G, Stolting G*, et al.* Somatic and germline CACNA1D calcium channel mutations in aldosterone-producing adenomas and primary aldosteronism. *Nat Genet*. 2013;45:1050-1054.

89. Azizan EA, Poulsen H, Tuluc P*, et al.* Somatic mutations in ATP1A1 and CACNA1D underlie a common subtype of adrenal hypertension. *Nat Genet*. 2013;45:1055-1060.

90. Nishikawa T, Omura M, Satoh F*, et al.* Guidelines for the diagnosis and treatment of primary aldosteronism--the Japan Endocrine Society 2009. *Endocr J*. 2010;58:711-721.

91. Toffelmire EB, Slater K, Corvol P*, et al.* Response of plasma prorenin and active renin to chronic and acute alterations of renin secretion in normal humans - studies using a direct immunoradiometric assay. *J Clin Invest*. 1989;83:679-687.

92. Güngör S. Retail price quotation for Aldactone® and Inspra®. 2015.

93. Vonend O, Ockenfels N, Gao X*, et al.* Adrenal venous sampling: evaluation of the German Conn's registry. *Hypertension*. 2011;57:990-995.

94. Fischer E, Beuschlein F, Degenhart C*, et al.* Spontaneous remission of idiopathic aldosteronism after long-term treatment with spironolactone: results from the German Conn's Registry. *Clin Endocrinol (Oxf)*. 2012;76:473-477.

95. Montori VM, Schwartz GL, Chapman AB*, et al.* Validity of the aldosterone-renin ratio used to screen for primary aldosteronism. *Mayo Clin Proc*. 2001;76:877-882.

96. Burton TJ, Mackenzie IS, Balan K*, et al.* Evaluation of the sensitivity and specificity of (11)C-metomidate positron emission tomography (PET)-CT for lateralizing aldosterone secretion by Conn's adenomas. *The Journal of clinical endocrinology and metabolism*. 2012;97:100-109.

97. Nanba K, Tsuiki M, Sawai K*, et al.* Histopathological diagnosis of primary aldosteronism using CYP11B2 immunohistochemistry. *The Journal of Clinical Endocrinology & Metabolism*. 2013;98:1567-1574.

98. Bettegowda C, Sausen M, Leary RJ*, et al.* Detection of circulating tumor DNA in early- and late-stage human malignancies. *Science translational medicine*. 2014;6:224ra224.

99. Beuschlein F. Animal models of primary aldosteronism. *Ann Endocrinol (Paris)*. 2009;70:168-172.

100. Nobel Foundation. The Nobel Prize in Physiology or Medicine 2007. 2007;2015.

101. Heitzmann D, Derand R, Jungbauer S*, et al.* Invalidation of TASK1 potassium channels disrupts adrenal gland zonation and mineralocorticoid homeostasis. *The EMBO journal*. 2008;27:179-187.

102. Davies LA, Hu C, Guagliardo NA*, et al.* TASK channel deletion in mice causes primary hyperaldosteronism. *Proceedings of the National Academy of Sciences of the United States of America*. 2008;105:2203-2208.

103. Guagliardo NA, Yao J, Hu C*, et al.* TASK-3 channel deletion in mice recapitulates low-renin essential hypertension. *Hypertension*. 2012;59:999-1005.

104. Penton D, Bandulik S, Schweda F*, et al.* Task3 potassium channel gene invalidation causes low renin and salt-sensitive arterial hypertension. *Endocrinology*. 2012;153:4740-4748.

105. Sausbier M, Arntz C, Bucurenciu I*, et al.* Elevated blood pressure linked to primary hyperaldosteronism and impaired vasodilation in BK channel-deficient mice. *Circulation*. 2005;112:60-68.

106. Kos CH. Methods in nutrition science: Cre/loxP system for generating tissue-specific knockout mouse models. *Nutr Rev*. 2004;62:243-246.

107. Spyroglou A, Wagner S, Gomez-Sanchez C*, et al.* Utilization of a mutagenesis screen to generate mouse models of hyperaldosteronism. *Endocrinology*. 2011;152:326-331.

108. Ng SB, Turner EH, Robertson PD*, et al.* Targeted capture and massively parallel sequencing of 12 human exomes. *Nature*. 2009;461:272-276.

109. Choi M, Scholl UI, Ji W*, et al.* Genetic diagnosis by whole exome capture and massively parallel DNA sequencing. *Proceedings of the National Academy of Sciences*. 2009;106:19096-19101.

110. Boulkroun S, Beuschlein F, Rossi GP*, et al.* Prevalence, clinical, and molecular correlates of KCNJ5 mutations in primary aldosteronism. *Hypertension*. 2012;59:592-598.

111. Williams TA, Monticone S, Schack VR*, et al.* Somatic ATP1A1, ATP2B3, and KCNJ5 mutations in aldosterone-producing adenomas. *Hypertension*. 2014;63:188-195.

112. Nadeau JH. Transgenerational genetic effects on phenotypic variation and disease risk. *Human molecular genetics*. 2009;18:R202-R210.

113. Fisher RA. XV.—The correlation between relatives on the supposition of Mendelian inheritance. *Transactions of the royal society of Edinburgh*. 1919;52:399-433.

114. Galton F. The history of twins, as a criterion of the relative powers of nature and nurture. *Journal of the Anthropological Institute of Great Britain and Ireland*. 1876:391-406.

115. Siemens HW. *Die zwillingspathologie; ihre bedeutung, ihre methodik, ihre bisherigen ergebnisse*. Berlin: J. Springer; 1924..

116. Inglis GC, Ingram MC, Holloway CD*, et al.* Familial pattern of corticosteroids and their metabolism in adult human subjects--the Scottish Adult Twin Study. *The Journal of clinical endocrinology and metabolism*. 1999;84:4132-4137.

117. Lynch M, Walsh B. *Genetics and analysis of quantitative traits*. Sinauer; 1998..

118. Harris H, Hopkinson D, Luffman J. Enzyme diversity in human populations. *Ann N Y Acad Sci*. 1968;151:232-242.

119. Hirschhorn JN, Lohmueller K, Byrne E, Hirschhorn K. A comprehensive review of genetic association studies. *Genetics in Medicine*. 2002;4:45-61.

120. Murray JC, Buetow KH, Weber JL*, et al.* A comprehensive human linkage map with centimorgan density. Cooperative Human Linkage Center (CHLC). *Science*. 1994;265:2049-2054.

121. Altmüller J, Palmer LJ, Fischer G*, et al.* Genomewide scans of complex human diseases: true linkage is hard to find. *The American Journal of Human Genetics*. 2001;69:936-950.

122. Hirschhorn JN, Daly MJ. Genome-wide association studies for common diseases and complex traits. *Nat Rev Genet*. 2005;6:95-108.

123. Tabor HK, Risch NJ, Myers RM. Candidate-gene approaches for studying complex genetic traits: practical considerations. *Nat Rev Genet*. 2002;3:391-397.

124. Tan E-K. Genome-wide association studies: Promises and pitfalls. *Annals Academy of Medicine Singapore*. 2010;39:77-78.

125. Risch N, Merikangas K. The future of genetic studies of complex human diseases. *Science*. 1996;273:1516-1517.

126. Venter JC, Adams MD, Myers EW*, et al.* The sequence of the human genome. *science*. 2001;291:1304-1351.

127. Gibbs RA, Belmont JW, Hardenbol P*, et al.* The international HapMap project. *Nature*. 2003;426:789-796.

128. Ramsay G. DNA chips: state-of-the art. *Nature biotechnology*. 1998;16:40-44.

129. Matsuzaki H, Loi H, Dong S*, et al.* Parallel genotyping of over 10,000 SNPs using a one-primer assay on a high-density oligonucleotide array. *Genome research*. 2004;14:414-425.

130. Strittmatter WJ, Saunders AM, Schmechel D*, et al.* Apolipoprotein E: high-avidity binding to beta-amyloid and increased frequency of type 4 allele in late-onset familial Alzheimer disease. *Proceedings of the National Academy of Sciences*. 1993;90:1977-1981.

131. Collins FS, Guyer MS, Chakravarti A. Variations on a theme: Cataloging human DNA sequence variation. *Science*. 1997;278:1580-1581.

132. Laitinen T, Polvi A, Rydman P*, et al.* Characterization of a common susceptibility locus for asthma-related traits. *Science*. 2004;304:300-304.

133. Welter D, MacArthur J, Morales J*, et al.* The NHGRI GWAS Catalog, a curated resource of SNP-trait associations. *Nucleic acids research*. 2014;42:D1001-D1006.

134. Newton-Cheh C, Johnson T, Gateva V, *et al.* Genome-wide association study identifies eight loci associated with blood pressure. *Nat Genet*. 2009;41:666-676.

135. Levy D, Ehret GB, Rice K, *et al.* Genome-wide association study of blood pressure and hypertension. *Nat Genet*. 2009;41:677-687.

136. Org E, Eyheramendy S, Juhanson P, *et al.* Genome-wide scan identifies CDH13 as a novel susceptibility locus contributing to blood pressure determination in two European populations. *Human molecular genetics*. 2009;18:2288-2296.

137. Li Y, Willer C, Sanna S, Abecasis G. Genotype imputation. *Annual review of genomics and human genetics*. 2009;10:387-406.

138. Ehret GB, Munroe PB, Rice KM, *et al.* Genetic variants in novel pathways influence blood pressure and cardiovascular disease risk. *Nature*. 2011;478:103-109.

139. Klein RJ, Zeiss C, Chew EY, *et al.* Complement factor H polymorphism in age-related macular degeneration. *Science*. 2005;308:385-389.

140. Nordgren RN, Elkeeb AM, Godley BF. Age-related macular degeneration treatment in the era of molecular medicine. *World J Ophthalmol*. 2014;4:130-139.

141. Tolentino MJ, Dennrick A, John E, Tolentino MS. Drugs in Phase II clinical trials for the treatment of age-related macular degeneration. *Expert opinion on investigational drugs*. 2015;24:183-199.

142. Visscher Peter M, Brown Matthew A, McCarthy Mark I, Yang J. Five years of GWAS discovery. *Am J Hum Genet*. 2012;90:7-24.

143. Alvarez-Madrazo S, Padmanabhan S, Mayosi BM, *et al.* Familial and phenotypic associations of the aldosterone Renin ratio. *The Journal of clinical endocrinology and metabolism*. 2009;94:4324-4333.

144. Pearson TA, Manolio TA. How to interpret a genome-wide association study. *Jama*. 2008;299:1335-1344.

145. Maher B. Personal genomes: The case of the missing heritability. *Nature*. 2008;456:18-21.

146. Manolio TA, Collins FS, Cox NJ, *et al.* Finding the missing heritability of complex diseases. *Nature*. 2009;461:747-753.

147. Gomez-Sanchez CE, Foecking MF, Ferris MW, *et al.* The production of monoclonal antibodies against aldosterone. *Steroids*. 1987;49:581-587.

148. Huang da W, Sherman BT, Lempicki RA. Systematic and integrative analysis of large gene lists using DAVID bioinformatics resources. *Nat Protoc*. 2009;4:44-57.

149. Wang H, Maurano MT, Qu H, *et al.* Widespread plasticity in CTCF occupancy linked to DNA methylation. *Genome Research*. 2012;22:1680-1688.

150. Ashburner M, Ball CA, Blake JA, *et al.* Gene ontology: tool for the unification of biology. The Gene Ontology Consortium. *Nat Genet*. 2000;25:25-29.

151. Su AI, Wiltshire T, Batalov S, *et al.* A gene atlas of the mouse and human protein-encoding transcriptomes. *Proceedings of the National Academy of Sciences of the United States of America*. 2004;101:6062-6067.

152. International HapMap Consortium, Frazer KA, Ballinger DG, *et al.* A second generation human haplotype map of over 3.1 million SNPs. *Nature*. 2007;449:851-861.

153. Schneider CA, Rasband WS, Eliceiri KW, *et al.* NIH Image to ImageJ: 25 years of image analysis. *Nature methods*. 2012;9.

154. Kanehisa M, Goto S, Sato Y, *et al.* Data, information, knowledge and principle: back to metabolism in KEGG. *Nucleic acids research*. 2014;42:D199-205.

155. Glaab E, Schneider R. PathVar: analysis of gene and protein expression variance in cellular pathways using microarray data. *Bioinformatics*. 2012;28:446-447.

156. van Iersel MP, Kelder T, Pico AR, *et al.* Presenting and exploring biological pathways with PathVisio. *BMC bioinformatics*. 2008;9:399.

157. Untergasser A, Cutcutache I, Koressaar T, *et al.* Primer3--new capabilities and interfaces. *Nucleic acids research*. 2012;40:e115.

158. Lindberg DA. Internet access to the National Library of Medicine. *Effective clinical practice : ECP*. 2000;3:256-260.

159. Milacic M, Haw R, Rothfels K, *et al.* Annotating cancer variants and anti-cancer therapeutics in reactome. *Cancers*. 2012;4:1180-1211.

160. Pruitt KD, Brown GR, Hiatt SM, *et al.* RefSeq: an update on mammalian reference sequences. *Nucleic acids research*. 2014;42:D756-763.

161. Friedman RC, Farh KK-H, Burge CB, Bartel DP. Most mammalian mRNAs are conserved targets of microRNAs. *Genome Research*. 2009;19:92-105.

162. Rosenbloom KR, Armstrong J, Barber GP*, et al.* The UCSC Genome Browser database: 2015 update. *Nucleic acids research*. 2015;43:D670-681.

163. Kelder T, van Iersel MP, Hanspers K*, et al.* WikiPathways: building research communities on biological pathways. *Nucleic acids research*. 2012;40:D1301-1307.

164. Prie D, Friedlander G, Coureau C*, et al.* Role of adenosine on glucagon-induced cAMP in a human cortical collecting duct cell line. *Kidney international*. 1995;47:1310-1318.

165. Wichmann HE, Gieger C, Illig T, Group MKS. KORA-gen--resource for population genetics, controls and a broad spectrum of disease phenotypes. *Gesundheitswesen (Bundesverband der Arzte des Offentlichen Gesundheitsdienstes (Germany))*. 2005;67 Suppl 1:S26-30.

166. Hannemann A, Bidlingmaier M, Friedrich N*, et al.* Screening for primary aldosteronism in hypertensive subjects: results from two German epidemiological studies. *European journal of endocrinology / European Federation of Endocrine Societies*. 2012;167:7-15.

167. Korn JM, Kuruvilla FG, McCarroll SA*, et al.* Integrated genotype calling and association analysis of SNPs, common copy number polymorphisms and rare CNVs. *Nat Genet*. 2008;40:1253-1260.

168. Marchini J, Howie B, Myers S*, et al.* A new multipoint method for genome-wide association studies by imputation of genotypes. *Nat Genet*. 2007;39:906-913.

169. Mulatero P, Rabbia F, Milan A*, et al.* Drug effects on aldosterone/plasma renin activity ratio in primary aldosteronism. *Hypertension*. 2002;40:897-902.

170. Fischer E, Beuschlein F, Bidlingmaier M, Reincke M. Commentary on the Endocrine Society Practice Guidelines: Consequences of adjustment of antihypertensive medication in screening of primary aldosteronism. *Reviews in Endocrine and Metabolic Disorders*. 2011;12:43-48.

171. Forlino A, Piazza R, Tiveron C*, et al.* A diastrophic dysplasia sulfate transporter (SLC26A2) mutant mouse: morphological and biochemical characterization of the resulting chondrodysplasia phenotype. *Human molecular genetics*. 2005;14:859-871.

172. Manolopoulou J, Bielohuby M, Caton SJ*, et al.* A highly sensitive immunofluorometric assay for the measurement of aldosterone in small sample volumes: validation in mouse serum. *The Journal of endocrinology*. 2008;196:215-224.

173. Dressendorfer RA, Kirschbaum C, Rohde W*, et al.* Synthesis of a cortisol-biotin conjugate and evaluation as a tracer in an immunoassay for salivary cortisol measurement. *The Journal of steroid biochemistry and molecular biology*. 1992;43:683-692.

174. Neuhofer W, Bartels H, Fraek ML, Beck FX. Relationship between intracellular ionic strength and expression of tonicity-responsive genes in rat papillary collecting duct cells. *The Journal of physiology*. 2002;543:147-153.

175. Beck F, Dorge A, Rick R, Thurau K. Intra- and extracellular element concentrations of rat renal papilla in antidiuresis. *Kidney international*. 1984;25:397-403.

176. Spyroglou A, Bozoglu T, Rawal R*, et al.* Diastrophic dysplasia sulfate transporter (SLC26A2) is expressed in the adrenal cortex and regulates aldosterone secretion. *Hypertension*. 2014;63:1102-1109.

177. Miller L. Analyzing gels and western blots with ImageJ. 2011;2015.

178. Walter M, Lucet IS, Patel O*, et al.* The 2.7 A crystal structure of the autoinhibited human c-Fms kinase domain. *Journal of molecular biology*. 2007;367:839-847.

179. Haila S, Hastbacka J, Bohling T*, et al.* SLC26A2 (diastrophic dysplasia sulfate transporter) is expressed in developing and mature cartilage but also in other tissues and cell types. *The journal of histochemistry and cytochemistry : official journal of the Histochemistry Society*. 2001;49:973-982.

180. Dmitrieva NI, Burg MB, Ferraris JD. *DNA damage and osmotic regulation in the kidney*. 2005..

181. Lichtenauer UD, Shapiro I, Osswald A*, et al.* Characterization of NCI-H295R cells as an in vitro model of hyperaldosteronism. *Hormone and metabolic research = Hormon- und Stoffwechselforschung = Hormones et metabolisme*. 2013;45:124-129.

182. Parmar J, Key RE, Rainey WE. Development of an adrenocorticotropin-responsive human adrenocortical carcinoma cell line. *The Journal of clinical endocrinology and metabolism*. 2008;93:4542-4546.

183. Smith H. Discovery of the anthrax toxin: the beginning of in vivo studies on pathogenic bacteria. *Trends in Microbiology*. 2000;8:199-200.

184. Doi M, Takahashi Y, Komatsu R*, et al.* Salt-sensitive hypertension in circadian clock-deficient Cry-null mice involves dysregulated adrenal Hsd3b6. *Nat Med*. 2010;16:67-74.

185. Grundy HM, Simpson SA, Tait JF. Isolation of a highly active mineralocorticoid from beef adrenal extract. *Nature*. 1952;169:795-796.

186. Simpson SA, Tait JF, Wettstein A*, et al.* Konstitution des Aldosterons, des neuen Mineralocorticoids. *Experientia*. 1954;10:132-133.
187. Verrey F. *Early aldosterone action: toward filling the gap between transcription and transport*. 1999..
188. Conn JW, Louis LH. Primary aldosteronism, a new clinical entity. *Ann Intern Med*. 1956;44:1-15.
189. Stowasser M, Gordon RD, Tunny TJ*, et al.* Familial hyperaldosteronism type II: five families with a new variety of primary aldosteronism. *Clinical and experimental pharmacology and physiology*. 1992;19:319-322.
190. Geller DS, Zhang J, Wisgerhof MV*, et al.* A novel form of human mendelian hypertension featuring nonglucocorticoid-remediable aldosteronism. *The Journal of clinical endocrinology and metabolism*. 2008;93:3117-3123.
191. Berglund G, Andersson O, Wilhelmsen L. Prevalence of primary and secondary hypertension: studies in a random population sample. *British medical journal*. 1976;2:554-556.
192. Mosso L, Carvajal C, Gonzalez A*, et al.* Primary aldosteronism and hypertensive disease. *Hypertension*. 2003;42:161-165.
193. Conn JW, Knopf RF, Nesbit RM. Clinical characteristics of primary aldosteronism from an analysis of 145 cases. *Am J Surg*. 1964;107:159-172.
194. Hunter DJ, Altshuler D, Rader DJ. From Darwin's finches to canaries in the coal mine — mining the genome for new biology. *New England Journal of Medicine*. 2008;358:2760-2763.
195. Klein C, Lohmann K, Ziegler A. The promise and limitations of genome-wide association studies. *Jama*. 2012;308:1867-1868.
196. Cirulli ET, Goldstein DB. Uncovering the roles of rare variants in common disease through whole-genome sequencing. *Nature Reviews Genetics*. 2010;11:415-425.
197. Gibson G. Hints of hidden heritability in GWAS. *Nat Genet*. 2010;42:558-560.
198. McKinney BA, Pajewski NM. Six degrees of epistasis: Statistical network models for GWAS. *Frontiers in Genetics*. 2011;2:109.
199. Gibson G. Rare and common variants: twenty arguments. *Nat Rev Genet*. 2012;13:135-145.
200. Zuk O, Hechter E, Sunyaev SR, Lander ES. The mystery of missing heritability: Genetic interactions create phantom heritability. *Proceedings of the National Academy of Sciences*. 2012;109:1193-1198.
201. Stahl EA, Wegmann D, Trynka G*, et al.* Bayesian inference analyses of the polygenic architecture of rheumatoid arthritis. *Nat Genet*. 2012;44:483-489.
202. Yang J, Ferreira T, Morris AP*, et al.* Conditional and joint multiple-SNP analysis of GWAS summary statistics identifies additional variants influencing complex traits. *Nat Genet*. 2012;44:369-375.
203. Zhu X, Feng T, Tayo Bamidele O*, et al.* Meta-analysis of correlated traits via summary statistics from GWASs with an application in hypertension. *The American Journal of Human Genetics*. 2015;96:21-36.
204. The 1000 Genomes Project Consortium, Abecasis GR, Auton A*, et al.* An integrated map of genetic variation from 1,092 human genomes. *Nature*. 2012;491:56-65.
205. Sheridan C. Illumina claims [dollar]1,000 genome win. *Nat Biotech*. 2014;32:115-115.
206. Wellcome Trust Case Control Consortium. Genome-wide association study of 14,000 cases of seven common diseases and 3,000 shared controls. *Nature*. 2007;447:661-678.
207. Nalls MA, Pankratz N, Lill CM*, et al.* Large-scale meta-analysis of genome-wide association data identifies six new risk loci for Parkinson's disease. *Nat Genet*. 2014;46:989-993.
208. Hindorff LA MJ, Morales J, Junkins HA, Hall PN, Klemm AK, and Manolio TA. A catalog of published genome-wide association studies. 2015;2015.
209. Sawcer S. *The complex genetics of multiple sclerosis: pitfalls and prospects*. 2008..
210. Teumer A, Rawal R, Homuth G*, et al.* Genome-wide association study identifies four genetic loci sssociated with thyroid volume and goiter risk. *The American Journal of Human Genetics*. 2011;88:664-673.
211. Steffens M, Lamina C, Illig T*, et al.* SNP-based analysis of genetic substructure in the German population. *Human Heredity*. 2006;62:20-29.
212. Wacholder S, Rothman N, Caporaso N. Counterpoint: bias from population stratification is not a major threat to the validity of conclusions from epidemiological studies of common polymorphisms and cancer. *Cancer Epidemiology Biomarkers & Prevention*. 2002;11:513-520.
213. Dastani Z, Hivert MF, Timpson N*, et al.* Novel loci for adiponectin levels and their influence on type 2 diabetes and metabolic traits: a multi-ethnic meta-analysis of 45,891 individuals. *PLoS Genet*. 2012;8:e1002607.
214. Kottgen A, Albrecht E, Teumer A*, et al.* Genome-wide association analyses identify 18 new loci associated with serum urate concentrations. *Nat Genet*. 2013;45:145-154.

215. Scott RA, Lagou V, Welch RP*, et al.* Large-scale association analyses identify new loci influencing glycemic traits and provide insight into the underlying biological pathways. *Nat Genet*. 2012;44:991-1005.

216. Visscher PM. Sizing up human height variation. *Nat Genet*. 2008;40:489-490.

217. Speliotes EK, Willer CJ, Berndt SI*, et al.* Association analyses of 249,796 individuals reveal 18 new loci associated with body mass index. *Nat Genet*. 2010;42:937-948.

218. Watkins WS, Rohrwasser A, Peiffer A*, et al.* AGT genetic variation, plasma AGT, and blood pressure: An analysis of the Utah Genetic Reference Project pedigrees. *American Journal of Hypertension*. 2010;23:917-923.

219. Young WF, Jr. Primary aldosteronism: A common and curable form of hypertension. *Cardiol Rev*. 1999;7:207-214.

220. Young Jr WF. Pheochromocytoma and primary aldosteronism: diagnostic approaches. *Endocrinology and metabolism clinics of North America*. 1997;26:801-827.

221. Funder JW. Primary aldosteronism and low-renin hypertension: a continuum? *Nephrol Dial Transplant*. 2013;28:1625-1627.

222. Gouli A, Kaltsas G, Tzonou A*, et al.* High prevalence of autonomous aldosterone secretion among patients with essential hypertension. *European journal of clinical investigation*. 2011;41:1227-1236.

223. Grim CE, Miller JZ, Luft FC*, et al.* Genetic influences on renin, aldosterone, and the renal excretion of sodium and potassium following volume expansion and contraction in normal man. *Hypertension*. 1979;1:583-590.

224. Kotchen TA, Kotchen JM, Grim CE*, et al.* Genetic determinants of hypertension: Identification of candidate phenotypes. *Hypertension*. 2000;36:7-13.

225. Vinck WJ, Fagard RH, Vlietinck R, Lijnen P. Heritability of plasma renin activity and plasma concentration of angiotensinogen and angiotensin-converting enzyme. *J Hum Hypertens*. 2002;16:417-422.

226. Brookfield JF. Q&A: promise and pitfalls of genome-wide association studies. *BMC biology*. 2010;8:41.

227. Ehret GB, Morrison AC, O'Connor AA*, et al.* Replication of the Wellcome Trust genome-wide association study of essential hypertension: the Family Blood Pressure Program. *Eur J Hum Genet*. 2008;16:1507-1511.

228. Hong K-W, Jin H-S, Cho YS*, et al.* Replication of the Wellcome Trust genome-wide association study on essential hypertension in a Korean population. *Hypertens Res*. 2009;32:570-574.

229. Schirpenbach C, Seiler L, Maser-Gluth C*, et al.* Automated chemiluminescence-immunoassay for aldosterone during dynamic testing: comparison to radioimmunoassays with and without extraction steps. *Clin Chem*. 2006;52:1749-1755.

230. Tomaschitz A, Pilz S. Aldosterone to renin ratio--a reliable screening tool for primary aldosteronism? *Hormone and metabolic research = Hormon- und Stoffwechselforschung = Hormones et metabolisme*. 2010;42:382-391.

231. Fischer E, Reuschl S, Quinkler M*, et al.* Assay characteristics influence the aldosterone to renin ratio as a screening tool for primary aldosteronism: results of the German Conn's registry. *Hormone and metabolic research = Hormon- und Stoffwechselforschung = Hormones et metabolisme*. 2013;45:526-531.

232. Hiura Y, Tabara Y, Kokubo Y*, et al.* A genome-wide association study of hypertension-related phenotypes in a Japanese population. *Circulation journal: official journal of the Japanese Circulation Society*. 2010;74:2353-2359.

233. Lieb W, Chen M-H, Teumer A*, et al.* Genome-wide meta-analyses of plasma renin activity and concentration reveal association with the kininogen 1 and prekallikrein genes. *Circulation: Cardiovascular Genetics*. 2014:CIRCGENETICS. 114.000613.

234. Smit AF, Riggs AD. Tiggers and DNA transposon fossils in the human genome. *Proceedings of the National Academy of Sciences of the United States of America*. 1996;93:1443-1448.

235. Marshall O, Choo KHA. Putative CENP-B paralogues are not present at mammalian centromeres. *Chromosoma*. 2012;121:169-179.

236. Ueda T, Yoshida M. HMGB proteins and transcriptional regulation. *Biochimica et biophysica acta*. 2010;1799:114-118.

237. Yanai H, Ban T, Wang Z*, et al.* HMGB proteins function as universal sentinels for nucleic-acid-mediated innate immune responses. *Nature*. 2009;462:99-103.

238. Lindskog C, Korsgren O, Pontén F, *et al.* Novel pancreatic beta cell-specific proteins: Antibody-based proteomics for identification of new biomarker candidates. *Journal of Proteomics*. 2012;75:2611-2620.

239. Sherr CJ. Colony-stimulating factor-1 receptor. *Blood*. 1990;75:1-12.

240. Dai XM, Ryan GR, Hapel AJ, *et al.* Targeted disruption of the mouse colony-stimulating factor 1 receptor gene results in osteopetrosis, mononuclear phagocyte deficiency, increased primitive progenitor cell frequencies, and reproductive defects. *Blood*. 2002;99:111-120.

241. Cecchini MG, Dominguez MG, Mocci S, *et al.* Role of colony stimulating factor-1 in the establishment and regulation of tissue macrophages during postnatal development of the mouse. *Development (Cambridge, England)*. 1994;120:1357-1372.

242. Cohen PE, Nishimura K, Zhu L, Pollard JW. Macrophages: important accessory cells for reproductive function. *Journal of leukocyte biology*. 1999;66:765-772.

243. He L, Hristova K. Physical-chemical principles underlying RTK activation, and their implications for human disease. *Biochimica et biophysica acta*. 2012;1818:995-1005.

244. Leung AY, Man CH, Kwong YL. FLT3 inhibition: a moving and evolving target in acute myeloid leukaemia. *Leukemia*. 2013;27:260-268.

245. El-Gamal MI, Anbar HS, Yoo KH, Oh CH. FMS kinase inhibitors: Current status and future prospects. *Medicinal research reviews*. 2013;33:599-636.

246. Nes WD, Lukyanenko YO, Jia ZH, *et al.* Identification of the lipophilic factor produced by macrophages that stimulates steroidogenesis. *Endocrinology*. 2000;141:953-958.

247. Ohana E, Shcheynikov N, Park M, Muallem S. Solute carrier family 26 member a2 (Slc26a2) protein functions as an electroneutral SOFormula/OH-/Cl- exchanger regulated by extracellular Cl. *The Journal of biological chemistry*. 2012;287:5122-5132.

248. Heneghan JF, Akhavein A, Salas MJ, *et al.* Regulated transport of sulfate and oxalate by SLC26A2/DTDST. *American journal of physiology. Cell physiology*. 2010;298:C1363-1375.

249. Hastbacka J, de la Chapelle A, Mahtani MM, *et al.* The diastrophic dysplasia gene encodes a novel sulfate transporter: positional cloning by fine-structure linkage disequilibrium mapping. *Cell*. 1994;78:1073-1087.

250. Cornaglia AI, Casasco A, Casasco M, *et al.* Dysplastic histogenesis of cartilage growth plate by alteration of sulphation pathway: a transgenic model. *Connective tissue research*. 2009;50:232-242.

251. Yusa A, Miyazaki K, Kimura N, *et al.* Epigenetic silencing of the sulfate transporter gene DTDST induces sialyl Lewisx expression and accelerates proliferation of colon cancer cells. *Cancer research*. 2010;70:4064-4073.

252. Dawson PA, Rakoczy J, Simmons DG. Placental, renal, and ileal sulfate transporter gene expression in mouse gestation. *Biol Reprod*. 2012;87:43.

253. Simard J, Ricketts ML, Gingras S, *et al.* Molecular biology of the 3beta-hydroxysteroid dehydrogenase/delta5-delta4 isomerase gene family. *Endocr Rev*. 2005;26:525-582.

254. Caroccia B, Fassina A, Seccia TM, *et al.* Isolation of human adrenocortical aldosterone-producing cells by a novel immunomagnetic beads method. *Endocrinology*. 2010;151:1375-1380.

255. Beuschlein F. Regulation of aldosterone secretion: from physiology to disease. *European journal of endocrinology / European Federation of Endocrine Societies*. 2013;168:R85-93.

256. Gomez-Sanchez CE. Channels and pumps in aldosterone-producing adenomas. *The Journal of clinical endocrinology and metabolism*. 2014;99:1152-1156.

257. Valverde MA, Hardy SP, Sepulveda FV. Chloride channels: a state of flux. *FASEB J*. 1995;9:509-515.

258. Gallo-Payet N, Cote M, Chorvatova A, *et al.* Cyclic AMP-independent effects of ACTH on glomerulosa cells of the rat adrenal cortex. *The Journal of steroid biochemistry and molecular biology*. 1999;69:335-342.

259. Bandulik S, Penton D, Barhanin J, Warth R. TASK1 and TASK3 potassium channels: determinants of aldosterone secretion and adrenocortical zonation. *Hormone and metabolic research = Hormon- und Stoffwechselforschung = Hormones et metabolisme*. 2010;42:450-457.

260. Chapman J, Karniski L. Protein localization of SLC26A2 (DTDST) in rat kidney. *Histochem Cell Biol*. 2010;133:541-547.

261. Nogueira EF, Xing Y, Morris CA, Rainey WE. Role of angiotensin II-induced rapid response genes in the regulation of enzymes needed for aldosterone synthesis. *Journal of molecular endocrinology*. 2009;42:319-330.

262. Ritchie W, Flamant S, Rasko JE. mimiRNA: a microRNA expression profiler and classification resource designed to identify functional correlations between microRNAs and their targets. *Bioinformatics*. 2010;26:223-227.

263. Haecker I, Gay LA, Yang Y*, et al.* Ago HITS-CLIP expands understanding of Kaposi's sarcoma-associated herpesvirus miRNA function in primary effusion lymphomas. *PLoS pathogens*. 2012;8:e1002884.

264. Levy Y, Arbel-Goren R, Hadari YR*, et al.* Galectin-8 functions as a matricellular modulator of cell adhesion. *Journal of Biological Chemistry*. 2001;276:31285-31295.

265. Chatr-aryamontri A, Breitkreutz B-J, Oughtred R*, et al.* The BioGRID interaction database: 2015 update. *Nucleic acids research*. 2014.

266. Xu C, Bailly-Maitre B, Reed JC. Endoplasmic reticulum stress: cell life and death decisions. *J Clin Invest*. 2005;115:2656-2664.

267. Soh JW, Lee EH, Prywes R, Weinstein IB. Novel roles of specific isoforms of protein kinase C in activation of the c-fos serum response element. *Mol Cell Biol*. 1999;19:1313-1324.

268. Brown MJ. Platt versus Pickering: what molecular insight to primary hyperaldosteronism tells us about hypertension. *JRSM cardiovascular disease*. 2012;1:17.

269. El Wakil A, Bandulik S, Guy N*, et al.* Dkk3 is a component of the genetic circuitry regulating aldosterone biosynthesis in the adrenal cortex. *Human molecular genetics*. 2012;21:4922-4929.

270. Romero DG, Yanes LL, de Rodriguez AF*, et al.* Disabled-2 is expressed in adrenal zona glomerulosa and is involved in aldosterone secretion. *Endocrinology*. 2007;148:2644-2652.

271. Yang DH, Fazili Z, Smith ER*, et al.* Disabled-2 heterozygous mice are predisposed to endometrial and ovarian tumorigenesis and exhibit sex-biased embryonic lethality in a p53-null background. *Am J Pathol*. 2006;169:258-267.

272. Bielohuby M, Herbach N, Wanke R*, et al.* Growth analysis of the mouse adrenal gland from weaning to adulthood: time- and gender-dependent alterations of cell size and number in the cortical compartment. *Am J Physiol Endocrinol Metab*. 2007;293:E139-146.

273. Bielohuby M, Sawitzky M, Johnsen I*, et al.* Decreased p44/42 mitogen-activated protein kinase phosphorylation in gender- or hormone-related but not during age-related adrenal gland growth in mice. *Endocrinology*. 2009;150:1269-1277.

274. Spyroglou A, Sabrautzki S, Rathkolb B*, et al.* Gender-, strain-, and inheritance-dependent variation in aldosterone secretion in mice. *The Journal of endocrinology*. 2012;215:375-381.

275. Akerstrom T, Crona J, Delgado Verdugo A*, et al.* Comprehensive re-Sequencing of adrenal aldosterone producing lesions reveal three somatic mutations near the KCNJ5 potassium channel selectivity filter. *PloS one*. 2012;7:e41926.

276. Fernandes-Rosa FL, Williams TA, Riester A*, et al.* Genetic spectrum and clinical correlates of somatic mutations in aldosterone-producing adenoma. *Hypertension*. 2014;64:354-361.

277. Sealey JE, Blumenfeld J, Laragh JH. Prorenin cryoactivation as a possible cause of normal renin levels in patients with primary aldosteronism. *J Hypertens*. 2005;23:459-460; author reply 460.

278. Náray-Fejes-Tóth A, Fejes-Tóth G. *Novel mouse strain with Cre recombinase in 11β-hydroxysteroid dehydrogenase-2-expressing cells*. 2007..

279. Dawson PA, Beck L, Markovich D. Hyposulfatemia, growth retardation, reduced fertility, and seizures in mice lacking a functional NaS(i)-1 gene. *Proceedings of the National Academy of Sciences of the United States of America*. 2003;100:13704-13709.

280. Aronson PS. Essential roles of CFEX-mediated Cl--oxalate exchange in proximal tubule NaCl transport and prevention of urolithiasis. *Kidney international*. 2006;70:1207-1213.

281. Bailey JE. Life is complicated. *Technological and Medical Implications of Metabolic Control Analysis*. Springer; 2000:41-47..

7. Appendix

7.1. Abbreviations

$[Ca^{2+}]_I$	intracellular calcium concentration
$[Ca^{2+}]_O$	extracellular calcium concentration
$[K^+]_O$	extracellular potassium concentration
°C	degree Celsius
µl	microliter
µM	micromolar
11βHSD	11-β-hydroxysteroid dehydrogenase
12-HETE	12-Hydroxyeicosatetraenoic acid
3βHSD	3-β-hydroxysteroid dehydrogenase / Δ-5-4 isomerase
ACE	angiotensin-converting enzyme
ACTH	adrenocorticotropic hormone
ADH	anti-diuretic hormone
AngI	angiotensin I
AngII	angiotensin II
ANOVA	analysis of variance
APA	aldosterone producing adenoma
ARR	aldosterone to renin ratio
AT_1	angiotensin II receptor type 1
AT_2	angiotensin II receptor type 2
ATF	activator transcription factor
ATP	adenosine triphosphate
ATPase	adenosine triphosphatase
AVS	adrenal vein sampling
BAH	bilateral adrenal hyperplasia
BCA	bicinchoninic acid
BK	Ca^{2+}-activated K^+ channel
BSA	bovine serum albumin fraction
CaM	calmodulin
CAMK	calcium / calmodulin dependent kinases
cAMP	cyclic adenosine monophosphate
CDCV	common disease - common variant
cDNA	complementary DNA

CHIF	corticosteroid hormone-induced factor
cm	centimeter
cM	centimorgan
CRE	cAMP response element
CREB	CRE binding protein
cRNA	complementary RNA
CT	computed tomography
CYP11B	11β-hydroxylase
DAB	3,3'-diaminobenzidine
DAG	1,2-diacylglycerol
DIN	Deutsches Institut für Normung
DMEM	Dulbecco's modified Eagle's medium
DNA	deoxyribonucleic acid
DNase	deoxyribonuclease
DOCA	11-desoxycorticosterone acetate
DTD	diastrophic dysplasia
DTDST	diastrophic dysplasia sulfate transporter
DTPA	diethylenetriaminepentaaceticacid
DTT	dithiothreitol
ECL	enhanced chemiluminescence
EDTA	ethylene diamine tetraacetic acid
EIA	enzyme immunoassay
ENaC	amiloride-sensitive epithelial sodium channel
ENU	N-ethyl-N-nitrosourea
ER	endoplasmic reticulum
ES	embryonic stem (cell)
EtBr	ethidium bromide
EtOH	ethanol
FBS	fetal bovine serum
FH	familial hyperaldosteronism
GO	Gene Ontology
GTP	guanosine triphosphate
GWA	genome-wide association
GWAS	genome-wide association study

h^2	narrow-sense heritability
HDL	high-density lipoprotein
HEPES	4-(2-hydroxyethyl)-1-piperazineethanesulfonic acid
HRP	horseradish peroxidase
HSP	heat shock protein
IgG	immunoglobulin G
IHC	immunohistochemistry
IP_3	inositol 1,4,5-triphosphate
IQR	interquartile range
ITS	insulin–transferrin–selenium
KD	Knockdown
kg	kilogram
KHP	potassium-hydrogen-phthalate
Ki-RasA	Kirsten Ras GTP-binding protein-2A
KORA	Cooperative Health Research in the Region of Augsburg
L	liter
LD	linkage disequilibrium
LDL	low-density lipoprotein
LKC	immunoassay buffer
LREH	low-renin essential hypertension
M	molar
MAPK	mitogen-activated protein kinase
M-CSF	macrophage colony-stimulating factor
mg	milligram
min	minute
miRNA	microRNA
ml	milliliter
mM	millimolar
mmol	millimole
MR	mineralocorticoid receptor
mRNA	messenger RNA
NCC	thiazide-sensitive sodium-chloride cotransporter
NCI	National Cancer Institute
ng	nanogram

NGFI-B	neuronal growth factor-induced clone B
NHE1	sodium–hydrogen antiporter
NKCC2	Na^+-K^+-$2Cl^-$ cotransporter
nm	nanometer
nmol	nanomolar
NURR1	nuclear receptor related 1
oligo(dT)$_{18}$	18-mer deoxythymidine
PA	primary aldosteronism
PAC	plasma aldosterone concentration
PAGE	polyacrylamide gel electrophoresis
PBS	phosphate buffered saline
PCR	polymerase chain reaction
PDE3A	phosphodiesterase 3A
PEG	polyethylenglycol
Pen-Strep	penicillin / streptomycin
PET	positron emission tomography
PFA	paraformaldehyde
pg	picogram
PI3K	phosphoinositide 3-kinase
PKA	protein kinase A
PKC	protein kinase C
PLC	phospholipase C
pmol	picomole
PMSF	phenylmethylsulfonyl fluoride
PRA	plasma renin activity
PRC	plasma renin concentration
PTFE	polytetrafluoroethylene
PVDF	polyvinylidene fluoride
qPCR	quantitative polymerase chain reaction
RAAS	renin-angiotensin-aldosterone system
Ras	rat sarcoma
RIA	radioimmunoassay
RIPA	radioimmunoprecipitation assay
RNA	ribonucleic acid

RNAi	RNA interference
RNase	ribonuclease
ROMK	renal outer medullary potassium channel
RPMI	Roswell Park Memorial Institute
RT-PCR	real-time polymerase chain reaction
SDS	sodium dodecyl sulfate
SF1	steroidogenic factor 1
SGK1	serum and glucocorticoid-regulated kinase 1
shRNA	short hairpin RNA
siRNA	short interfering RNA
SNP	single-nucleotide polymorphism
TASK	TWIK-like, acid-sensitive K^+ channel
TBE	tris / borate / EDTA
TBST	tris-buffered saline - Tween 20
TOPO	tri-N-octylphosphinoxide
TRIS	tris-hydroxymethylaminomethane
TTFA	thenoyltrifluoroacetone
TWIK	tandem of P domains in a weak inward rectifying K^+ channel
UT-A	urine transporter SLC14A2
v/v	volume per volume
w/v	weight per volume
WB	Western blot
WNK	with no lysine kinase
WT	wild type
x g	relative centrifugal force
ZF	zona fasciculata
ZG	zona glomerulosa
ZP	progenitor zone
ZR	zona reticularis

7.2. Acknowledgments

7.3. Curriculum Vitae

PERSONAL DETAILS
Name: Tarik Bozoglu

EDUCATION
June 2009 –Present:
Ph.D. in Human Biology
Ludwig-Maximilians-University, Medical Clinic IV, Endocrine Research Unit, Munich, Germany

Sept. 2005 –Nov. 2008:
M.Sc. in Molecular Biology & Genetics
Bogazici University, Department of Molecular Biology and Genetics, Istanbul, Turkey

Sept. 2001 –June 2005:
B.Sc. in Biological Sciences & Bioengineering Program
Sabanci University, Faculty of Engineering and Natural Sciences, Istanbul, Turkey

Sept.1998 –June 2001
Math & Science Section
Izmir Science High School, Izmir, Turkey

PUBLICATIONS
The diastrophic dysplasia sulfate transporter (SLC26A2) is expressed in the adrenal cortex and regulates aldosterone secretion; Spyroglou A, Bozoglu T, et al.; Hypertension, 2014 May;63(5):1102-09.

Gender-, strain-, and inheritance-dependent variation in aldosterone secretion in mice; Spyroglou A, Sabrautzki S, Rathkolb B, Bozoglu T, et al.; J Endocrinol. 2012 Dec;215(3):375-81.

Low SLC26A2 expression in adrenal cells is associated with high aldosterone output; Bozoglu T, et al.; BioScientifica, 2012 May;29.

Detecting PORCN microdeletions in a large family with the Focal Dermal Hypoplasia; Güven A, Seven M, Bozoglu T, et al.; Genetic Counseling, accepted 2014 Nov.

Novel NDE1 homozygous mutation resulting in microhydranencephaly and not microlyssencephaly; Guven A, Gunduz A, Bozoglu TM, et al.; Neurogenetics. 2012 Aug;13(3):189-94.

Familial microhydranencephaly, a family that does not map to 16p13.13-p12.2: relationship with hereditary fetal brain degeneration and fetal brain disruption sequence; Behunova J; Zavadilikova E; Bozoglu T; et al.; Clin Dysmorph. 2010 Jul;19(3):107-18.

A mouse model with hyperaldosteronism carrying an ENU induced mutation on chromosome 9; Spyroglou A, Wagner S, Bidlingmaier M, Bozoglu M, et al.; BioScientifica 2010 April;22.